National Technical University of Athens

Laboratory of Marine Engineering

Development of a Semi-Empirical Combustion Model for a Dual Fuel Two-Stroke Low-Pressure Marine Engine

Diploma Thesis

Klagkou Margarita

Supervisor: Professor N. P. Kyrtatos

Athens, December 2019

Contents

Motivation and Objectives of the Thesis 1

Abstract 2

Acknowledgements 4

1 Chapter: Dual Fuel Engines 5

1.1 Brief History of Dual Fuel Engines 5

1.2 DF engines as a solution to the shipping sector 6

1.2.1 DF engine emissions- Compliance with regulations 6

1.2.2 Other Benefits of Dual Fuel Engines in Shipping 9

1.2.3 Challenges of DF technology 10

1.3 Types of Marine Dual Fuel Engines 11

1.3.1 Four-Stroke, DF engines 11

1.3.2 Two-Stroke, DF engines 13

2 Chapter: Dual Fuel Combustion Modelling 17

2.1 Combustion Modelling Types 17

2.2 Existing DF Combustion Models 18

2.3 Selected model approach 20

2.3.1 WIEBE FUNCTION 20

2.3.2 Multi-Wiebe Applications 24

2.3.3 Determination of the problem to be solved 25

3 Chapter: Dual Fuel Model Development 27

3.1 Model Fitting Approach 29

3.2 Model Development 37

3.2.1 Regression Analysis 37

3.2.2 Linear Regression Application 40

3.2.3 Non-Linear Regression Application 43

3.2.4 Final form of DF model 44

4 Chapter: Results 47

4.1 Double-Wiebe Parameters Variation 47

4.1.1 Pilot and Main Fuel Characteristic Exponents Variation 48

4.1.2 Pilot Fuel Weighting Factor Variation 51

4.1.3 Pilot Fuel Start of Combustion Angle Variation 52

4.1.4 Main Fuel Start of Combustion Angle Variation 54

4.1.5 Main Fuel Combustion Duration Variation 56
4.1.6 Pilot Fuel Combustion Duration Variation 58
4.2 Model Validation 59
5 Chapter: Conclusions 65
5.1 Discussion 65
5.2 Recommendations for future research 66
References 68
APPENDIX 71
A1: Tables 71
A2: Figures 72
Engine load variation results 79
Equivalence ratio variation results 81
Pilot fuel injection timing variation results 84
Engine speed variation results 86
Exhaust valve closing variation results 89

Motivation and Objectives of the Thesis

Increasingly stringent emission regulations combined with the advancements in extraction technologies that have significantly increased the available reserves of natural gas make up a very strong motive for engine designers to consider the use of natural gas for ship propulsion applications. However, the attractive dual-fuel, natural-gas engine concept is also very complex and still requires further research to be conducted in order to be better understood and applied.

In this respect, the intention of this diploma thesis is to suggest a model that describes the complicated combustion process of a dual fuel, marine engine as a heat release phenomenon and makes accurate predictions based on the values of the combustion variables at different operation points.

The aim of the present work is to achieve a satisfactory level of prediction ability along with a reasonably light calculation load, using the currently available data. It is also desired to make observations and reach conclusions about the characteristics of dual fuel combustion that identify with general valid concepts and agree with the available literature.

The final combustion model will be tested against reliable validation data in order to improve and ensure its accuracy. After the model is validated and completed it can be used for future research by being integrated into an engine simulation tool.

In short, the present thesis starts with an abstract of the work and a discussion about dual fuel concept in marine propulsion in terms of historical background, factors that make it an attractive choice and also the available dual fuel engine types and their operation principals in the "1st Chapter". In the "2nd Chapter", a presentation of the already existing models is given along with an in depth introduction to the model type that was chosen. "Chapter 3" provides a detailed demonstration of the modelling procedure that was followed while in "Chapter 4" are given the results along with some comments and observations. In the "5th Chapter", are made the conclusions of the thesis alongside with some suggestions about future research and study on relevant subjects.

Abstract

The “Dual-Fuel Engine” (DF) concept has gained grown popularity during the last years among both researchers and shipping companies as it provides a realistic way to meet the demands set by the recent and the upcoming emission regulations.

In this scope, the marine engine manufacturing companies have developed several dual-fuel solutions of different types. In particular, firstly, there are the four-stroke, dual-fuel engines that operate as conventional four-stroke, diesel engines except that when in “dual-fuel mode” natural gas is used as main fuel and also the air-fuel mixture is ignited by a small amount of pilot, diesel fuel that is injected at the end of the compression stroke. As for the two stroke applications of this technology they are encountered in two types, the “high pressure” and the “low pressure”. In “high pressure”, two-stroke, DF engines, gas is injected into the compressed air at high pressure leading to a diffusion combustion that follows the “Diesel” cycle. On the other hand, in the “low pressure” version of the two-stroke DF engine the main fuel is injected earlier, at low pressures, leading to a lean burn, “Otto” combustion. In both cases, the start of the combustion is supported by diesel, pilot fuel injection at the Top Dead Center.

The combustion process in dual-fuel engines is a phenomenon of high complexity that requires further research to be conducted to be better understood. So, in order to study such a phenomenon, a combustion model needs to be developed. In the present work, the produced model corresponds to the DF combustion of a two-stroke, low pressure, marine engine. In terms of modelling types, a zero-dimensional, semi-empirical approach was selected that represents the combustion as a heat release phenomenon with the use of a mathematical function whose parameters are calibrated by heat release data. In this work, a double-“Wiebe” function was utilized to describe the heat release process by dividing it into two separate parts, the main and the pilot fuel combustion. Wiebe function was selected as it is an analytical tool of high computational efficiency that is widely used in terms of performance prediction of internal combustion engines. As for the calibration of the model, it was based on validation data provided by the available literature (1).

By evaluating the model using proper mathematical criteria and comparing its results to the validation data, it was found that it is able to make accurate predictions within its calibration range.

The model fitting outcome led to conclusions that seem to be in good agreement with the recent results found in literature. In terms of “Ignition Delay” of the pilot fuel, it was found that it is reduced in cases of high engine loads and low overall equivalence ratios. Also, the “pre-ignition” phenomenon of the main fuel, meaning the spontaneous ignition of gas prior

to pilot flame front arrival, became more pronounced at high overall equivalence ratio and engine speed values and also at late pilot injection timing and early exhaust valve closing. Moreover, the combustion of both fuels is accelerated when load, equivalence ratio, engine speed and pilot injection angle are increased.

In addition to the above conclusions, the present work indicates that the complex dual fuel combustion can be accurately represented by the relatively simple analytical Wiebe function and produce reliable outcomes. In fact, the program codes that have been created in the scope of developing the combustion model make up a useful and computational effective tool for the production of a combustion model for any DF engine even in high pressure or four stroke concepts provided that an adequate amount of trustworthy calibration data is available.

Acknowledgements

Firstly, I would like to thank the supervisor of my thesis, Professor N. P. Kyrtatos for giving me the chance to conduct my Diploma Thesis at the Laboratory of Marine Engineering (LME) of the National and Technical University of Athens (NTUA) and also express my gratitude for the support, guidance and help he provided me with from the beginning until the end of my work.

Moreover, I specially thank the members of the examination committee, Professor of school of Marine Engineering and Naval Architecture of the NTUA, Lampros Kaiktsis and Professor of school of Mechanical Engineering of the NTUA, Maria Founti.

I would also like to express my thanks to senior Research Associate of LME, Mr. S. Tzanos and Dr. M. Foteinos for their supervision and assistance throughout the course of the thesis as well as for the willingness and availability they showed in discussing any issues that came up.

Lastly, I would like to thank my family, friends and colleagues for their support during this very important period of my life.

1 Chapter: Dual Fuel Engines

1.1 Brief History of Dual Fuel Engines

Even though the interest in the use of natural gas as main fuel for ship propulsion has risen only during the past few years, the gas engine concept is dating back to the early 19th century.

At that time, a lot of experiments were conducted concerning the use of gaseous fuels in internal combustion engines with the first practical successful attempt being the one of the Belgian engineer Étienne Lenoir in 1860.

Some years later, his work was further researched and improved by the cooperation of two German engineers Nikolaus August Otto and Eugen Langen who introduced in 1867 an engine which worked by drawing a mixture of gas and air into a vertical cylinder. After the rise of about eight inches of the piston, the gas and air mixture was ignited by a small pilot flame burning outside, which forced the piston (which was connected to a toothed rack) upwards, creating a partial vacuum beneath it. The work was produced when the piston and toothed rack descended under the effects of atmospheric pressure and their own weight, turning the main shaft and flywheels as they fell (2).

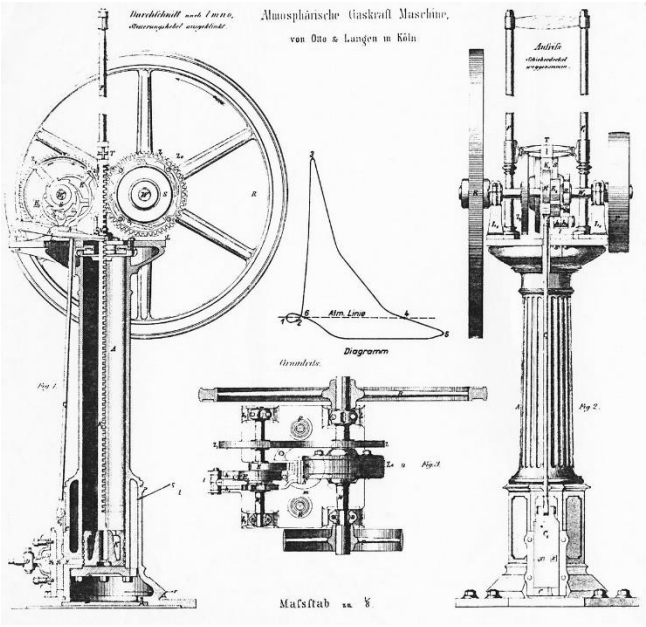

Figure 1: Otto-Langen gas engine 1867 (3)

Several years later, in 1901, the also German engineer Rudolf Christian Karl Diesel in a patent entitled “Method of Igniting and Regulating Combustion for Internal Combustion Engines”

proposed that "if a given mixture is compressed to a degree below its igniting-point, but higher than the igniting-point of a second or auxiliary combustible, then injecting this latter into the first compressed mixture will induce immediate ignition of the secondary fuel and gradual combustion of the first mixture, the combustion after ignition depending on the injection of the igniting or secondary combustible" (4). In this way, he introduced the idea of using and igniting a less reactive gaseous fuel in a four-stroke internal combustion engine using a second more reactive fuel.

However, the dual fuel engine did not become a commercial product, due to its mechanical complexity and rough running caused by auto-ignition and knocking, until 1939 when the first one was produced by the "National Gas and Oil Engine Co." in Great Britain.

During the Second World War the need to make effective use of the natural gas produced as a byproduct of oil extraction, led to the burning of the gas in diesel engines by mixing it with the intake air. It was then that a dual fuel engine was used in marine propulsion applications for the first time. Different types of dual-fuel marine engines have been developed since then, that are either diesel-ignited gas engines that use liquid fuel to ignite the gas fuel, or mixed combustion engines in which LNG tanker boil-off gas or the byproduct natural gas from oil extraction is used together with another fuel (5).

In order to meet the demands of the ship classification technical guidelines about safety, further improvements had to be made to the dual-fuel technology so that the engines would have the ability to switch between gas and liquid fuel when needed. As a result, the first four-stroke marine dual fuel engines appeared in the late 1990's and respectively, the first two-stroke marine dual fuel engine showed up in 2010 (5).

1.2 DF engines as a solution to the shipping sector

1.2.1 DF engine emissions- Compliance with regulations

The utilization of natural gas is increasingly seen as a realistic solution to some of the current issues that concern the shipping industry. The main driver of this trend is the need to comply with the upcoming progressively stringent regulations about the acceptable levels of a vessel's air emissions without the use of costly after-treatment systems.

Natural gas has gained a lot of interest as an alternative fuel to marine diesel and heavy fuel oils for merchant shipping due to its potential to reduce emissions of:

- Carbon Dioxide (CO_2)
- Nitrogen Oxides (NO_X)
- Sulphur Oxides (SO_X)
- Particular Matter (PM)

In order to reduce the greenhouse gases (GHGs) the International Maritime Organization (IMO) has set ambitious targets for a drastic CO_2 emission reduction over the following decades. Newly built ships need to meet the Energy Efficiency Design Index (EEDI) limits for CO_2 emissions that require a 20% reduction by 2020 (5). The EEDI provides a specific figure for an individual ship design, expressed in grams of carbon dioxide (CO_2) per ship's capacity-mile (the smaller the EEDI the more energy efficient ship design) and is calculated by a formula based on the technical design parameters for a given ship (6).Because of having methane (CH_4) as its main component, natural gas is characterized by low carbon to hydrogen ratio which leads to the reduction of CO_2 emissions (1).

Regarding the emissions of Nitrogen Oxides, that contribute to the formation of smog and acid rain, regulations specified under the 1997 IMO/MARPOL Convention came into force in 2005 (Tier I regulations) setting the limit to 9.8-17 g/kWh. This limit was about to drop to 7.7-14 g/kWh in 2011 by the revised Tier II regulations and finally to 2-3.4 g/kWh in January 1st 2016 in compliance with the Tier III requirements (80% reduction on Tier I) (5). Strategies such as 2-stage turbocharging, EGR or extreme Miller timing that were employed for Tier II are not applicable to the Tier III demands. The combustion process of the lean-burn Otto Cycle of the dual fuel engines ensures a very equal combustion temperature distribution, leading to low combustion temperature. As a result, combustion-induced NO_X emissions are kept low, while fuel-induced NO_X emissions do not exist as the chemical elements of natural gas are nitrogen-free (7).

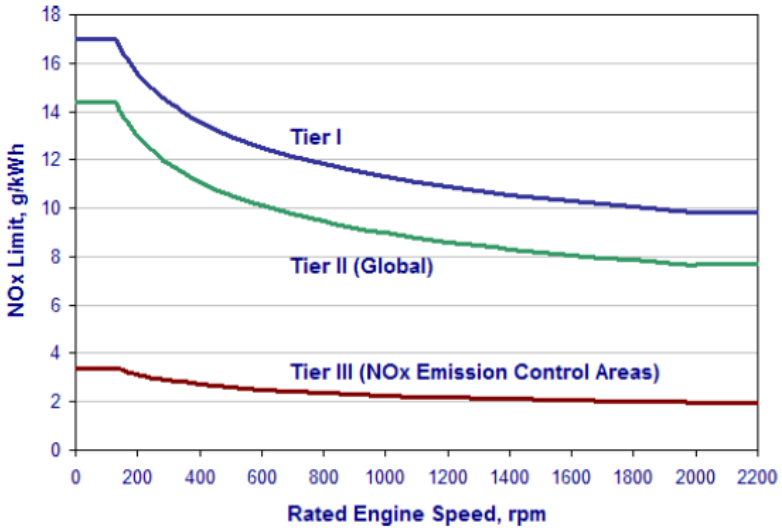

Figure 2: Overview of IMO NOx emission regulations (8)

Sulphur Oxides emissions contribute to acid rain and also cause harmful effects to trees and plants as well as to human health. The formation of SO_X mostly depends on the fuel quality and just like the NO_X their maximum allowed quantity in a ship's emissions is being reduced step to step. Following the implementation of the 0.1% limit in Emissions Control Areas (ECAs)

from 2015, IMO is challenging the marine industry by forcing a global Sulphur cap of maximum 0.5% (3.5% from 2012) by January 1st 2020 (9). At the moment, there is a tendency for many shipping companies to adopt scrubbers in order to meet with the upcoming regulations. However, when it comes to natural gas it is practically a Sulphur free fuel and thus represents a simple and economically sound solution.

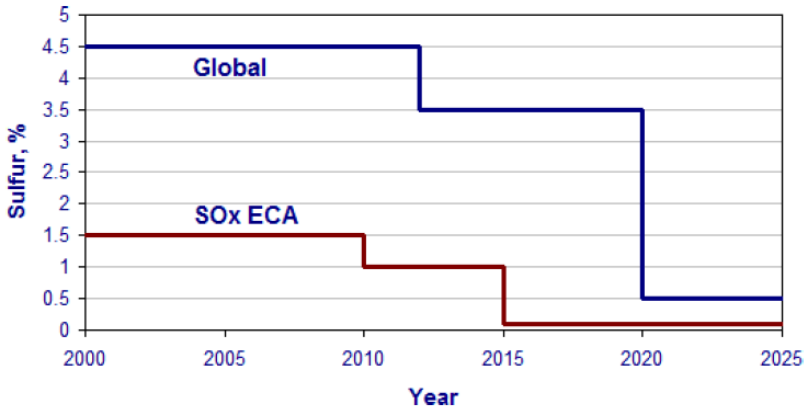

Figure 3: Overview of IMO SOx emission regulations (5)

As for the particular matter, even though there are regulations (EPA Tier 2, 3, 4) that define the limits of their emissions for vehicles no such limits have yet been set for marine engine applications. Nevertheless, it is worth noting that in dual fuel engine combustion, the lean gas-air mixture ensures that each fuel molecule can combine with sufficient oxygen for complete combustion, avoiding PM formation (7).

For the aforementioned reasons it can be deduced that the use of dual fuel engines provides a good solution to the emissions reduction issue compared to the conventional marine diesel engines.

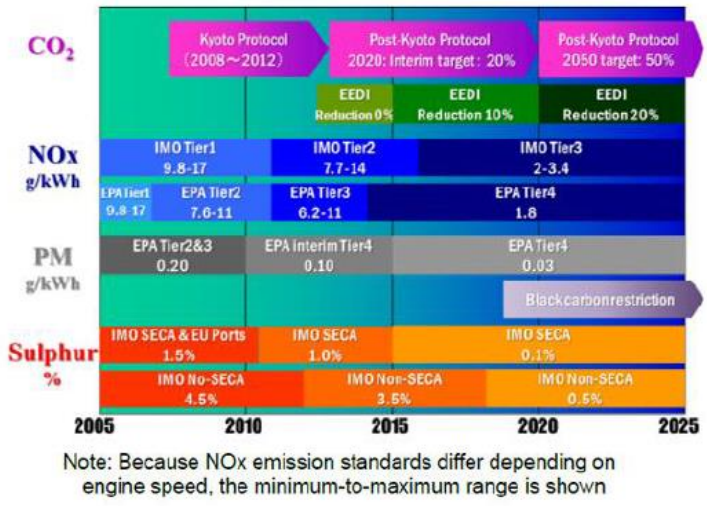

Figure 4: Schedule for Reductions in Emissions from Ships (5)

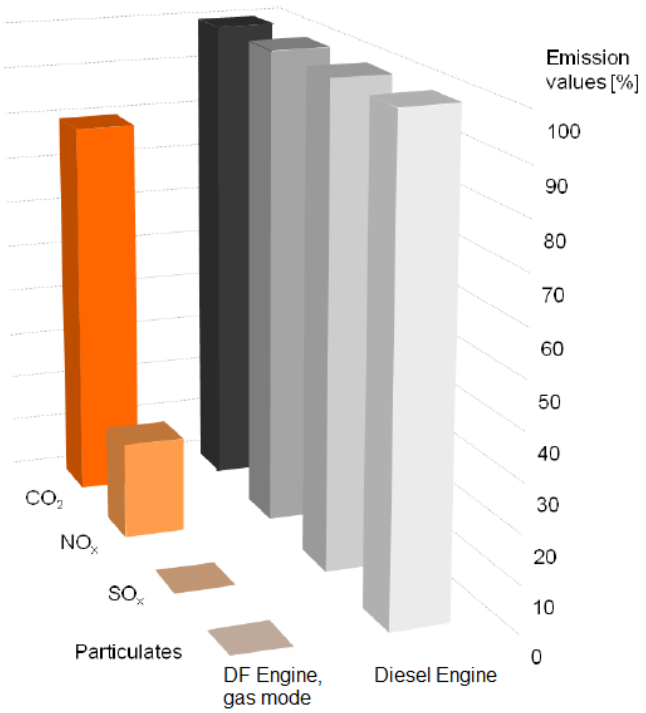

Figure 5: Comparison of emissions for a Diesel and DF engine (1)

1.2.2 Other Benefits of Dual Fuel Engines in Shipping

Apart from the use of natural gas as main fuel being a sustainable solution for meeting the upcoming regulations about a vessel's emissions, it also represents a cost-effective choice for shipping companies.

The recent advances in extraction technologies have greatly increased the estimated natural gas reserves. As a result, it is indicated that its price will remain lower than that of diesel fuel during the next decades in order to stimulate the increase of its use. It is indicatively mentioned that as of 2015, the diesel price was US $22.08/BTU while natural gas was only US $9.97/BTU (10).

Another important economic advantage of the natural gas technology is the capability to comply with emissions limits without expensive exhaust gas after-treatment systems or engine internal measures.

Also, these engines can be operated using two different fuels depending on the fuel price, or they can be operated in a fuel sharing mode to maximize the economic benefit (11).

Lastly, in the case of dual-fuel engines, the conversion from a conventional diesel engine requires little hardware modification. High compression ratio is retained and the engine can operate in the lean mode. Hence, there is a prospect of achieving roughly the same thermal efficiency as the diesel baseline (10).

At the same time, another benefit of the dual fuel engine is that it can achieve rapid acceleration when operating in diesel mode, in order to cover the ship propulsion needs or power generation back-up purposes (11).

Finally, the fact that the engine operation can be switched from gas mode to diesel mode increases the safety of its use even in emergency situations.

1.2.3 Challenges of DF technology

Despite the fact of being a promising solution to the matters that the marine industry will have to deal with in the near future, the dual fuel technology is linked with certain issues that need to be considered and resolved in order for it to become even more competitive.

Several problems have been identified and studied concerning the whole spectrum of the dual fuel engine operation. In specific, at high load conditions, when the thermal load and combustion pressure increase, the unburned fuel mixture may ignite spontaneously prior to being reached by the propagating flame. This could trigger a chain reaction known as "knocking" that could cause serious damage to the engine due to high levels of pressure and temperature (5).

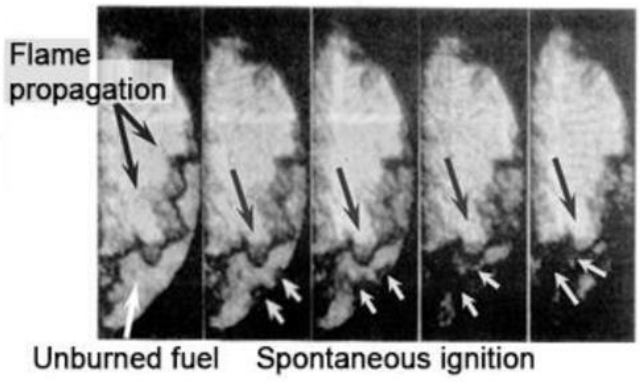

Figure 6: Gas Combustion (Knocking) (5)

On the other hand, when operating at light loads, the combination of the small injected amount of fuel into the cylinder and the abundant air supply result in an extremely lean air-fuel mixture. As a result, the combustion becomes slow and unstable with this instability exacerbating when significant cylinder-to-cylinder variations occur. In addition to this, the lean mixture also leads to low combustion efficiencies and high CO and unburned hydrocarbon emissions (12).

Incomplete combustion and flame quenching contribute to methane slip, a phenomenon that occurs when unburned methane is emitted in the air. Currently, there are no official regulations concerning the limitations of methane slip for marine engine applications

however, methane has about 25 times the greenhouse effect of CO_2 and thus the environmental impact of the phenomenon is critical (10).

It is important to point out that the combustion characteristics of dual-fuel engines are not yet fully understood. Questions regarding the ignition delay of diesel and the auto-ignition of NG in a dual-fuel setting have yet to be answered. That is mainly due to the combustion process complexity. The interaction between the fuel jet, the diesel auto ignition process and the flame front development make the combustion difficult to analytically be modeled and subsequently studied and thoroughly understood.

Finally, another factor that practically limits the use of gas in marine applications is the availability of a fuel bunker infrastructure. Without it the dual fuel marine engines will be constrained to operate in diesel mode even in situations when it would be against their efficiency.

1.3 Types of Marine Dual Fuel Engines

In order to make the utilization of dual fuel technology as much efficient and competitive as possible for each application, several types of these engines have been produced.

Initially, the dual fuel marine engines could be separated in two large categories according to whether they operate on a four-stroke or two-stroke cycle.

Both of these engines can operate in diesel and dual fuel modes and switch between them freely. In the following paragraphs will be given a short description of the dual fuel running procedure of each type as the diesel procedure does not differ from that of the conventional diesel engine.

1.3.1 Four-Stroke, DF engines

As in all four stroke engines, the cycle begins with the intake stroke during which the gas fuel is supplied from a gas valve in the air intake manifold where it flows into the cylinder as a mixture with air, while the piston is moving downwards.

The engine features two diesel fuel injectors, the “Main Fuel Injector” used for diesel mode and the “Micro-Pilot Fuel injector” that supplies a small quantity of diesel fuel at the end of the compression stroke. This small amount of diesel is ignited by the high levels of pressure and temperature inside the cylinder and triggers the ignition of the fuel-air mixture at the start of the combustion stroke when the piston is once again moving downwards and the mechanical work is being produced (5).

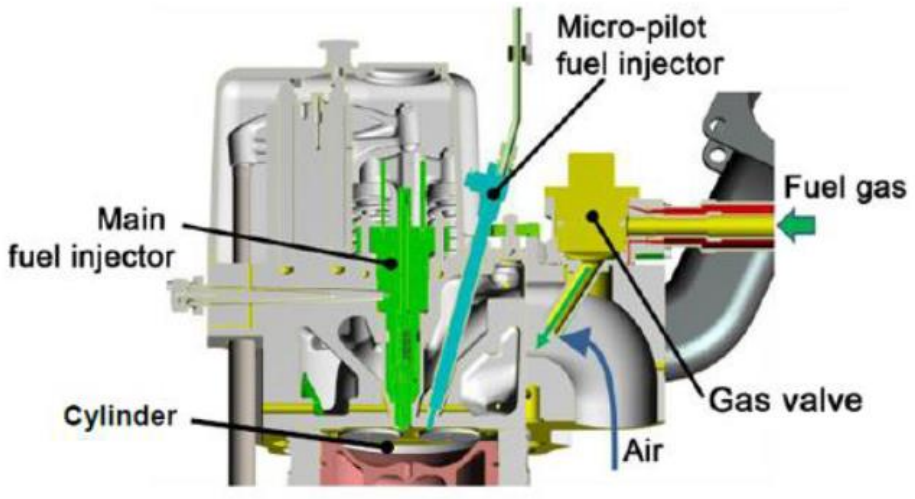

Figure 7: Cross-Section of Four Stroke Dual-Fuel Engine (5)

Finally comes the exhaust stroke, when the piston returns from the "Bottom Dead Center" (BDC) to the "Top Dead Center" (TDC) expelling the spent air-fuel mixture through the open exhaust valve. The exhaust emissions vary according to the proportions of diesel in the total fuel amount that must be reduced to 2-3% in order to achieve the IMO Tier III regulations (5).

The biggest Marine Engine manufacture companies "WinGD - Winterthur Gas & Diesel/ Wärtsilä" "MAN B&W" and "Hyundai" have put four-stroke dual fuel engines on the market. In the below table are presented the currently available models as displayed on the websites of the companies (13) (14) (15).

Table 1: four-stroke dual fuel marine engine models currently available on the market

Engines	*Output/cylinder [kW/cyl]*	*Speed [rpm]*
Wärtsilä		
20DF	*185*	*1200*
31DF	*550*	*750*
34DF	*500*	*750*
46DF	*1145*	*600*
50DF	*950, 975*	*500, 514*
MAN B&W		
35/44DF	*510, 530*	*720, 750*
51/60DF	*975, 1000*	*500, 514*
HYUNDAI		
H22CDFP	*220*	*1000*
H27DFP	*310*	*1000*
H35DFP	*500*	*750*
H35DFVP	*500*	*750*

1.3.2 Two-Stroke, DF engines

As is known, in a two-stroke engine a power cycle is completed within two strokes of the piston during one crankshaft revolution. During the first stroke begins the intake when the piston is near the BDC. Air is let in through ports in the cylinder wall and is compressed by the upwards movement of the piston forcing at the same time out the remaining combustion gases (scavenging). Near the TDC, fuel is injected and ignited by the high levels of temperature and pressure caused by the compression. Then the second stroke starts with the piston moving downwards producing work.

There are two types of two-stroke dual fuels engines that even though having in common the aforementioned power cycle, they differ in the injection of the LNG into the combustion chamber in high or low pressure that leads to a diffusion or lean combustion respectively.

1.3.2.1 High Pressure, Two-stroke, DF engines

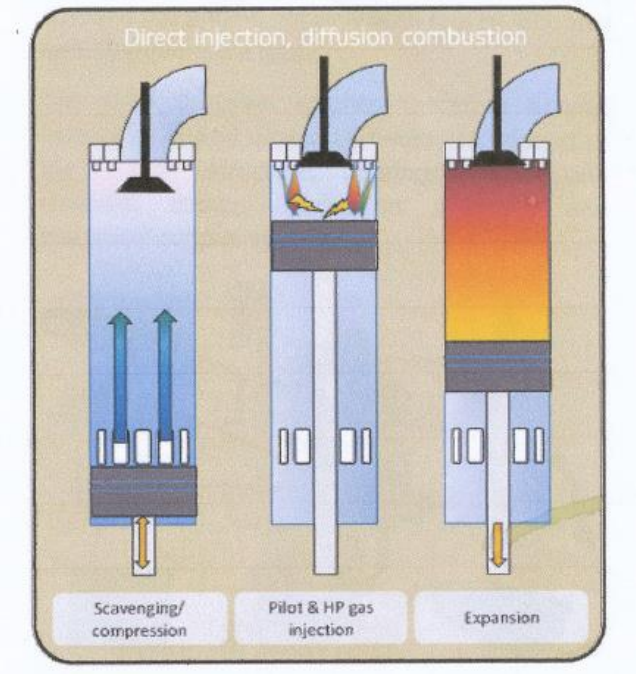

Figure 8: High Pressure Gas Injection, Diesel Cycle, Diffusion flame (16)

In these engines the gas is being injected into the compressed air near the Top Dead Center in the same way as in the conventional diesel two-stroke engine. The compression pressure can exceed 150 bar meaning that the gas must be injected with pressures of about 300 bar in order to mix quickly and good with air and lead to an efficient combustion following the Diesel cycle.

With high pressure injection the gas could, theoretically, burn directly after injection through a diffusion flame however, its burning speed would be too slow. Therefore, in order to

increase the heat and turbulence and thus the combustion acceleration, a small amount of diesel pilot fuel is also injected via a micro-pilot fuel injector (9).

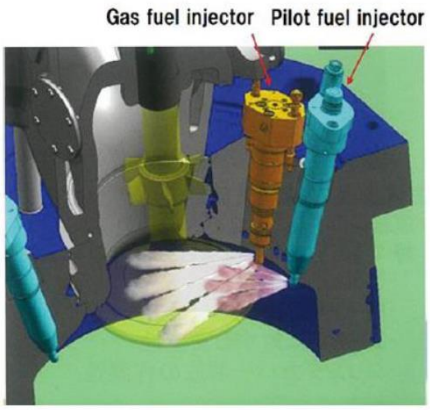

Figure 9: Cylinder Cover-Fuel Injectors (5)

Because of having a diffusion combustion, the CO_2 and CO emissions are critically reduced while there is no risk of "knocking" phenomena to occur (5).

However, the required proportion of diesel pilot fuel ranges between 5-10% of the total fuel energy and so Tier III compliance can be met only by installing exhaust gas after-treatment or recirculation systems.

Such engine applications are available on the market by "MAN B&W" (ME-GI concept) and are based on a diesel type combustion process with gas injection pressure between 150 and 315 bar depending on engine load (17).

1.3.2.2 Low Pressure, Two-stroke, DF engines

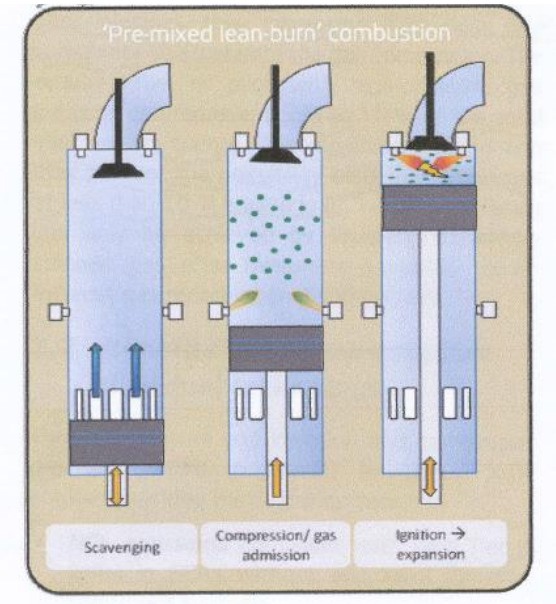

Figure 10: Low pressure, Otto cycle, lean mixture (16)

In this case, the gas is being injected into the chamber during the first phase of the compression in other words, close to the BDC where the pressure is low. This allows the gas to be injected at also low pressure (less than 16 bar) (7) and mix with the air. The piston continues to move up and the compression increases the temperature of the lean gas-air mixture. When the piston is almost at TDC, pilot fuel is injected to support the start of combustion.

In order to secure stable ignition, the pilot fuel is usually injected into a pre-chamber which concentrates the energy of the fuel leading to higher temperature and rapid pressure increase. A powerful torch is then created that penetrates into the main combustion chamber giving a high energy ignition source for the main fuel charge in the cylinder (18).

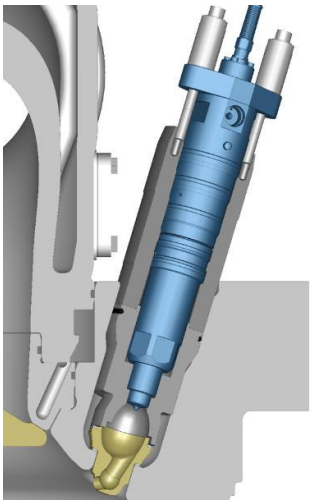

Figure 11: Injector and Pre-Chamber of Diesel Pilot Fuel (19)

The lean burn, Otto combustion is characterized by minimal pilot fuel oil needed as well as high speed and low maximum combustion temperatures leading to low NO_X emissions that comply with the IMO Tier III regulations without additional equipment.

In addition to this, the simple and reliable gas supply system compared to that required by the high pressure direct injection technology is a far more low investment in terms of purchase and maintenance.

Even though the lean fuel mixture helps to decrease the risk of pre-ignition and knocking nonetheless at high loads it increases the risk of misfiring as the misfiring limit is nearing the knocking limit. This means that extra care should be given in ensuring that the engine operates in the safe operation area (20).

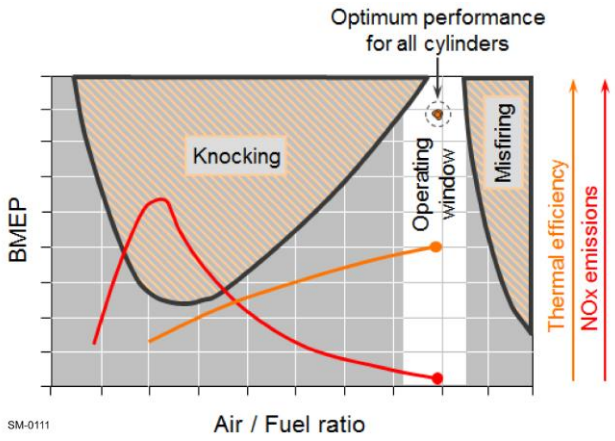

Figure 12: Lean Burn Operation Area (5)

WinGD was the first company to introduce in 2013 the low-pressure X-DF engines which were based on the existing RT-flex and X-diesel engine series and until now there has been no such application produced by other companies.

2 Chapter: Dual Fuel Combustion Modelling

As it has been already stated, this diploma thesis focuses on the development of a model for the combustion process in a dual fuel, two stroke, low pressure marine engine.

In the following paragraphs will be presented the existing combustion modelling types as well as some of the models that already have been developed concerning the dual fuel combustion concept. Finally, there will be given a detailed introduction to the modelling method that was chosen for the present work.

2.1 Combustion Modelling Types

When it comes to the modelling of a combustion process regardless of whether it is defined as conventional or alternative there are three main categories of combustion models, the "zero-dimensional", the "quasi-dimensional" and the "multi-dimensional" all three of which are briefly presented below (1):

- Zero-Dimensional models represent empirical or semi-empirical approximation methods of the combustion. Usually, the approach is achieved with a use of one or several mathematical functions that represent the Heat Release Fracture or Rate of the combustion and whose parameters are calibrated by measured heat release data. The data used for parameter calibration are selected so that the produced model can give valid results for several operation ranges or even several engines. Physics and chemical kinetics are excluded by zero-dimensional modelling methods and also uniformity is assumed in each zone (usually one or two) that is assumed for the in cylinder processes. These models offer a fast solution in terms of computational time and also a well predictive tool within the calibration range.

- Quasi-dimensional models are an intermediate step between zero and multi-dimensional ones. In this case, physical and chemical phenomena and also turbulence terms are taken into account along with the spatial differences of the thermodynamic values within the same zone. In addition to this, energy and mass equations are being solved within the combustion space and thus, this kind of model can predict well the emissions and all the combustion products. The computational effort of this category is bigger than that of the zero-dimensional but remains reasonable.

- Lastly, multi-dimensional CFD (Computational Fluid Dynamics) models offer the most general and theoretically supported approaches by solving in detail the energy, mass and momentum conservation equations. Moreover, they include chemical

concentrations, turbulence within the calculation entity and spatial differences. Their reliability depends on initial boundary conditions and the utilized methodologies and tools, while high computational effort is required.

2.2 Existing DF Combustion Models

Even though in the past little effort was put to research and development of suitable models for multi-fuel combustion due to flexibility of environmental regulations and lack of expertise still, there have been developed several noteworthy dual fuel combustion models within the last two decades.

Starting from the "zero-dimensional" available applications, an empirical approach of the combustion in a 4-sroke dual fuel marine engine was presented in 2014 by Xu et al. (21). The motivation behind their work was to study and improve transient response which is one of the biggest challenges of DF technology due to its increased complexity. The model uses a triple Wiebe function each of the three parts representing the heat release in "premixed", "main" and "trail" combustion phase of both diesel and fuel operation. Ignition delay and injection timings are calculated based on Start of Combustion (SOC) and a predictive ignition delay correlation. The proposed model was integrated into the 1-D GT-Suite simulation environment and used for transient simulations producing satisfactory results.

Another 0-D combustion modelling way for a medium speed, four stroke DF engine was given by Park et al. in 2019 (11) that used a double Wiebe function to represent the combustion of pilot and main fuel respectively. The model was designed in order to examine the impact of the heat release parameters in the combustion process and derive ways to improve the engine performance. It was developed for operating condition variations mainly in micro pilot (MP) injection timing, MP injection duration, MP injection pressure, air chamber conditions and compression ratio. The combustion model seems to predict the desired parameters with sufficient accuracy leading to a reliable distribution of the HR curve of an operation point.

An empirical model for a diesel engine with maximum 40% natural gas substitution rate (SR) was published by Hountalas and Papagiannakis (22) to give results derived from a theoretical investigation and model simulation for the soot emissions reduction. In this a case, two zones have been assumed in each of which details of diesel fuel spray formation and mixing with the surrounding mixture of air and gas have been considered. It is also assumed that the burning of the gas starts after the ignition of the diesel fuel and that its burning rate is a function of the rate of entrainment of surrounding gas inside the fuel jet. It utilizes a soot model, an equilibrium model for concentration of chemical species calculations and the "Zeldovich mechanism" for NO_X. The model has been tested and found to work properly on a one-cylinder laboratory engine for variable loads and quantities of substitution gas. It is however assumed that it could not be used in lean burn, micro-pilot applications as it doesn't take into account the related phenomena.

There have also been released several “quasi-dimensional” models. In this category belongs the phenomenological model for the combustion in large low speed, two stroke, dual fuel, marine engines that was proposed by Filip Černík in his doctoral thesis (1). The goal of this work was to identify generally valid concepts for describing diesel and dual fuel combustion in such engines and to undertake engine performance analysis and optimization under both steady state and transient operation conditions. In the development procedure were taken into account both pilot fuel controlled and self-triggered ignition of the air-fuel mixture along with interactions between pilot and main fuel, cylinder purity, stratification of gaseous fuel and in-cylinder turbulence. The cylinder volume was discretized into a number of zones in order to capture spatial differences given by the scavenging process and the admission of the gaseous fuel. The ignition delay of the pilot fuel was defined by “Livengood-Wu” integral approach while in the case of main fuel, tabulated values originating from the detailed kinetics were used. By assuming a homogenous fuel oxidizer mixture, even distribution of temperature and pressure within the cylinder and also uniform turbulence level the laminar and turbulent flame speeds are estimated. Furthermore, the model was implemented into the commercial 1-D GT-Suite simulation tool by means of a user routine in order for full cycle calculations to be performed. Validation was made through comparison with full scale engine data and as for the sub-models used, their results were evaluated by being compared to those of multi-dimensional CFD simulations. From the validation’s outcome and its theoretical background this model seems to be a reliable one.

One more multi-zonal, quasi-dimensional model came out in 2017 by Taritas et al. (23) that has been integrated within a commercial engine system simulation framework and is based on two sub-models. The first is a modified multi-zone model which handles the part of the combustion process that is governed by the mixing-controlled combustion while the other is a modified fractal combustion model that handles the part that is governed by the flame propagation. In this work spray processes, i.e. liquid spray break-up, fresh charge entrainment and evaporation process are phenomenological described and special tables have been made for determination of ignition delay and chemical reaction time scale. Concerning the sub-models used, an existing turbulence model has been extended to account for the effect of diesel pilot injection on the increase of in-cylinder turbulence level and a newly developed, based on knock integral calculation, model was employed for flame propagation. Since in the conventional dual fuel combustion process multiple flames propagate through the combustion chamber, a multiple flame propagation model has also been developed. The validation data for variable loads and diesel substitution ratios were derived from the operation of a Diesel engine modified to perform a conventional dual fuel combustion.

A multi-dimensional, CFD approach was made by Eder et al. (24). Their work target was the numerical modelling of a diesel ignited gas engine using a 3D-CFD tool with special focus on pilot injection and the interaction between the two fuels. As for the gas injection modelling, a specific approach was proposed that improves the modelling of the ballistic region of the needle lift that was evaluated by comparison to experimental data from an inert spray

chamber. The approach describes a two-stage ignition method depending on temperature and dual fuel mixture fraction, which combines two different tables with an interpolation function. It also suggests improvements in ignition delay modelling of the diesel ignited gas engine. The predictive capability of the models was investigated using data from single cylinder engine.

Tulwin and Sochaczewski in their work (25), produced a dual-fuel CFD combustion model in order to examine direct and indirect CNG injection. In the indirect injection, the injector was placed in intake channel and the injection occurred during the intake stroke. On the other hand, in the direct injection the injector was installed in the plow plug. The results allow a mixture homogeneity analysis and its impact on combustion process and heat transfer.

2.3 Selected model approach

After having examined the already existing models and methods for modelling the combustion process of dual fuel marine engines, it was decided for the present work to employ a "Double-Wiebe function" so as to describe the heat release process of the combustion.

This function has been selected for being a simple but powerful correlation model with high computational efficiency that is well suited for zero and one dimensional engine cycle simulations. Furthermore, its applicability in different combustion processes regardless of the systems and fuels used makes it a suitable choice for a dual fuel application.

2.3.1 WIEBE FUNCTION

The analytical "Wiebe function" was introduced by a Russian engineer and scientist, born in Ukraine in 1902, named Ivan Ivanovitch Wiebe in 1962 when he published his monograph (26). The function is a derivative of the normal distribution of a continuous random variable and is until today the best known among the others of this type in terms of performance prediction of internal combustion engines.

Wiebe function is based on the theory of chemical reactions kinetics and chain reactions. Briefly explained, along with the chain reactions that occur in a combustion system, intermediate, high reactive species are formatted (free atoms, radicals) that Wiebe called "active centers" and are crucial to the reaction path. In fact, in order for the reaction to start a certain amount of active centers is required to be generated by heating the air-fuel mixture. As combustion proceeds more active centers are produced starting new reaction cycles however, total concentration of reactants decreases and so does the reaction rate. In this scope, Wiebe assumed that the incremental change in the number of molecules of the main reactants dN of the reaction in the time interval t

to t+dt is directly proportional to the change in the number of active centers dN_e where n is the constant of proportionality (27):

$$-\left(\frac{dN}{dt}\right) = n \cdot \left(\frac{dN_e}{dt}\right) \tag{2-1}$$

Subsequently, he defined the density of the active centers as:

$$\rho = \left(\frac{dN_e}{dt}\right)\Big/_{N} \tag{2-2}$$

,where N is the instantaneous number of molecules of the initial reactants and then expressed it as follows with k and m being constant values:

$$\rho = k \cdot t^m \tag{2-3}$$

Finally, he introduced the burn fraction value x in the following manner:

$$x = \left(\frac{N_0 - N}{N_0}\right) \tag{2-4}$$

After integrating Equation (2-1), making the necessary replacements and switching time variable with crank angle Wiebe established the final form of his equation of burn fraction that has the form of a “S-type” curve:

$$x = 1 - exp\left[C \cdot \left(\frac{\theta - \theta_0}{\Delta\theta}\right)^{m+1}\right] \tag{2-5}$$

Equation (2-5) represents the fraction of the fuel mass burnt at crank angle θ to the total fuel mass injected into the cylinder per cycle. Accordingly, by simply calculating the derivative of this equation the burning rate of the fuel w was obtained:

$$w = \frac{dx}{d\theta} = \frac{-C \cdot (m+1)}{\Delta\theta} \cdot \left(\frac{\theta - \theta_0}{\Delta\theta}\right)^{m} \cdot exp\left[C \cdot \left(\frac{\theta - \theta_0}{\Delta\theta}\right)^{m+1}\right] \tag{2-6}$$

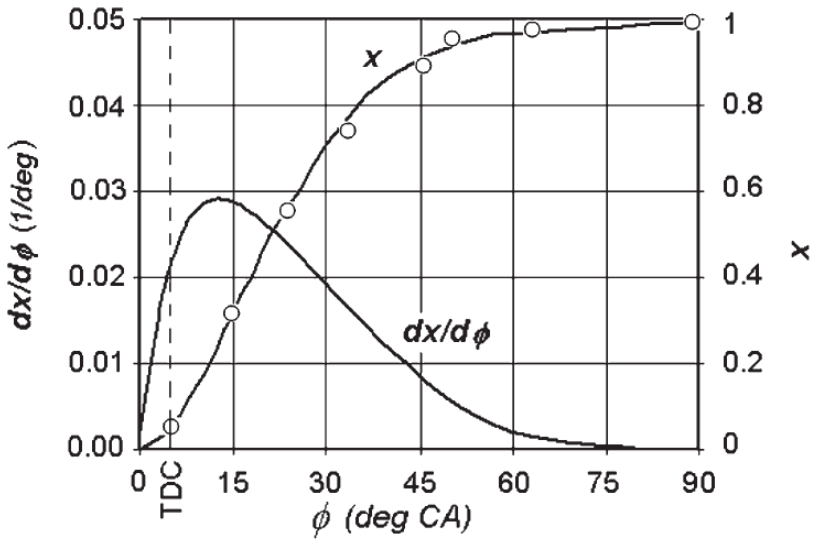

Figure 13: Burn Fraction x and Burn Rate dx/dθ diagrams (27)

As depicted above, the S-curve of the mass burn fraction starts from zero in the beginning of the combustion when no fuel has been burnt yet and stops when it reaches one, meaning that all the fuel injected in the cylinder has been burnt by the end of the combustion. Regarding the burn rate w curve, it also starts from zero in the beginning of the phenomenon, reaching its maximum value after the TDC and arrives gradually to zero again by the end of combustion.

Both the burn fraction and burn rate equations include a number of constants that are further described below:

- "Efficiency parameter" of the Wiebe function **C** is a function of the mass fraction of the fuel burnt by the end of combustion x_d:

$$C = \ln(1 - x_d) \tag{2-7}$$

  In many applications it is assumed that x_d = 0.999 in every cycle and so C value is rounded off to C=-6.908.

- "Form factor" or "Combustion characteristic exponent" **m** was given a physical explanation by Wiebe who concluded that "for a given combustion duration t_d the time t_m it takes for maximum burn fraction (/burn rate) to be reached is determined solely by the magnitude of m, which, in turn, determines the magnitude of the maximum burn fraction equation (/burn rate) x_m" (27). Indicatively, are displayed below the two equations that represent the aforementioned relationships.

$$x_m = 1 - exp\left[\frac{-m}{m+1}\right] \tag{2-8}$$

$$t_m = t_d \cdot \left[\frac{m}{-C \cdot (m+1)}\right]^{\frac{1}{m+1}} \quad (2\text{-}9)$$

In the following graphs is depicted the influence of parameter m on the burn fraction and burn rate curves:

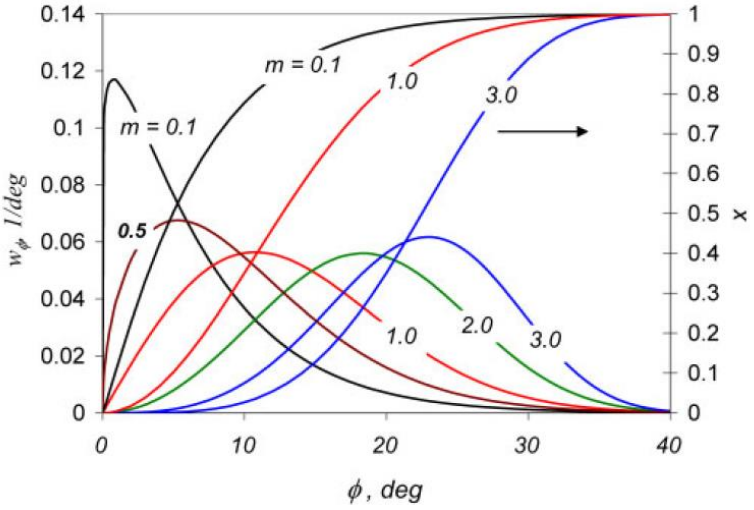

Figure 14: Burn Fraction/Rate graphs for θd=40deg and m=0.1-3.0 (27)

- **θ_0** represents the angle of the crank angle at the start of combustion
- **$\Delta\theta$** stands for the combustion duration in angle units

These two functions introduced by Wiebe are very important in terms of combustion modelling. That is because, the heat released by the combustion is calculated by multiplying the mass of the burnt fuel m_{FUEL} with its lower calorific value (LCV) and by calculating the derivative of this function, a relationship between the Heat Release Rate and the burn rate w can be acquired. The Heat Release Rate function and diagram are representative of the combustion process and can be used for estimating the pressure-volume diagrams.

$$Q_A[kJ] = m_{FUEL}[kg] \cdot LCV \left[{}^{kJ}/_{kg}\right] \rightarrow \quad (2\text{-}10)$$

$$\frac{dQ_A}{d\theta} = \frac{dm_{FUEL}}{d\theta} \cdot LCV = m_{CYCLE} \cdot w \cdot LCV \quad (2\text{-}11)$$

,where Q_A represents the combustion's released heat and m_{CYCLE} the total fuel mass injected per cycle.

2.3.2 Multi-Wiebe Applications

In cases of engines that feature more sophisticated and advanced combustion systems that lead to more complex forms of the Heat Release Rate curves, single-Wiebe functions are no longer appropriate for their depiction.

For this reason, multi-wiebe correlations were introduced that divide the combustion into a number of multiple stages depending on its nature:

$$x = f_1 \cdot x_1 + f_2 \cdot x_2 + \cdots + f_N \cdot x_N \tag{2-12}$$

$$w = f_1 \cdot w_1 + f_2 \cdot w_2 + \cdots + f_N \cdot w_N \tag{2-13}$$

Where:

- $$x_i = 1 - exp\left[C_i \cdot \left(\frac{\theta - \theta_{0i}}{\Delta\theta_i}\right)^{m_i+1}\right], i = 1,2,\dots,N \tag{2-14}$$

- $$w_i = \frac{-C_i \cdot (m_i+1)}{\Delta\theta_i} \cdot \left(\frac{\theta-\theta_{0i}}{\Delta\theta_i}\right)^{m_i} \cdot exp\left[C_i \cdot \left(\frac{\theta-\theta_{0i}}{\Delta\theta_i}\right)^{m_i+1}\right], i = 1,2,\dots,N \tag{2-15}$$

- N : The number of stages of the multi-wiebe function

- f_i : The "Amplitude Correction Factor" of the Wiebe function that represents the contribution of each combustion stage to the heat release and for which the following rules are applied:

$$0 \le f_i \le 1$$
$$f_1 + f_2 + \cdots + f_N = 1 \tag{2-16}$$

2.3.3 Determination of the problem to be solved

In the present work, it was decided to make use of a double-Wiebe function. This has to do with the fact that, as is going to be further comprehended in the next chapters, the burn rate curve in a dual fuel engine exhibits in many cases two peaks, one for the pilot and one for the main fuel combustion. Thus, it was considered convenient to employ a double-wiebe function with its first part representing the pilot and the second the main fuel burning.

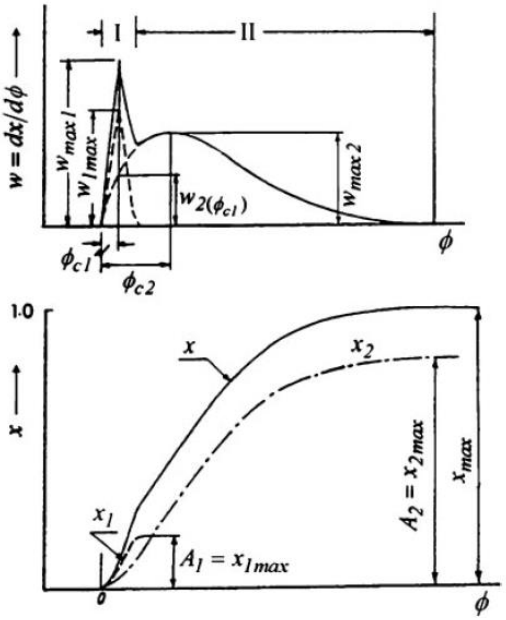

Figure 15: Example of double-Wiebe function application (27)

The functions that will be used are of the below form where, p indicates a pilot and m a fuel related term:

$$x_i = f_i \cdot \left(1 - exp\left[C_i \cdot \left(\frac{\theta - \theta_{0i}}{\Delta\theta_i}\right)^{m_i+1}\right]\right), i = p, m \tag{2-17}$$

$$w_i = f_i \cdot \frac{-C_i \cdot (m_i + 1)}{\Delta\theta_i} \cdot \left(\frac{\theta - \theta_{0i}}{\Delta\theta_i}\right)^{m_i} \cdot exp\left[C_i \cdot \left(\frac{\theta - \theta_{0i}}{\Delta\theta_i}\right)^{m_i+1}\right] \tag{2-18}$$
$$, i = p, m$$

$$\begin{aligned} x &= x_p + x_m \\ w &= w_p + w_m \end{aligned} \tag{2-19}$$

Summarizing the above, in order to produce the desired dual fuel combustion model utilizing the double-Wiebe function all that is required is to determine the values of those 10 parameters:

- ✓ f_p, f_m
- ✓ C_p, C_m
- ✓ $\Delta\theta_p$, $\Delta\theta_m$
- ✓ θ_{p0}, θ_{m0}
- ✓ m_p, m_m

3 Chapter: Dual Fuel Model Development

After having determined the problem that needs to be solved as the computation of the ten parameters that are required to establish the double-Wiebe function, the method of their estimation was yet to be figured out.

As it has already been mentioned, in an empirical or semi-empirical phenomenological combustion model the required parameters are usually calibrated by measured data. However no such data were available. Hence, model validation was carried out using data found in literature (1). One of the most prominent works on phenomenological combustion models applied on dual-fuel, two-stroke, marine engines is the one proposed by Filip Černík in his doctoral thesis "Phenomenological Combustion Modelling for Optimization of Large 2-stroke Marine Engines under both Diesel and Dual Fuel Operating Conditions".

The results of this work were used as validation data in this thesis. The specifications of the engine used in this work are presented in the following Table:

Table 2: Engine Specification overview at CMCR

Engine type	*RT-flex50DF*
Number of cylinders	6
Bore [mm]	500
Stroke [mm]	2050
Compression ratio	12.0
Engine speed [rpm]	124.0
BMEP [bar]	17.3
Gas Admission valves per cylinder	2
Injectors / Pilot Combustion Chambers per cylinder	2 / 2

In this work, the effect of each combustion model parameter on the overall Heat Release rate was examined. The examined parameters are listed below:

- Engine Load [%]
- Overall Equivalence ratio: $\varphi = \frac{m_{fuel}/m_{O2}}{\left(m_{fuel}/m_{O2}\right)_{st}}$, where m_{fuel} is the total mass of diesel fuel and NG, m_{O2} is the mass of available oxygen in the cylinder charge, and $\left(m_{fuel}/m_{O2}\right)_{st}$ is the stoichiometric fuel-to-oxygen ratio (10)
- Pilot Injection Timing [degrees after Top Dead Center]
- Engine Speed [rpm]

- Exhaust Valve Closing (EVC) [degrees after Top Dead Center]

For example, in the following figure the simulation results for overall equivalence ratio variation (0.33-0.46) / boost pressure (2.4-1.4 bar) are shown with blue lines and measurements are shown with red lines. All five simulations were made at steady 50% load, engine speed at 99 rpm, pilot injection timing at -2 crank angle degrees before Top Dead Center and exhaust valve closing at 266 crank angle degrees.

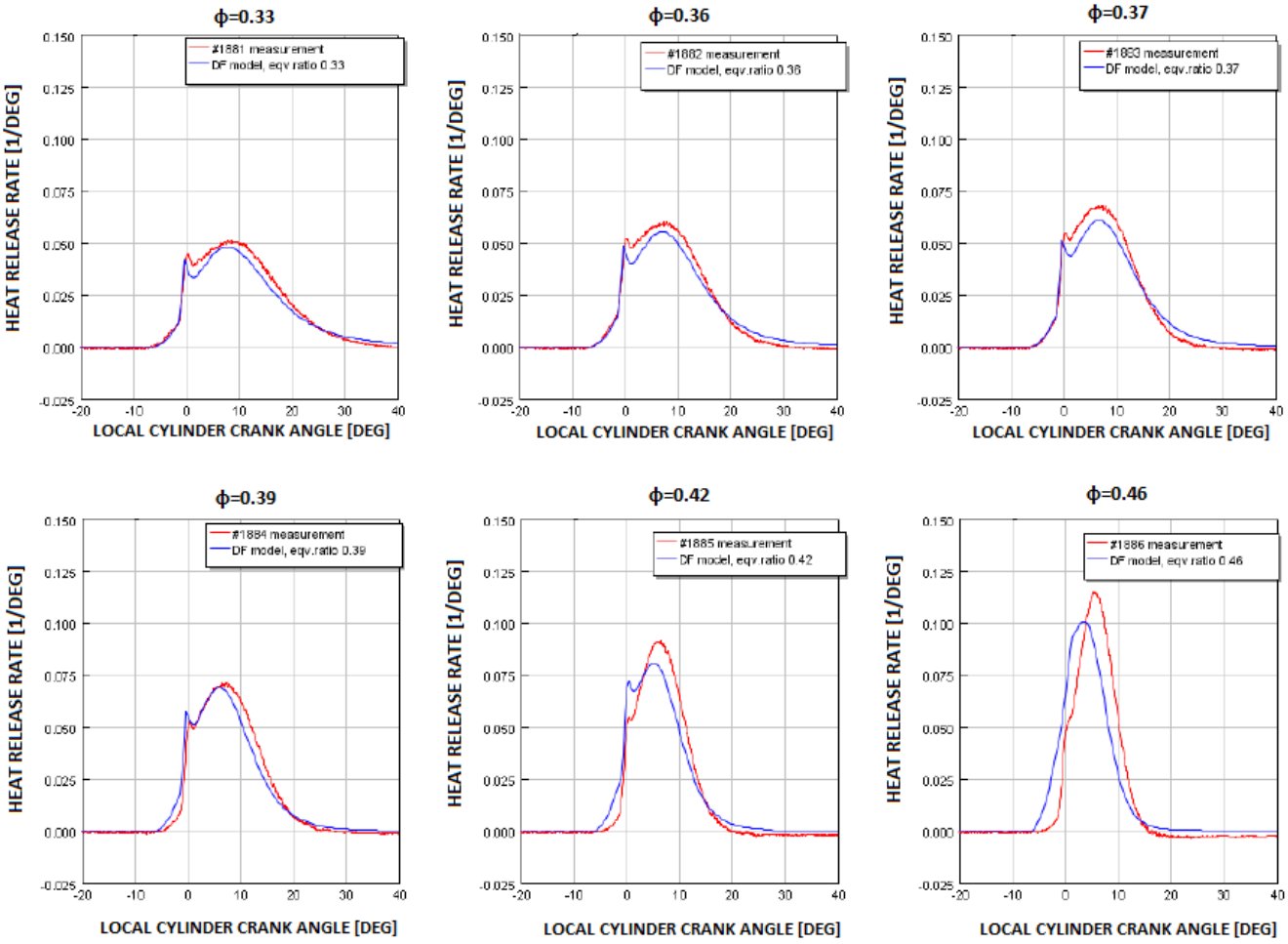

Figure 16: Comparison of model's predicted (blue) and measured (red) HRR profiles for equivalence ratio variation (1)

3.1 Model Fitting Approach

All the calculations in the present work were made using the "MATLAB 2015" software environment, therefore in the following segment of the chapter are presented in detail the steps that were taken in order to achieve a good fitting of the double-Wiebe function to the Heat Release curves of the calibration data:

- Before anything else, the aforementioned heat release rate curves had to be digitized. For this purpose, a "Plot-Digitizer" software was used to derive the coordinates (Crank angle, Specific Heat Release Rate) of the points of each curve.

- Subsequently, those points were inserted into the matlab code so as to be used in the fitting process. Then, trapezoidal integration was performed in order to calculate the points of the corresponding "Burn Fraction" curves. Afterwards, by finding the first non-zero point and the point where the burn fraction curve reaches its maximum value, the crank angles at "Start Of Combustion" (SOC) and "End Of Combustion" (EOC) respectively were estimated.

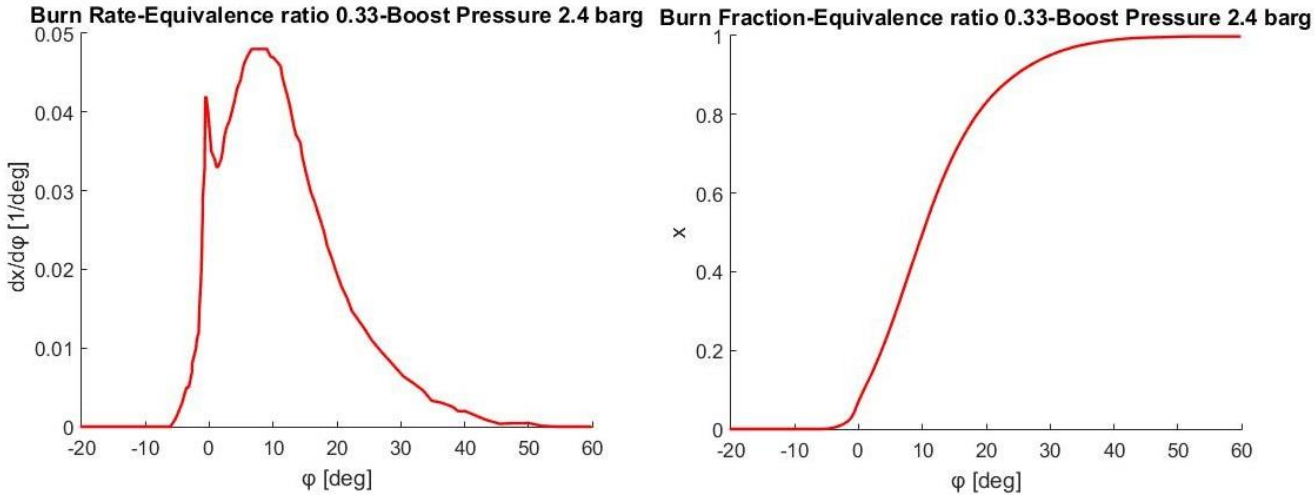

Figure 17: Inserted burn rate curve and calculated burn fraction curves

- At this point, some simplifications were made with the purpose to reduce the number of parameters to be calibrated in the fitting process:

  - The "Amplitude Correction Factor" of the main fuel wiebe function part f_m, was excluded from the calculation process as it is determined by the value of the corresponding factor of the pilot fuel f_p as indicated in Equation (2-16):

$$\boldsymbol{f_m = 1 - f_p} \quad (3\text{-}1)$$

- The "Efficiency parameters" of both pilot and main fuel C_p and C_m were given a fixed value that corresponds to 0.999 of each fuel burnt by the end of combustion, due to the fact that after several approximations their values did not show significant changes. According to Equation (2-7) the value of the two parameters is equal to :

$$\boldsymbol{C_p = C_m = \ln(1 - 0.999) = -6.908} \quad (3\text{-}2)$$

After having excluded the above parameters, the problem was reduced to the calibration of the **seven** highlighted parameters:

$$x = \boldsymbol{f_p} \cdot \left(1 - exp\left[C_p \cdot \left(\frac{\theta - \boldsymbol{\theta_{0p}}}{\boldsymbol{\Delta\theta_p}}\right)^{\boldsymbol{m_p}+1}\right]\right) + f_m \cdot \left(1 - exp\left[C_m \cdot \left(\frac{\theta - \boldsymbol{\theta_{0m}}}{\boldsymbol{\Delta\theta_m}}\right)^{\boldsymbol{m_m}+1}\right]\right) \quad (3\text{-}3)$$

➢ At this stage, begun the fitting procedure of the double Wiebe function at all the burn rate (and fraction) plots of each curve set of the validation data.

The fitting was achieved by minimizing the sum of squared differences between the predicted by the wiebe function Heat Release Rate and the one provided by the validation data. The smaller was this sum's final value, the better would be the fitting's quality.

In particular, this value was calculated in a matlab function that received as input the seven parameters, calculated the burn rate using the double wiebe function and then its deviation from the calibration data as the sum of squared errors:

$$SSE = \sum_{i=1}^{N} (w_w - w_{cd})^2 \quad (3\text{-}4)$$

Where:

- w_w is the predicted total burn rate by the wiebe function
- w_{cd} is the total burn rate given by the calibration data
- N is the number of points that were compared

➢ The minimization of the above sum was made with the use of non-linear programming solver that gives the user the option to put constraints to the values that can be given

to the parameters that are being calibrated. In this particular case, this feature was very helpful as most of the parameters bear a physical meaning and thus, cannot be given any value. Here are presented the applied constraints to the seven parameters of the problem:

1. $\mathbf{0} \leq \boldsymbol{f_p} \leq \mathbf{0.035}$, as the quantity of the pilot fuel rarely exceeds 3% of the total fuel energy (11) in dual fuel, low pressure, two-stroke marine engines

2. $\mathbf{0} \leq \boldsymbol{m_p} \leq \mathbf{4}$ and $\mathbf{0} \leq \boldsymbol{m_m} \leq \mathbf{4}$, as this is the usual range of the values used for the form factor of the Wiebe function

3. $\mathbf{0} \leq \boldsymbol{\Delta_{\theta p}} \leq \boldsymbol{EOC} - \boldsymbol{SOC}$ and $\mathbf{0} \leq \boldsymbol{\Delta_{\theta m}} \leq \boldsymbol{EOC} - \boldsymbol{SOC}$, as obviously the combustion duration of the main and even more of the pilot fuel could not be longer than that of the total combustion phenomenon

4. $\boldsymbol{\theta_p} \geq \boldsymbol{Pilot\ Injection\ Timing}\ (\boldsymbol{PIT})$, as it is certain that the pilot fuel will start burning after its injection

5. If pilot injection happens after the calculated start of combustion (**IF** $\boldsymbol{SOC} < \boldsymbol{PIT}$) it means that pre-ignition of the main fuel has occurred and so, the angle at the start of main fuel combustion is given the value of the total SOC angle $\boldsymbol{\theta_m} = \boldsymbol{SOC}$. Moreover, the pilot fuel is limited to ignite as following: $\boldsymbol{\theta_p} \leq \boldsymbol{PIT} + \boldsymbol{\Delta_{\theta p}} + \mathbf{5}$, where 5 is an excess estimate of the ignition delay that is used just to limit the range of values checked by the function for the parameter θ_p.

6. If pilot injection happens before the calculated start of combustion (**IF** $\boldsymbol{SOC} > \boldsymbol{PIT}$) it was assumed that the ignition starts with the burning of the pilot fuel $\boldsymbol{\theta_p} = \boldsymbol{SOC}$. Also, in this case the main fuel was constrained to start burning after the pilot fuel ignites and before its combustion is complete:

$$\boldsymbol{\theta_p} + \mathbf{0.0001} \cdot \boldsymbol{\Delta_{\theta p}} \leq \boldsymbol{\theta_m} \leq \boldsymbol{\theta_p} + \mathbf{0.999} \cdot \boldsymbol{\Delta_{\theta p}}$$

- Finally, in order to start the optimization process, the function requires an initial value to be determined for each parameter. These values were selected to be reasonable and close to the expected ones in order to give the function an accurate starting point:

  - m_{p0} = 0.1 (typical value for Diesel combustion)

- m_{m0} = 3 (typical value for Otto combustion)
- f_{p0} = 0.01
- θ_{p0} = PIT + 0.25
- θ_{m0} = SOC + 2.5
- $\Delta\theta_{p0}$ = 0.15 · (EOC-SOC) (The pilot fuel combustion duration is a small proportion of the total)
- $\Delta\theta_{m0}$ = EOC - SOC - 2.5

➢ With the constraints and initial values having been settled, the solver calculated the seven parameters that minimize the SSE. So, at that stage, it had to be checked whether with their use the Wiebe function would make an accurate prediction. The evaluation was made firstly by ensuring that the sums of squared errors of both the burn rate and burn fraction predictions were sufficiently low. Apart from this, the prediction was also checked visually by plotting both calibration and calculated data in the same graph as shown in the following figure.

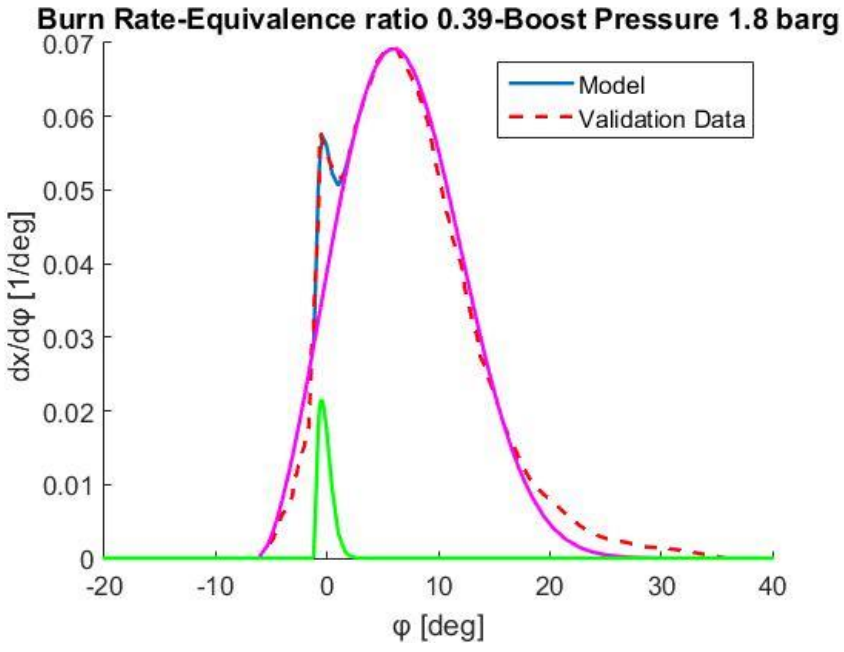

Figure 18: Fitting of Heat Release Curve with Double Wiebe function

The procedure described above was followed for all the heat release curves of all the five sets of diagrams of the calibration data. The achieved fitting was considered satisfactory in all cases. Demonstratively, are presented the results of the fitting with blue lines against the red, dashed lines of the calibration data for the group of diagrams that depict the Heat Release for engine load variation:

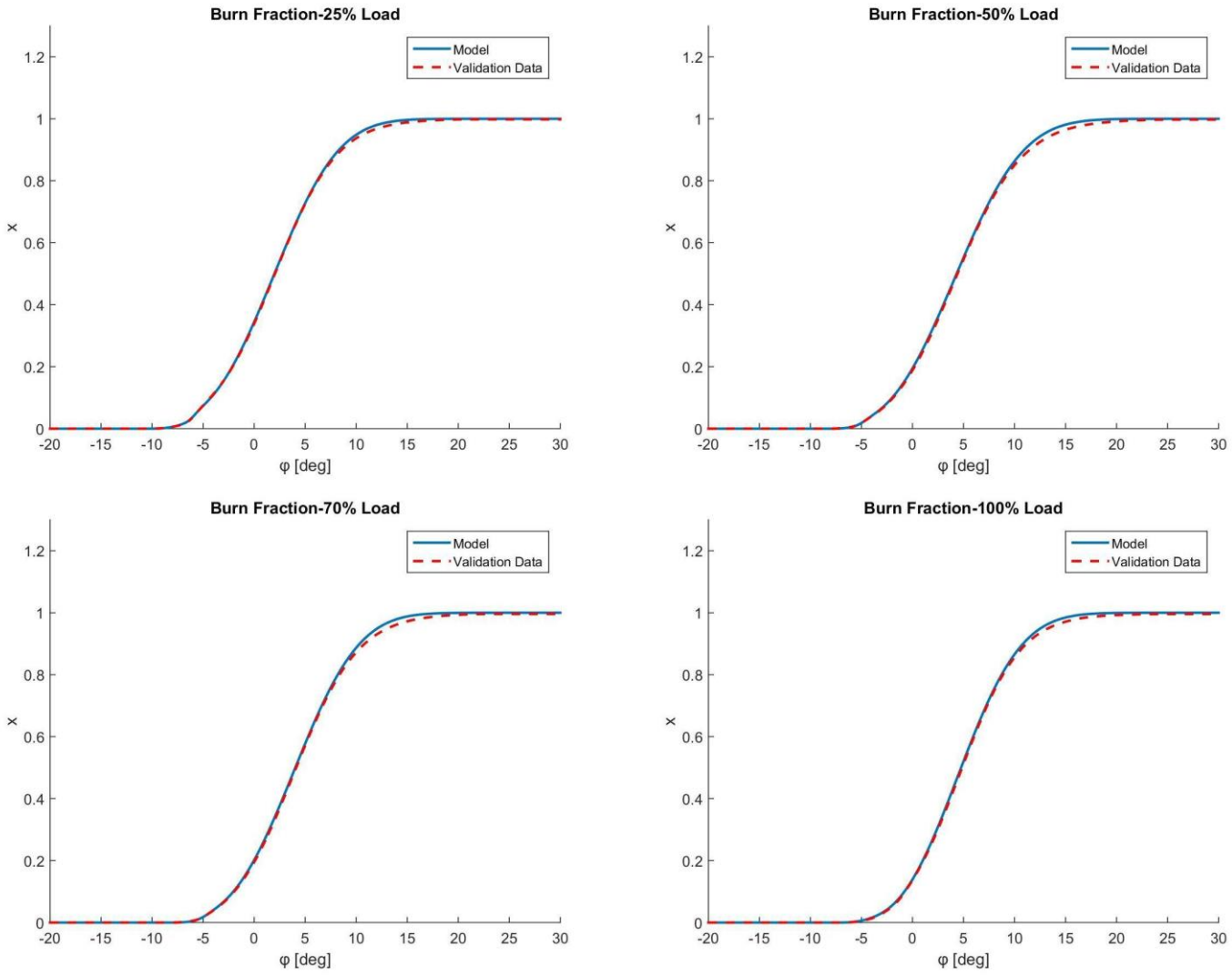

Figure 19: Burn Fraction fitting results (blue) against calibration (red dashed) curves

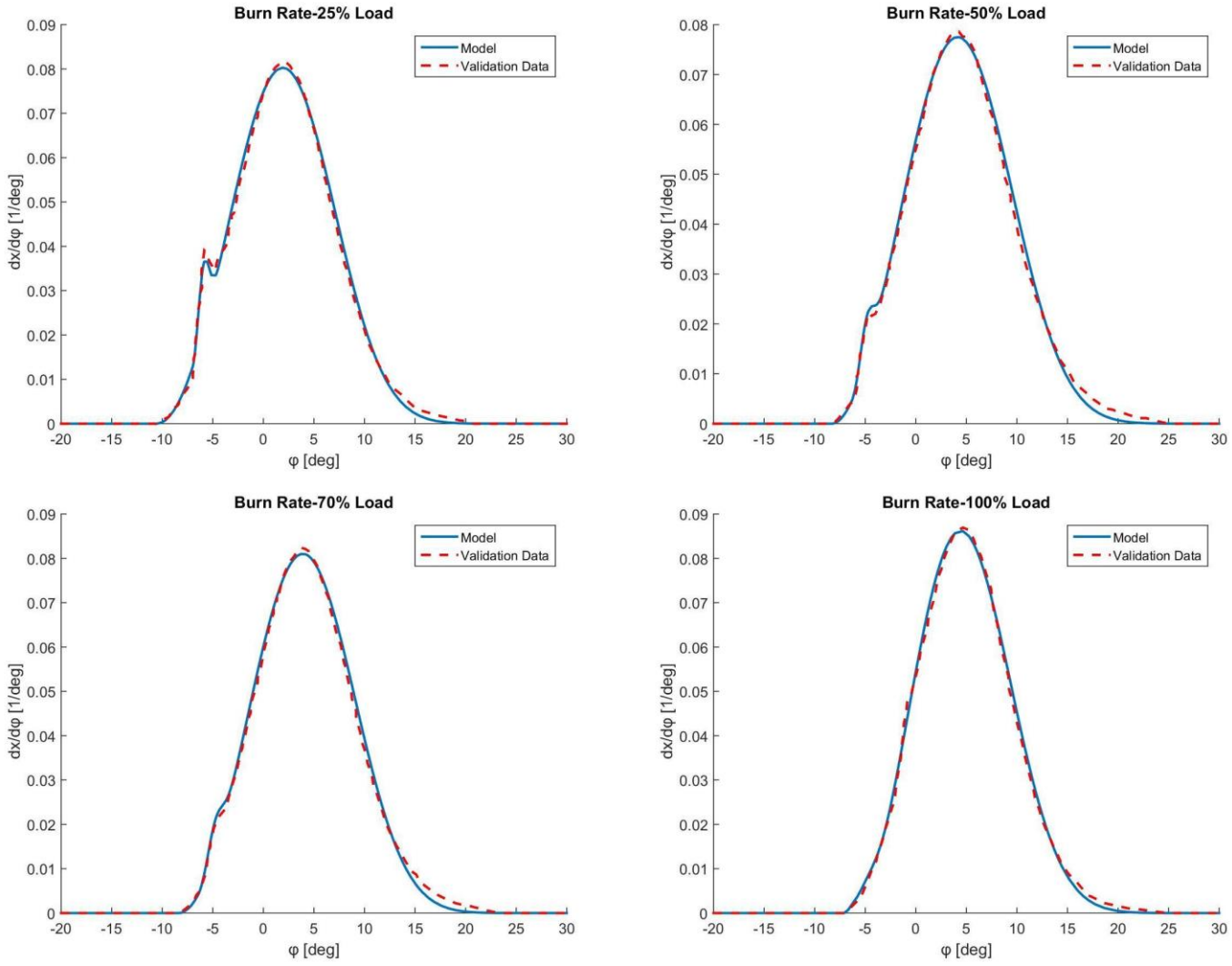

Figure 20: Burn Rate fitting results (blue) against calibration curves (red dashed)

- The last and most important step of the fitting was to produce functions that demonstrate how each Wiebe parameter (f_p, $\Delta\theta_p$, $\Delta\theta_m$, θ_{p0}, θ_{m0}, m_p, m_m) changes with the variation of one of the combustion parameters (load, equivalence ratio, PIT, engine speed, EVC).

  For this reason, after achieving the fitting of a group of curves that correspond to the variation of a combustion parameter, the calculated values of each Wiebe parameter

were collected and then approximated sufficiently by a (first-fifth degree) polynomial function of the particular combustion parameter.

For example, concerning the variation in equivalence ratio the main fuel combustion duration was estimated as is shown below:

Table 3: Main Fuel Combustion Duration Variation against equivalence ratio variation

Overall Equivalence Ratio (φ)	*$\Delta\vartheta_m$ [deg]*
0.33	*44.06*
0.36	*38.51*
0.37	*34.95*
0.39	*30.71*
0.42	*26.26*
0.46	*22.28*

This relationship was described by the second order polynomial:

$$\Delta\theta_m(\varphi) = 741.87 \cdot \varphi^2 - 759.98 \cdot \varphi + 214.75 \quad (3\text{-}5)$$

, which stands for the following graph:

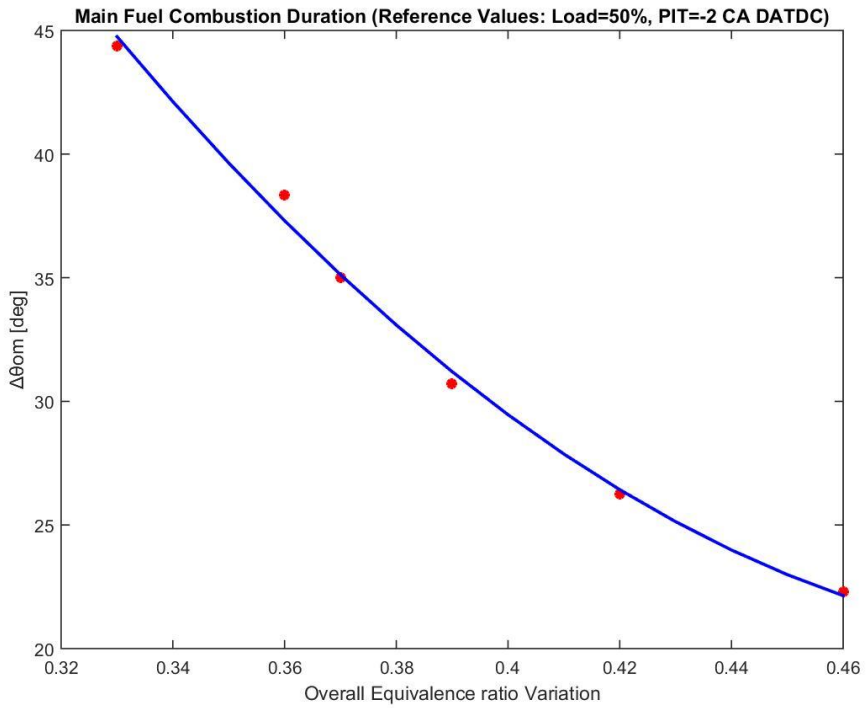

Figure 21: Main Fuel Combustion Duration variation as a function of equivalence ratio

In cases where the produced polynomial estimated values out of the constraint range of the corresponding parameter, its "weak-predictive" part was replaced by a linear one. For instance, as indicated with magenta color in the following graph, the initial m_p function of Pilot Injection Timing produced negative values for the parameter in a 3 degree range. So, this part of the function was replaced by a line.

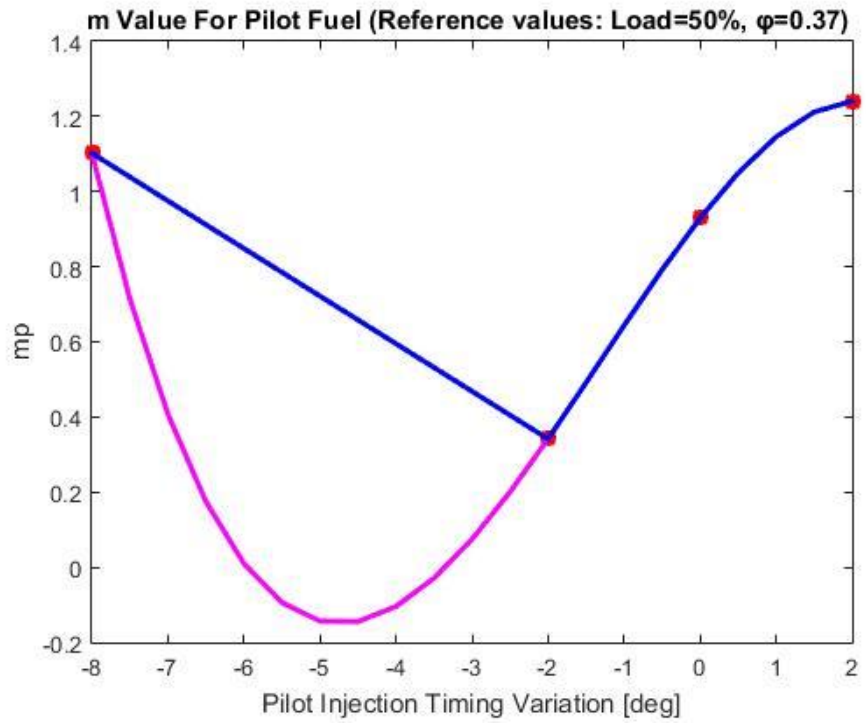

Figure 22: Pilot Fuel form factor variation as a function of PIT

So, by the end of the fitting process seven groups of functions, one for each Wiebe parameter, had been acquired. Each of these groups contained five equations describing the variation of the respective parameter as a function of each of the five combustion parameters alone:

$$i\,(Load) = f_{Li}(Load)$$

$$i\,(\varphi) = f_{\varphi i}(\varphi)$$

$$i\,(PIT) = f_{PITi}(PIT)$$

$$i\,(Engine\ Speed) = f_{ESi}(Engine\ Speed) \qquad (3\text{-}6)$$

$$i\,(EVC) = f_{EVCi}(EVC)$$

$$,where \quad i = m_p, m_m, f_p, \theta_p, \theta_m, \Delta\theta_p, \Delta\theta_m$$

3.2 Model Development

In the previous chapter, the fitting process was described which resulted in the production of seven groups of functions representing the relationship between the Wiebe Parameters and each of the combustion parameters separately (Equation (3-6)).

The goal of the present work, as stated in previous chapters, was to create a combustion model for the operation of a dual fuel engine. In other words, the developed model is expected to be able to receive as input any combination of the combustion parameters' values and provide as output a prediction for the Combustion Heat Release.

So, at this point, in order to complete the development of the model, it was required to find a way of combining the five equations of each wiebe parameter and produce one equation that predicts its value as a function of all five combustion variables. In short, the intention in this paragraph is to find a way to unite the equations of Equation (3-6), Ch.3 in only one multivariable function:

$$i\ (Load, \varphi, PIT, Engine\ Speed, EVC) = F_i(Load, \varphi, PIT, Engine\ Speed, EVC)$$

$$, where \quad i = m_p, m_m, f_p, \theta_p, \theta_m, \Delta\theta_p, \Delta\theta_m \tag{3-7}$$

3.2.1 Regression Analysis

The tool that was utilized to solve the mathematical problem that was presented above is a method of statistical modelling called "Regression Analysis" (28). This term refers to a set of statistical processes that contribute to the estimation of the relationships between a dependent variable (often called the 'outcome variable') and one or more independent variables (often called 'predictors', 'covariates', or 'features') in a fixed data set. This method is widely used for prediction and forecasting, where its use has substantial overlap with the field of machine learning.

Regression Analysis provides a way to estimate the conditional expectation of the dependent variable when the independent variables take on a given set of values. This is achieved by finding the curve that fits better the data according to a specific mathematical criterion. If this curve is a linear one then the procedure is called "Linear Regression" otherwise we have "Non-Linear Regression".

A regression model always consists of the following components:

- The unknown parameters, usually denoted as a scalar or vector β.
- The independent variables, which are observed in data and are usually denoted as a vector X_i (where i denotes a row of data).
- The dependent variable, which are observed in data and usually denoted using the scalar Yi.

Most Regression models propose that Y_i is a function of X_i and β with e_i representing an error term that may stand in for un-modeled determinants of Yi or random statistical noise:

$$Y_i = f(X_i, \beta) + e_i$$

$$, where\ f\ is\ a\ linear\ (linear\ regression)\ or\ a\ non-linear\ (non-linear\ regression)\ function \quad (3\text{-}8)$$

When it comes to evaluating the fitting of the data, achieved by the function that regression analysis generated, several mathematical criteria are usually being used. Here are presented three of them that are the most commonly utilized and also employed in the present work:

1. ***"Coefficient of determination" R^2***: In statistics the coefficient of determination or "R squared" depicts the proportion of the variance in the dependent variable that is predictable from the independent variables (29). Otherwise stated, it provides a measure of how well observed outcomes are replicated by a model, based on the proportion of total variation of outcomes explained by the model. The mathematical definition of its value is given below:

$$R^2 = 1 - \frac{\sum_i (y_i - f_i)^2}{\sum_i (y_i - \bar{y})^2}$$

$$, where\ y_i\ are\ the\ observed\ dependent\ values\ of\ the\ data\ set \quad (3\text{-}9)$$
$$f_i\ are\ the\ corresponding\ predicted\ by\ the\ model\ dependent\ values$$
$$and\ \ \bar{y} = \frac{1}{n}\sum_{1=1}^{n} y_i\ \ , the\ mean\ value\ of\ the\ n\ observations$$

R-squared can take values between 0 and 1, with 1 indicating that regression predicts perfectly the data and 0 that none of the data points fall within the results of the regression curve. The coefficient of determination could also take a negative value

which would mean that the produced model is a rather poor fit of the data and that the data's mean value would make a better one.

2. ***"Adjusted Coefficient of determination"*** R_{adj}^2: Adjusted R-squared (29) is an adjustment for the Coefficient of Determination that takes into account the number of variables in a data set. That is because every time a data point is added in regression analysis, R^2 increases. Therefore, the more points added, the better the regression will seem to "fit" the data even if these points are insignificant, meaning that they do not fit the model. On the other hand, the adjusted R-squared increases only when the increase in R^2 is more than one would expect to see by chance. Adjusted Coefficient of Determination is defined as:

$$R_{adj}^2 = 1 - (1 - R^2) \cdot \frac{n-1}{n-p-1} \tag{3-10}$$

$, where\ p\ is\ the\ total\ number\ of\ explanatory\ variables\ in\ the\ model\ and\ n\ the\ number\ of\ observations$

The range of possible values for the adjusted coefficient of determination is also from 0 to 1. The coefficient could take negative values as well, in case there are too many predictors chasing too little information. Generally, its value will always be less than or equal to that of R squared.

3. ***"Root Mean Square Error" RMSE***: The RMSE or root-mean-square deviation (RMSD) represents the square root of the variance, or "standard deviation", of the residuals, meaning the differences between predicted and observed values (30). RMSE is the square root of the average of squared errors. The effect of each error on RMSE is proportional to the size of the squared error thus, larger errors have a disproportionately large effect on RMSE. Its mathematical definition is the following:

$$RMSE = \sqrt{\frac{\sum_{i=1}^{n}(y_i - f_i)^2}{n}} \tag{3-11}$$

$, where\ y_i\ are\ the\ observed\ dependent\ values\ of\ the\ data\ set\ f_i\ are\ the\ corresponding\ predicted\ by\ the\ model\ dependent\ values\ and\ n\ the\ number\ of\ observations$

RMSE is always non-negative, and a value of 0 would indicate a perfect fit to the data. In general, a lower RMSE is better than a higher one and it is measured with the same units that the dependent variable is measured. Commonly, when someone is interested in evaluating the prediction ability of a model, the RMSE is considered the best criterion to be used.

3.2.2 Linear Regression Application

In the first attempt that was made to apply regression analysis to the fitting data, linear regression was used as it is the simplest form of the method. In Regression analysis, function (23) is a linear one and takes the form:

$$Y = X \cdot \beta \rightarrow$$

$$\begin{pmatrix} y_1 \\ y_2 \\ \vdots \\ y_n \end{pmatrix} = \begin{pmatrix} 1 & x_{11} & \dots & x_{1p} \\ 1 & x_{21} & \dots & x_{2p} \\ \vdots & \vdots & \ddots & \vdots \\ 1 & x_{n1} & \dots & x_{np} \end{pmatrix} \cdot \begin{pmatrix} \beta_0 \\ \beta_1 \\ \beta_2 \\ \vdots \\ \beta_p \end{pmatrix} \quad (3\text{-}12)$$

$$, where\ p\ is\ the\ number\ of\ predictor\ variables \\ and\ n\ the\ number\ of\ observations$$

Matlab offers a special tool for multiple linear regression applications. This tool is a function that receives as input parameters the vector Y_n of the observed dependent data and the table $X_{n(p+1)}$ of the observed independent data and returns a vector β_{p+1} of coefficient estimates for a multiple linear regression of the responses in vector Y_n on the predictors in matrix $X_{n(p+1)}$ (31).

In this case, linear regression had to be applied seven times, one for each parameter of the Wiebe function, with the number of predictor variables been taken equal to the number of combustion parameters p=5. So, in order to make use of the Matlab function, vector Y_n and table $X_{n(p+1)}$ should firstly be created for each of the seven parameters:

- Concerning the outcome vector Y_n, it was created by running the single variable functions (Equation (3-6)) for a range of values of their independent variables and then, merging their results in one vector. This range was the same in all seven cases and it was the following:
    - Load: [25:5:100]
    - Overall Equivalence Ratio: [0.33:0.01:0.46]
    - PIT: [-8:0.5:2]
    - Engine Speed: [99:0.1:123.4]
    - EVC: [248:1:272]

The number of observations resulting by these ranges was equal to n=321.

- When it comes to the determination of the predictors' table, it has n number of rows that correspond to each of the n outcomes (y_n). Also, the first element of each row is always equal to 1. The rest of the row elements are filled with the values of the combustion parameters (x_{i1}-x_{ip}) that produce the equivalent outcome for the dependent variable (y_n). The elements of the predictor table are taken equal to the ones (1) provided by the validation data. For example, the diagrams that relate to equivalence ratio variation are produced for the following values of the rest of the combustion parameters:

Table 4: Rest Combustion parameter values for overall equivalence ratio variation

φ	*Load [%]*	*PIT [deg ATDC]*	*Engine Speed [rpm]*	*EVC [deg ATDC]*
0.33	*50*	*-2.0*	*99*	*266*
0.36	*50*	*-2.0*	*99*	*266*
0.37	*50*	*-2.0*	*99*	*266*
0.39	*50*	*-2.0*	*99*	*266*
0.42	*50*	*-2.0*	*99*	*266*
0.46	*50*	*-2.0*	*99*	*266*

At this point, as some of the combustion details were not presented in the used literature (1) because they were considered confidential, some assumptions had to be made:

a) Concerning the Heat Release diagrams of the validation data for load variation, the angle of pilot injection is not notified. So, after observing the form of the curves it was desided to assume this value being equal to PIT=-8. This is because it was noticed that the pilot fuel combustion at all loads starts at about -7 degrees. Thus, a pilot's injection timing of -8 degrees was concided to be a reasonable assumption, meaning that its ignition delay takes values close to 1 degree of crank angle.

b) Secondly, even though the speed of the engine is provided in most of the results it was decided to make use of a propeller curve that predicts the engine speed as a function of the engine load, since the model is based on a "Fixed-Pitch Propeller" application. The propeller curve was calculated by information taken from the WinGD's General Technical Data (GTD) application run for an "RT-flex50DF" 6-cylinder engine (32). The produced curve was the following:

$$P[kW] = 0.0045 \cdot n^3 \rightarrow n[rmp] = \left(\frac{P[kW]}{0.0045}\right)^{\frac{1}{3}} \quad (3\text{-}13)$$

This propeller curve was found that fits well the data and provides correct engine speed values for an engine output at MCR taken from the GTD application equal to P_{MCR} = 8640 kW.

Before putting these data into the programming regression tool, a modification was made to the input data. Due to the fact that the smallest PIT angle that was used to the model was equal to -8 degrees, 9 degrees were added to all PIT angles in order to avoid having negative and zero values that may cause problems in the produced functions.

Subsequently, linear regression was applied to all of the parameters. The produced linear functions were the following:

$$\begin{aligned}
m_p &= 1.90 - 0.012 \cdot L + 19.66 \cdot \varphi - 0.054 \cdot (PIT + 9) + 0.0085 \cdot ES - 0.018 \cdot EVC \\
m_m &= 5.086 + 0.012 \cdot L - 1.092 \cdot \varphi - 0.02 \cdot (PIT + 9) + 0.006 \cdot ES - 0.016 \cdot EVC \\
f_p &= 0.0057 + 0 \cdot L - 0.0913 \cdot \varphi + 0.0014 \cdot (PIT + 9) - 0.0001 \cdot ES + 0.0002 \cdot EVC \\
\theta_p &= -6.75 + 0.0039 \cdot L + 5.57 \cdot \varphi + 0.98 \cdot (PIT + 9) - 0.0051 \cdot ES - 0.012 \cdot EVC \\
\theta_m &= -48.10 - 0.08 \cdot L + 49.88 \cdot \varphi + 0.17 \cdot (PIT + 9) - 0.19 \cdot ES + 0.17 \cdot EVC \\
\Delta\theta_p &= 22.26 + 0.26 \cdot L - 17.18 \cdot \varphi + 0.19 \cdot (PIT + 9) - 0.21 \cdot ES - 0.021 \cdot EVC \\
\Delta\theta_m &= -1.59 - 0.25 \cdot L, -53.71 \cdot \varphi + 0.41 \cdot (PIT + 9) + 0.13 \cdot ES + 0.21 \cdot EVC
\end{aligned} \quad (3\text{-}14)$$

$, where\ \ L: Engine\ Load, \varphi: Overall\ equivalence\ ratio, PIT: Pilot\ Injection\ Timing, ES: Engine\ Speed, EVC: Exhaust\ Valve\ Closing$

These functions achieved a good fitting according to the three mathematical criteria used as shown in the table:

Table 5: Mathematical Criteria for Linear Regression

Linear Regression Mathematical Criteria			
	R^2	R^2_{adj}	*RMSE*
m_p	*0.6663*	*0.661*	*0.2074*
m_m	*0.5447*	*0.5375*	*0.163*
f_1	*0.7582*	*0.7543*	*0.0019*
ϑ_m *[deg]*	*0.881*	*0.8791*	*0.8615*
ϑ_p *[deg]*	*0.9762*	*0.9758*	*0.2469*
$\Delta\vartheta_p$ *[deg]*	*0.9672*	*0.9666*	*0.5501*
$\Delta\vartheta_m$ *[deg]*	*0.5923*	*0.5858*	*2.3599*

3.2.3 Non-Linear Regression Application

In order to achieve the best possible fit to the data, it was decided to also apply non-linear regression assuming that the equation f of Equation (3-7) would be defined as following:

$$i = b_1 + b_2 \cdot L^{b_3} + b_4 \cdot \varphi^{b_5} + b_6 \cdot (PIT + 9)^{b_7} + b_8 \cdot ES^{b_9} + b_{10} \cdot ES^{b_{11}}$$

$$, where \quad i = m_p, m_m, f_p, \theta_p, \theta_m, \Delta\theta_p, \Delta\theta_m \qquad (20)$$

Concerning non-linear regression applications, plenty of such programming tools are available. The utilized tool (33) receives as input values the vector Y of the observed dependent data, the table X of the predictor data and also the model of the function that the user wants to use to fit the data. The produced output is a vector β of estimated coefficients for the nonlinear regression of the responses in Y on the predictors in X. The coefficients are estimated using iterative least squares estimation, with initial values specified by the user (33).

The input data Y and X were defined exactly as described in the linear regression procedure, with the same assumptions been made about the pilot injection timing at load variation diagrams (-8 crank angle degrees) and the engine speed determination by a propeller curve derived from GTD application data.

For initial values of vector β were used the ones given by the linear regression results. More specifically, coefficients b_i with i = 1, 2, 4, 6, 8, 10 were given values equal to the corresponding ones from the linear regression while the rest b_i initial coefficients were assumed being equal to 1.

The values of the b_i coefficients (Equation (3-15)) of each Wiebe parameter provided by the application of the non-linear regression are given in Table A1 of the appendix.

(Equation (3-15)) achieved a good fitting using the above mentioned coefficients, according to the three mathematical criteria of the table:

Table 6: Mathematical Criteria for Non-Linear Regression

Non-Linear Regression Mathematical Criteria			
	R^2	R^2_{adj}	*RMSE*
m_p	*0.7152*	*0.7107*	*0.1917*
m_m	*0.5795*	*0.5729*	*0.1567*
f_1	*0.8042*	*0.7931*	*0.0018*
ϑ_m *[deg]*	*0.9063*	*0.9048*	*0.7645*
ϑ_p *[deg]*	*0.9767*	*0.9763*	*0.2443*
$\Delta\vartheta_p$ *[deg]*	*0.979*	*0.9787*	*0.4398*
$\Delta\vartheta_m$ *[deg]*	*0.5369*	*0.5296*	*2.8088*

By comparing the values of the above table to the ones of Table 5, it is derived that the non-linear regression results lead to more satisfactory values of the mathematical regression criteria with the single exception of main fuel combustion duration parameter $\Delta\theta_m$.

Thus, it was decided to use the non-linear functions to predict all the Wiebe parameters apart from $\Delta\theta_m$ for which the linear function will be used.

3.2.4 Final form of DF model

In the previous paragraph, was made a detailed description of the method that was followed in order to produce the functions that make up the combustion model that the present work intends to introduce.

After testing the model by comparing its results to the validation data (1), it was realised that at 60% of the tests the model achieved a very good fit, at 25% the results were not as good but still acceptable and there was also a 15% of the results that was evaluated as having a bad fitting.

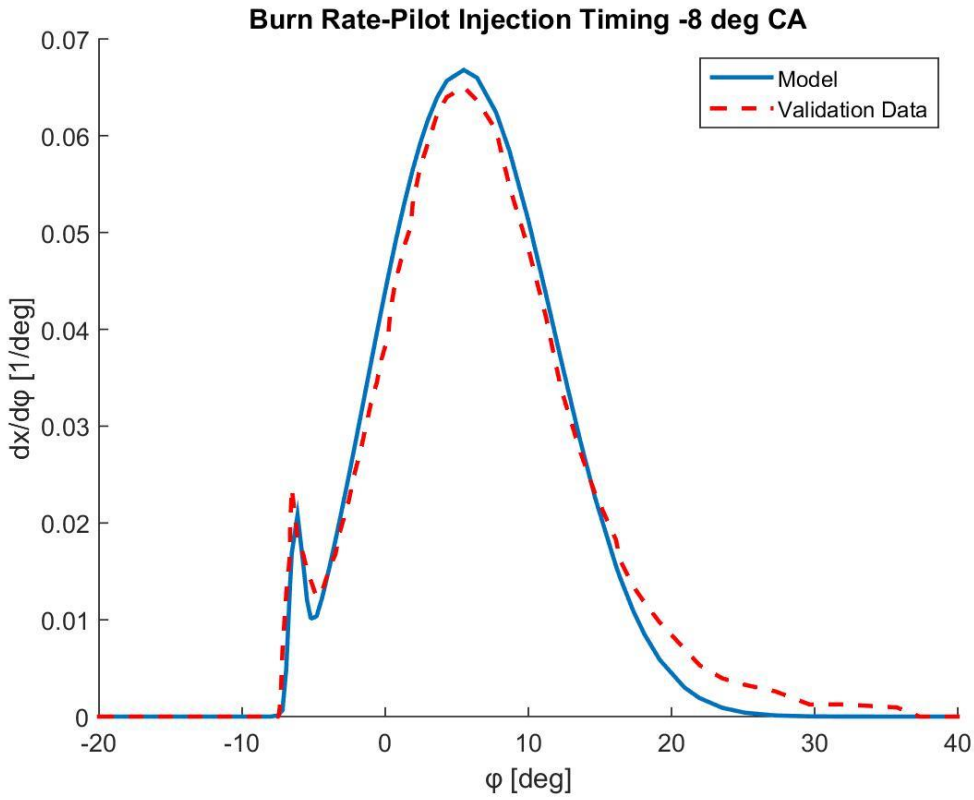

Figure 23: Example of good model fit

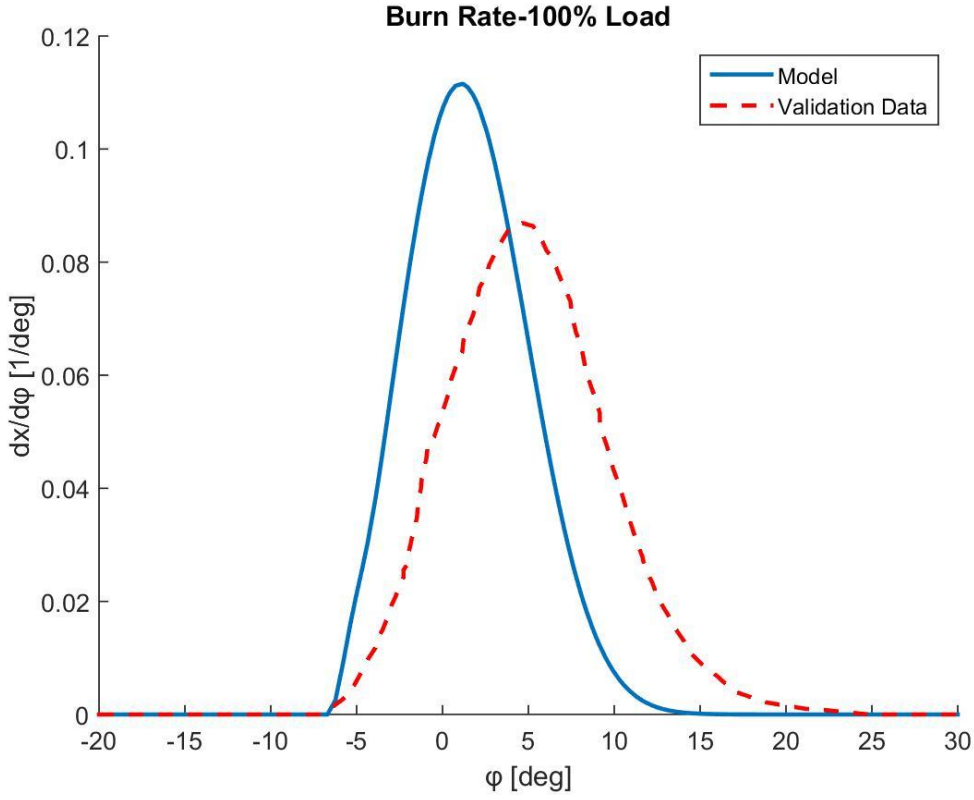

Figure 24: Example of bad model fit

In most of the cases of bad model fit, the parameter that caused the deviation was the combustion duration of main fuel $\Delta\theta_m$. This is because this parameter was approached the least adequately by the regression process as indicated by the mathematical criteria shown in Tables 5 and 6, Ch.3.

Upon further investigation it was found that this parameter also showed the greatest variance in its values that were estimated by the first fitting procedure. This problem could be solved if more diagrams or measured data were available and used in the regression.

Nevertheless, as no other calibration data were available at the moment, in order to enhance the model's reliability, it was decided to make $\Delta\theta_m$ a free parameter set by the user of the model who will chose a value by comparing the model's outcome to his calibration data.

The final combustion model of the dual fuel, two-stroke, low pressure, marine engine that was produced in this diploma thesis is the following:

$$i = b_1 + b_2 \cdot L^{b_3} + b_4 \cdot \varphi^{b_5} + b_6 \cdot (PIT + 9)^{b_7} + b_8 \cdot ES^{b_9} + b_{10} \cdot ES^{b_{11}}$$

$$, where \quad i = m_p, m_m, f_p, \theta_p, \theta_m, \Delta\theta_p \tag{3-15}$$

$$\Delta\theta_m: \text{Free Parameter}$$

$$b_1 - b_{11} : \text{values as defined in Table A1}$$

4 Chapter: Results

In this chapter, the results produced by the model are presented and divided in two groups.

The first contains the variation of the double-Wiebe model parameters as a function of the combustion parameters whereas, the second group includes the validation of the developed model.

4.1 Double-Wiebe Parameters Variation

After fitting the double-Wiebe function to the calibration data, a set of equations (Equation (3-6)) was produced for each of the seven function parameters describing its variation in relation with combustion variables change.

It is worthwhile to take a look at these relationships as Wiebe function parameters bear a physical meaning that could prove helpful in terms of better understanding of the dual fuel combustion characteristics.

Seven groups of diagrams were acquired by the fitting process, one for each Wiebe parameter showing its variation as a function of each of the five combustion parameters. It is noted that in this paragraph are presented some of those diagrams followed by comments; based on the observations that were made by examining them, while all of them can be found in the Appendix of the thesis:

4.1.1 Pilot and Main Fuel Characteristic Exponents Variation

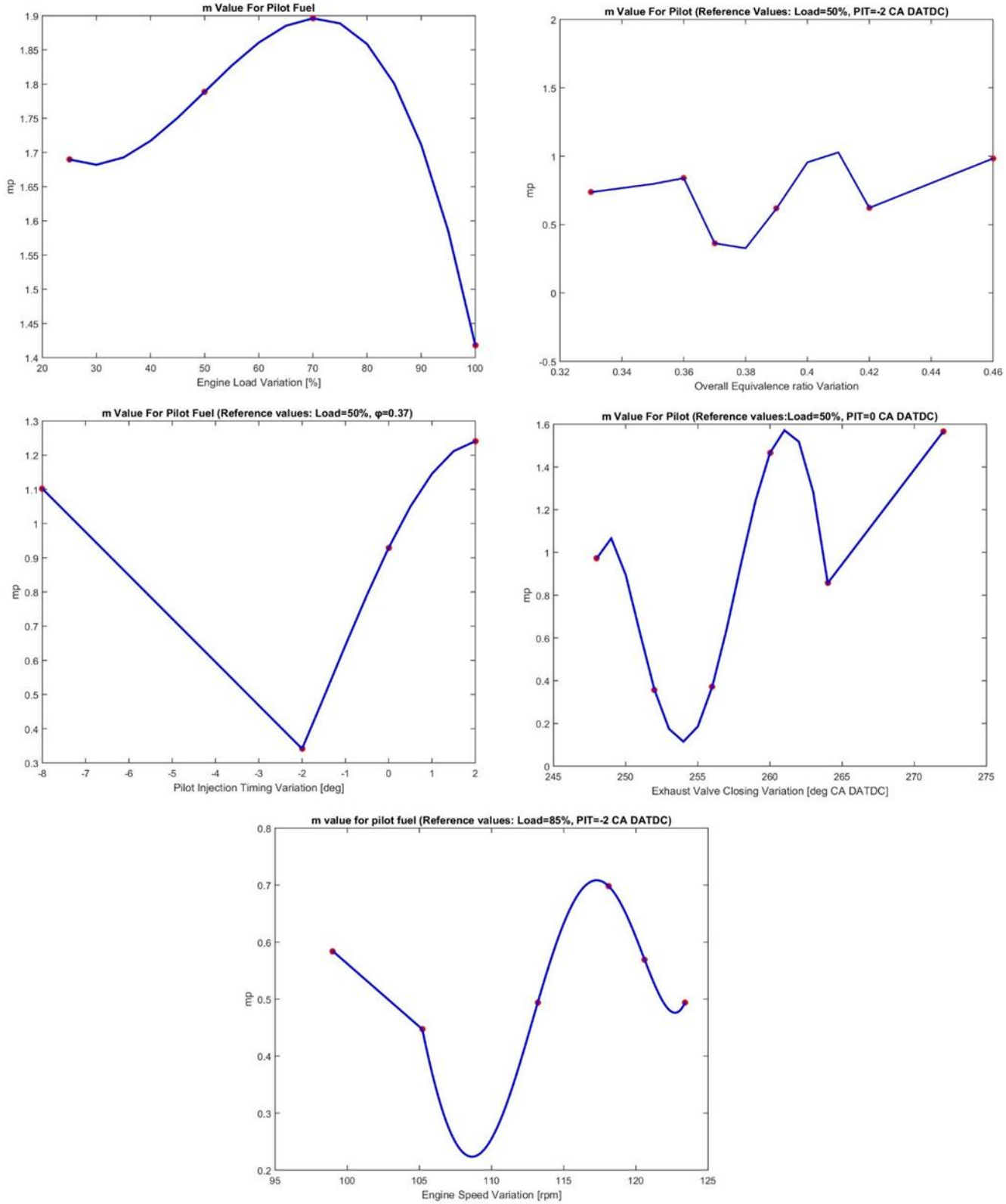

Figure 25: Pilot fuel "form factor" variation

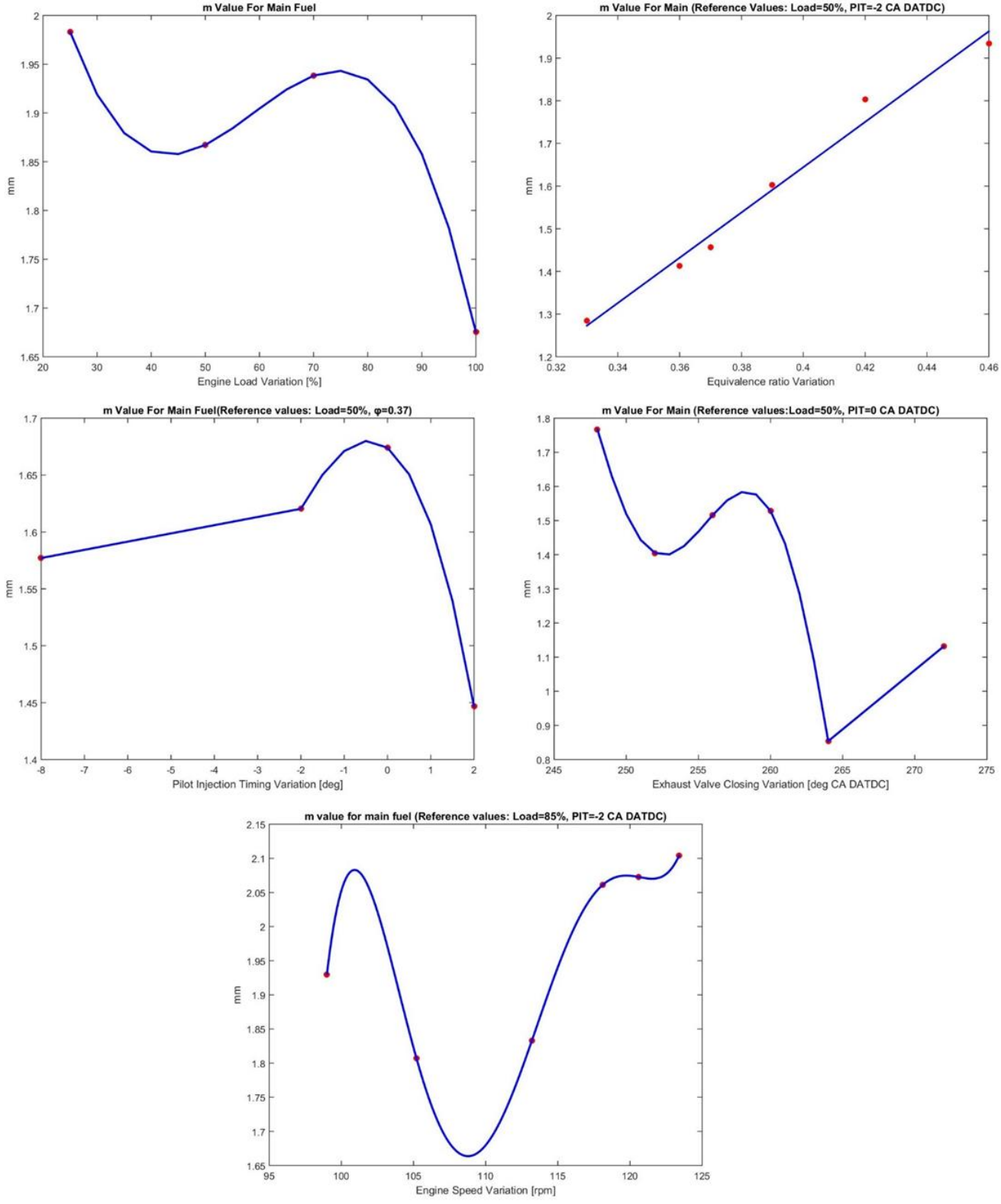

Figure 26: Main fuel "form factor" variation

The variations of pilot and main fuel "Combustion Characteristic Exponents" m_p and m_m are given in Figures 25 and 26 respectively. As explained in Equation (2-9), the "Combustion Characteristic Exponent" determines the time it takes for maximum burn rate to be reached for a given combustion duration. In particular, t_m is an increasing function of m: $t_m = t_d \cdot \left[\frac{m}{-C\cdot(m+1)}\right]^{\frac{1}{m+1}}$

By bearing in mind this relationship and observing closely the two groups of diagrams, these points can be made:

- The combustion characteristic exponents of both pilot and main fuel reduce substantially at high loads (over 70%) which according to Equation (2-9) indicates that the maximum heat release rate is reached faster at high load operation.

- The form factor of main fuel m_m increases linearly with equivalence ratio. This is probably because as the equivalence ratio increases so does the flame front propagation leading to smaller t_m values.

- Also at higher EVC angles, meaning lower effective Compression Ratios (CR), m_m is smaller. This can be reasoned by the fact that lower CR leads to lower flame velocity. As a result, it takes more time to reach the maximum heat release rates.

4.1.2 Pilot Fuel Weighting Factor Variation

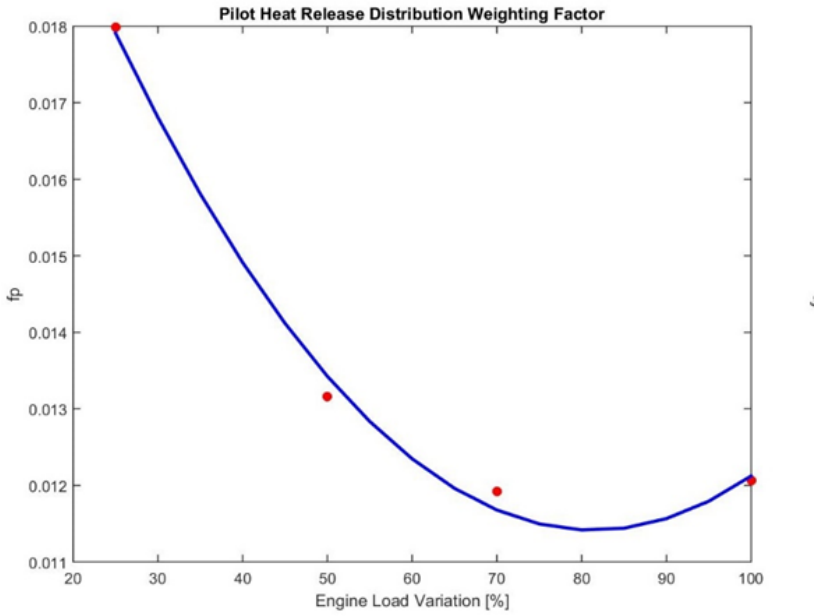

Figure 27: Pilot fuel "weighting factor" variation as a function of Load [%]

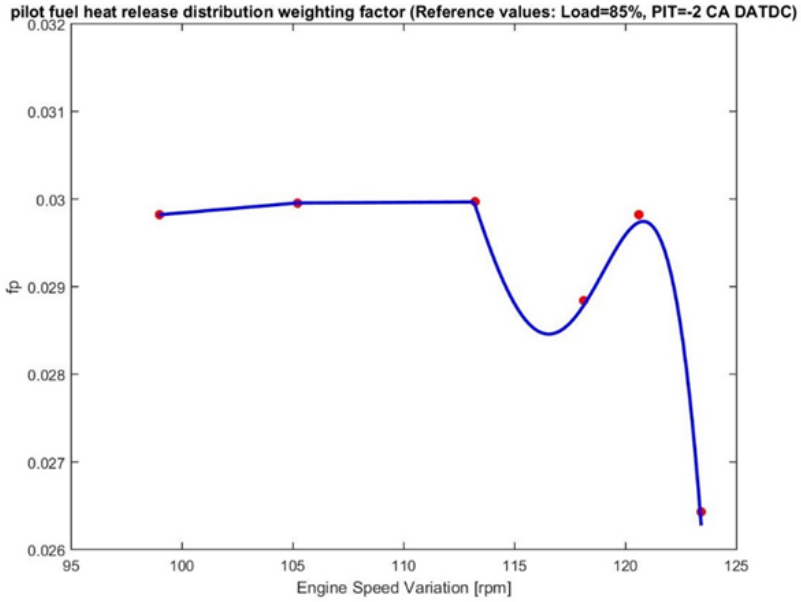

Figure 28: Pilot fuel "weighting factor" variation as a function of engine speed [rpm]

In Figures 27 and 28, the weighting factor of the pilot fuel is distributed against the variation of engine load and speed respectively. Its value seems to reduce when load and speed increase due to the fact that in these cases the high in-cylinder pressure leads to smaller amount of pilot fuel required in order to ignite the fuel-air mixture.

4.1.3 Pilot Fuel Start of Combustion Angle Variation

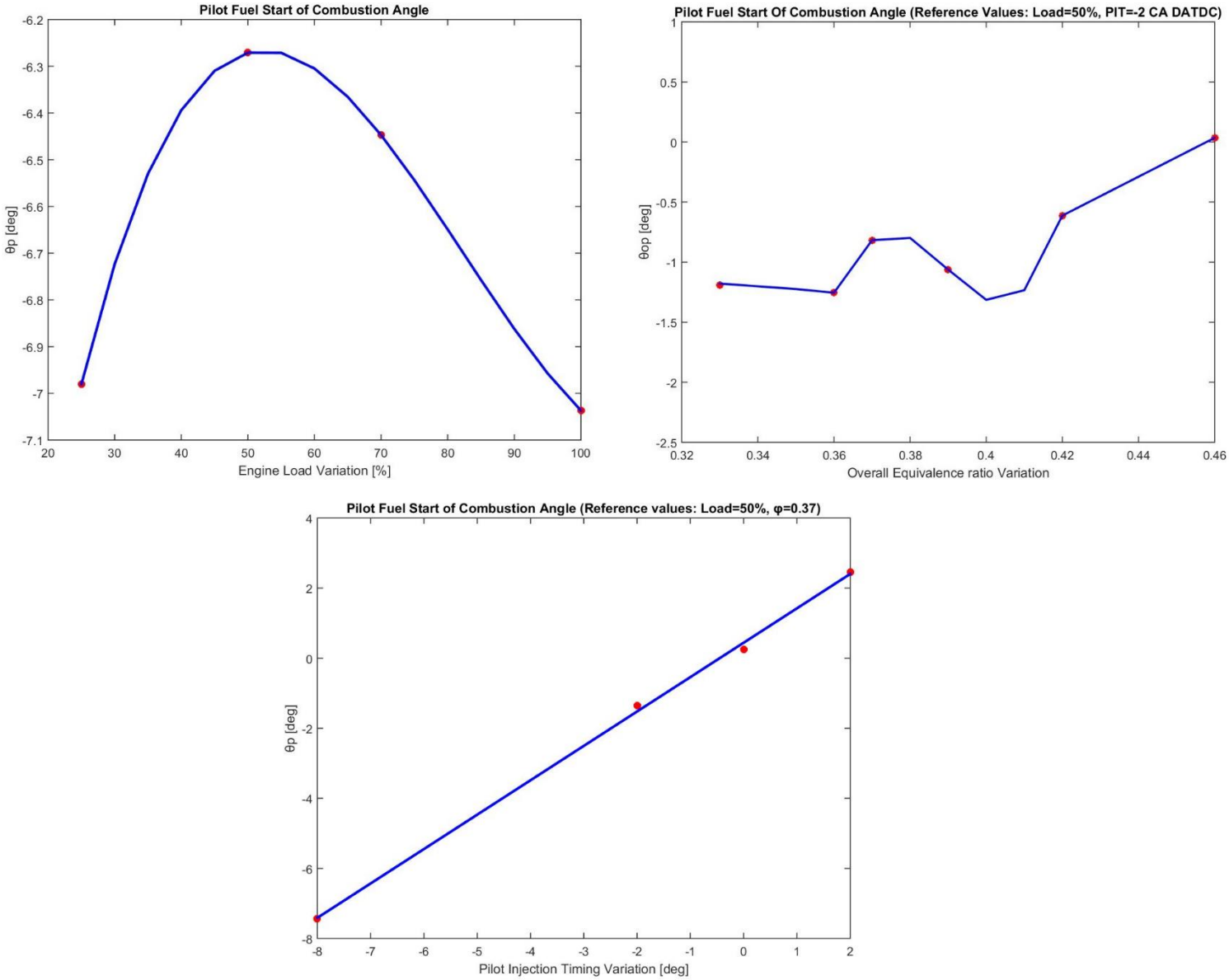

Figure 29: Pilot SOC angle as a function of Load [%], ϕ and PIT [deg]

The variation of start crank angle of pilot fuel combustion is demonstrated in the above figure as a function of load, equivalence ratio and PIT. Observation of this parameter's variation yields the following conclusions regarding pilot fuel's ignition delay:

- When the engine load increases so does the in-cylinder pressure and temperature. Thus, when the pilot is injected the conditions of the cylinder facilitate its ignition to occur faster than in lower load operation. This is depicted in the θ_{op} angle variation with load diagram where the angle significantly drops with the load increase after 50%. Ignition delay is also quite low in 25% load operation. This is probably because the total equivalence ratio at this operation point is relatively low (ϕ=0.37) and so the heat of the combustion chamber can be used to trigger pilot fuel's ignition.

- In the second diagram that corresponds to equivalence ratio variation at low load (50%) the ignition delay of the pilot fuel exhibits an increasing trend. This could be reasoned by the fact that when the air-fuel mixture becomes richer in fuel proportion then it absorbs greater heat amounts making it harder for the pilot fuel to concentrate enough energy for its ignition.

- In the PIT variation diagram the ignition delay is quite low and the pilot fuel seems to ignite soon after it is injected. Just as already explained, the low equivalence ratio conditions allow this immediate ignition.

4.1.4 Main Fuel Start of Combustion Angle Variation

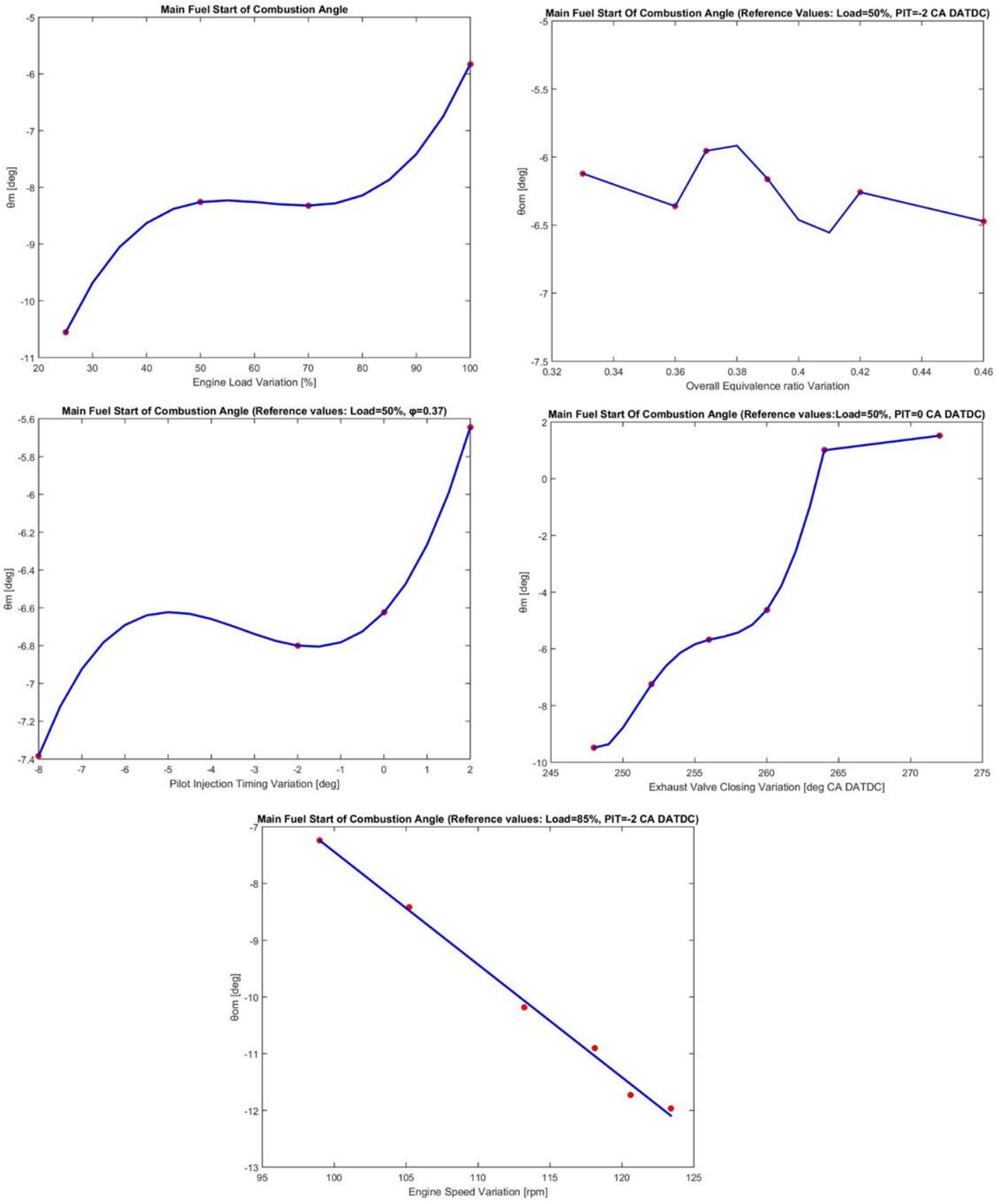

Figure 30: Main SOC angle as a function of the combustion parameters

When it comes to Figure 30 which shows the change in main fuel start combustion angle θ_{om} some noteworthy observations can be made about the cases when pre-ignition occurs. The pre-ignition phenomenon is defined as a spontaneous flame kernel ignition of the main fuel prior to flame front arrival:

- Firstly, as can be also seen in the validation data, pre-ignition takes place for all the spectrum of the equivalence ratio variation tests. However, the phenomenon becomes more pronounced for higher ϕ values when the mixture is richer and the flame propagation is accelerated.

- Moreover, as the injection of pilot fuel is delayed, the in-cylinder conditions become more likely to trigger a self-ignition of the main fuel as in-cylinder temperature and pressure rise. This relationship is displayed in the PIT variation diagram.

- Concerning the reduction of the pre-ignition with the increase of EVC angle it is to be expected as the effective CR drops causing a drop to the unburned zone temperature, which could result in pre-ignition of the main fuel if it became relatively high (1).

- When engine speed is low, the scavenging process is being prolonged and so the cylinder purity increases. Cylinder purity and hence lower gas temperature causes a slow down to the burning velocity and prevents the fuel from self-ignition (1). For this reason, a linear increase in pre-ignition phenomenon is noticed for engine speed increase.

- Even though experiments have shown that the pre-ignition phenomenon becomes more severe with increasing engine load (1), the fitting results show an inverted trend. The reason for this could be the fact that the validation data (blue lines) overpredict pre-ignition at low loads as shown in the following graph in which they are compared against measured data (red dashed lines):

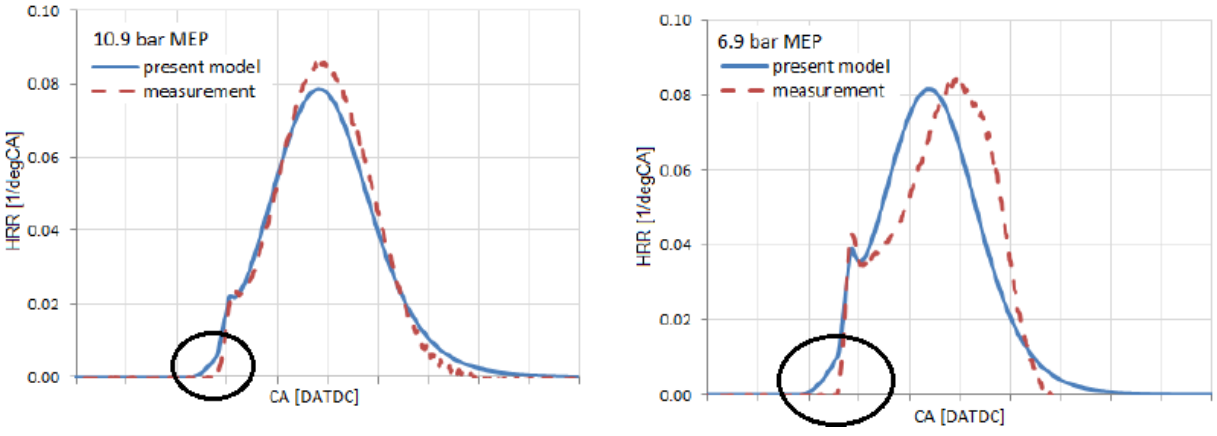

Figure 31: Over prediction of pre-ignition in 25% and 50% load by the validation data (1)

4.1.5 Main Fuel Combustion Duration Variation

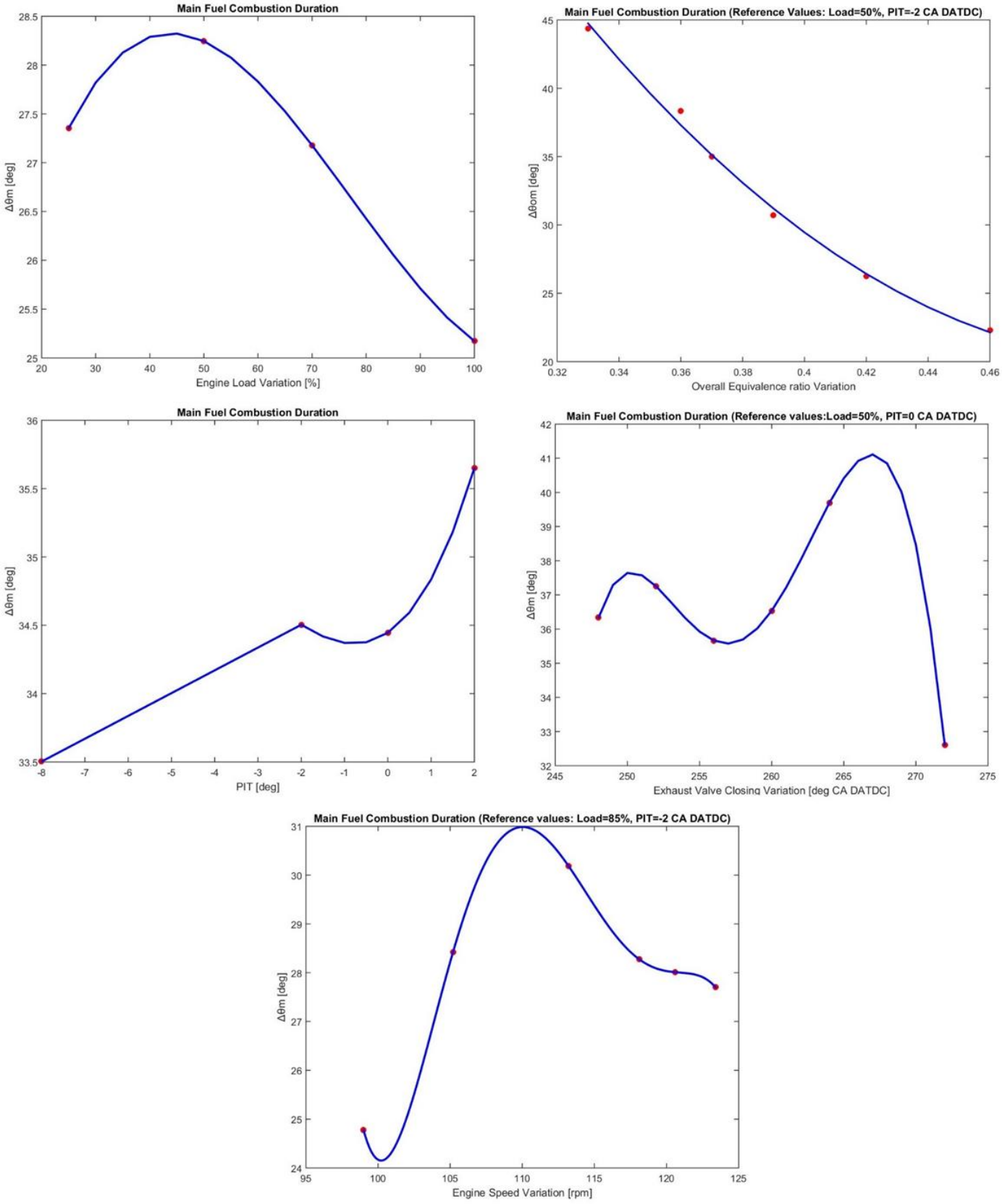

Figure 32: Main Fuel Combustion Duration Variation

In Figure 32 the variation of main fuel combustion duration is presented. The parameter shows the following behavior:

- $\Delta\theta_m$ is reduced with the increase in both load and overall equivalence ratio values. At low load operation, the combustion duration becomes longer because the combustion process is slowed down due to dilution by the large amount of the residual gases (34). Also, at high equivalence ratios the flame front propagation is being accelerated causing the combustion to end sooner.

- Concerning the pilot injection timing, it is observed that the later it occurs, the longer the main fuel combustion lasts. This is probably because as assumed above it is more likely for the main fuel to pre-ignite as the pilot fuel is injected at bigger crank angles and hence its combustion lasts exactly as the overall combustion does.

- Higher EVC angles and hence lower effective CR, cause a slow down to the flame velocity due to the fact that the end-of-compression temperature and pressure decrease and as a result the residual gases increase. This is why the combustion duration becomes higher along with the EVC angle.

- Finally, there is less available time for combustion due to higher engine speed. This is probably an effect of turbulence. As the engine speed increases, so does the turbulence inside the cylinder, leading to a better heat transfer between the burned and unburned zones (35).

4.1.6 Pilot Fuel Combustion Duration Variation

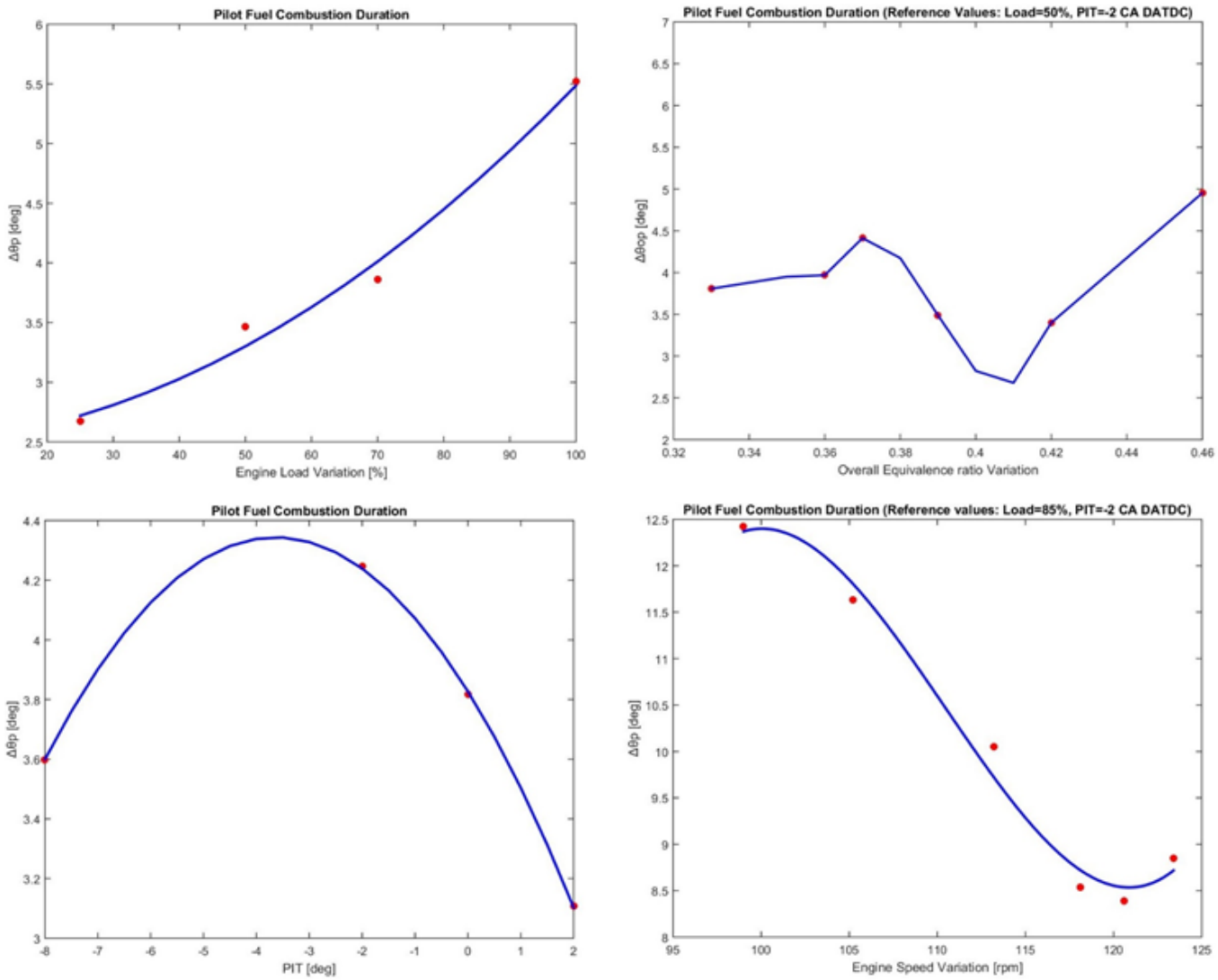

Figure 33: Pilot Fuel Combustion Duration Variation as a function of Load [%], ϕ, PIT [deg] and Engine Speed [rpm]

In Figure 33 the variation of pilot fuel combustion duration is shown. After close observation the below points can be derived:

- As load and equivalence ratio increase, $\Delta\theta_p$ is reduced. A reason that could be assumed for this behavior is that in these situations pre-ignition phenomena get more pronounced, thus when the pilot fuel is injected, the in-cylinder conditions lead to its faster burning. For the same reason as the PIT increases from -2 to +2 CA DATDC, pilot's combustion duration drops.

- Also in pilot fuel combustion, the duration of its burning is reduced with the increase of engine speed. This could as well be reasoned by the high turbulence in-cylinder conditions that lead to better transfer of the heat.

4.2 Model Validation

In this section, the proposed model is validated against the Heat Release curves derived from validation data found in available literature (1).

The validation results are presented in the appendix (Figures A8-A19) in five categories according to the combustion variable variation they correspond to. For each operation point the model is tested on, are given three diagrams. The first diagram depicts the comparison between the predicted (blue solid lines) and the validation (red dashed lines) Burn Fraction S-curves, while the second provides the same comparison between the Burn Rate curves. As for the third graph, it shows the deviation between the predicted and the target burn rate curves accompanied by the value of the mathematical fitting criterio of “Sum of Squared errrors” between the two curves. The smaller is the value of this sum is, the better is the estimation power of the model.

In the following two figures are presented demonstratively the results of the validation for engine load variation (25%, 50%, 70%, and 100%).

Afterwards, are given some comments related to all the validation results (Figures A8-A19).

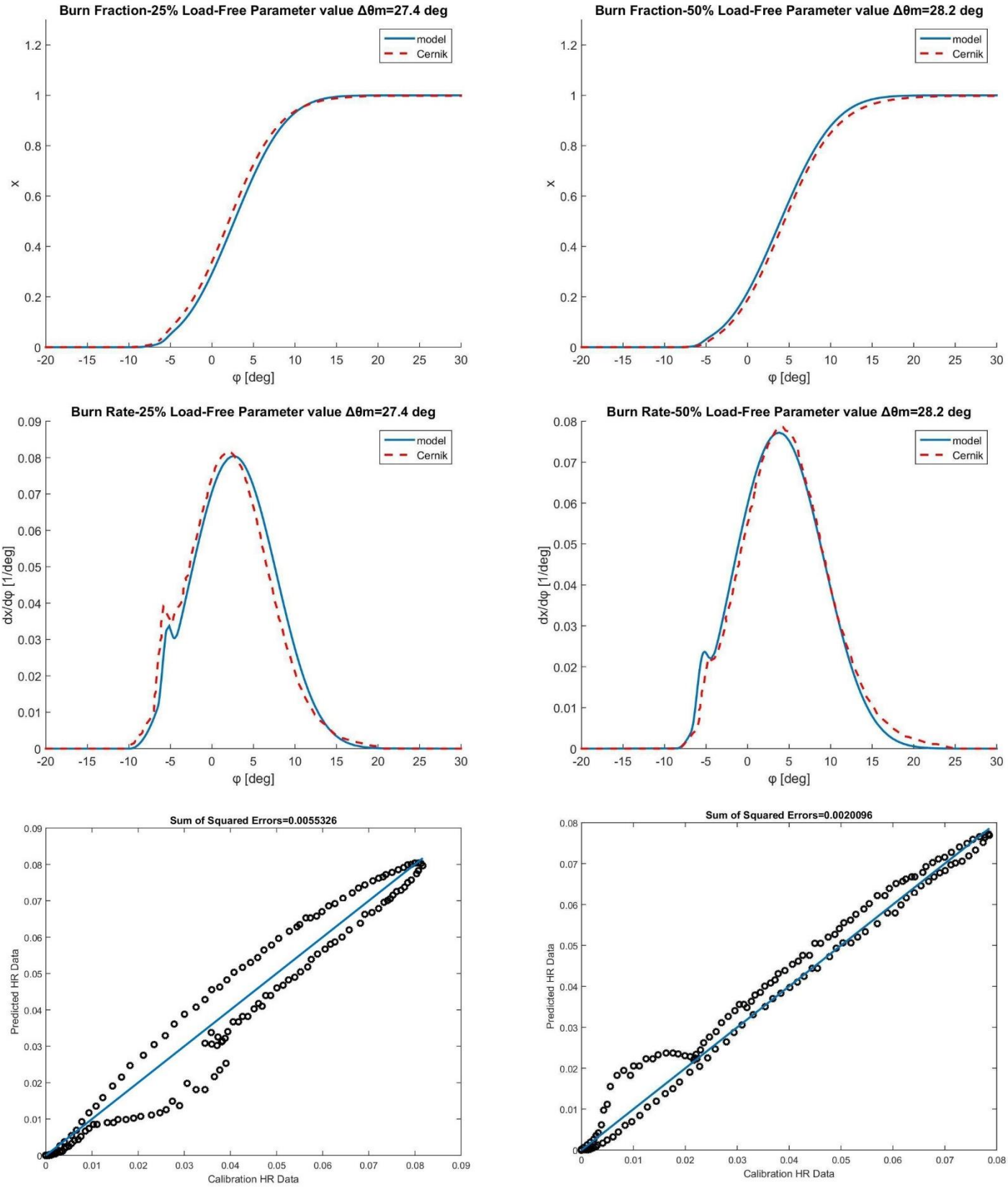

Figure 34: Model Validation at 25% and 50% Engine Load

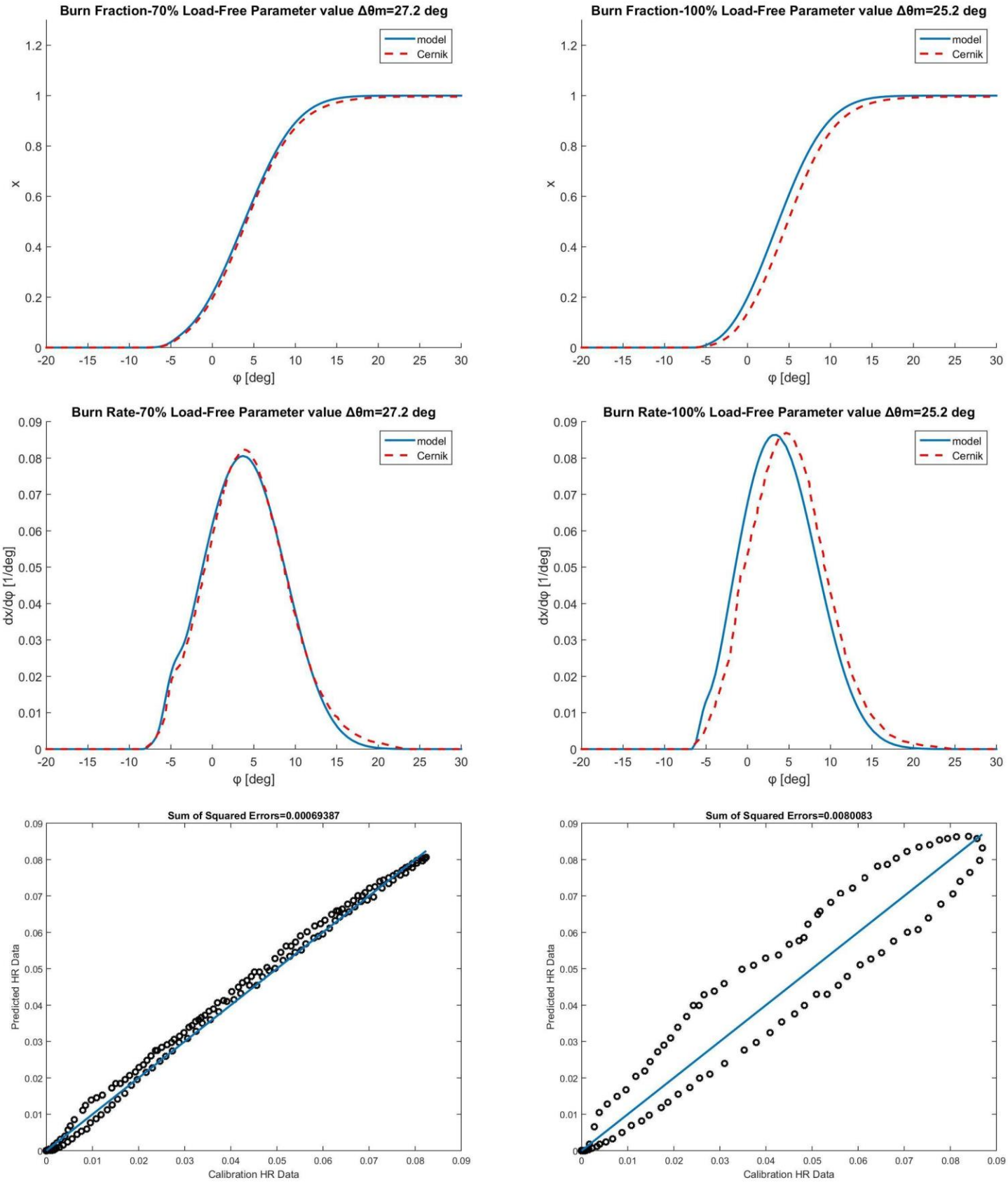

Figure 35: Model Validation at 70% and 100% Engine Load

➢ *Model Validation for Engine Load Variation:*

At all four load points, a good capture of the heat release curve's trend is achieved along with low deviation between the predicted and validation data. At 100% of engine load, an over-prediction of the main fuel start of combustion angle is observed and thus, the model produces an earlier development of the heat release phenomenon than it should.

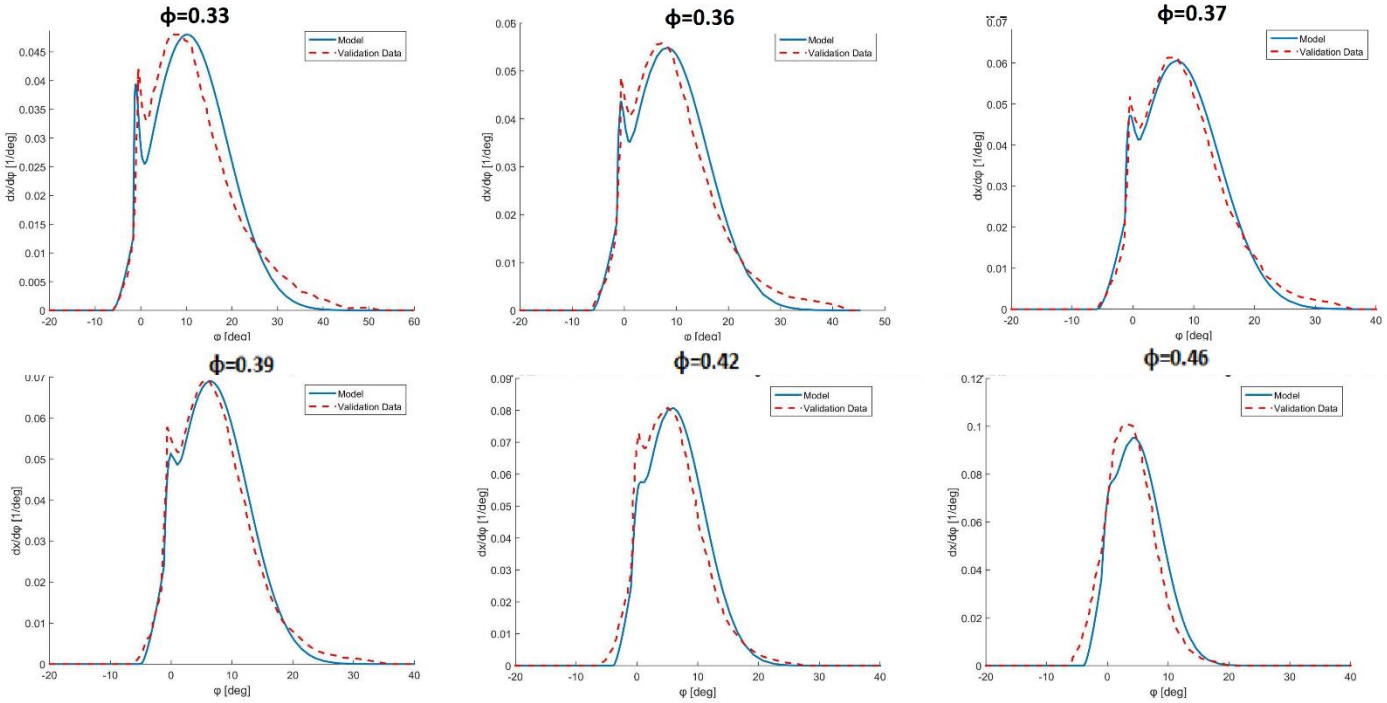

Figure 36: Model (blue lines) validation against validation data (red dashed lines) for ϕ variation

➢ *Model Validation for Overall Equivalence Ratio Variation:*

The predicted Heat Release curves show a good fit to the validation data for equivalence ratio variation as is shown in Figure 36. However, for values of ϕ over 0.39 a late prediction of the main fuel combustion angle can be noticed. Nevertheless, this is not considered to be a problem in terms of model's reliability as in this range of equivalence ratios the validation data do not depict accurately the main fuel ignition. In particular, as shown in the following graphs (1), they seem to over-predict the pre-ignition and thus, the present model is closer to the measurements.

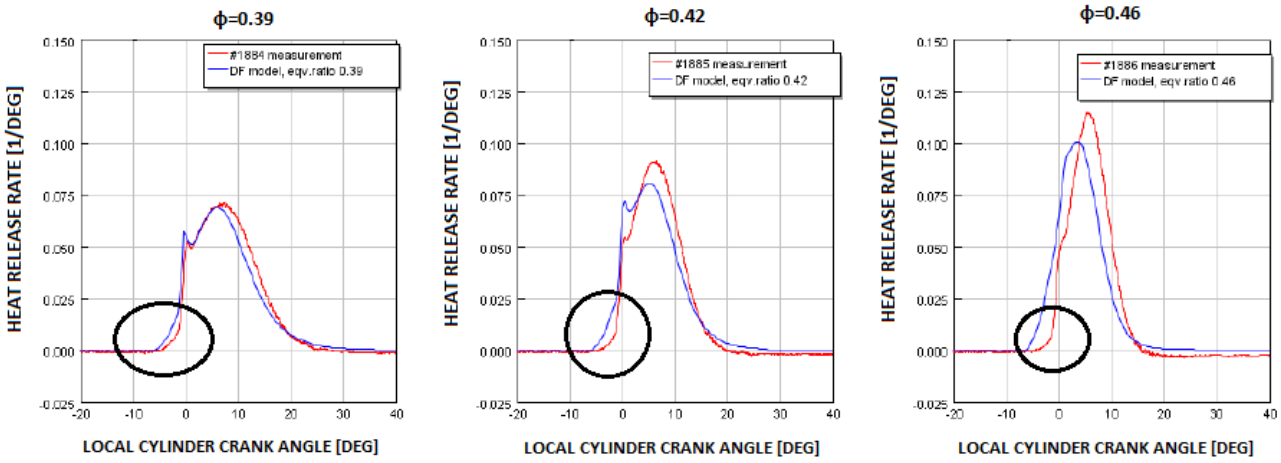

Figure 37: Validation data (blue lines) against measurements (red lines) for ϕ=0.39-0.46 (1)

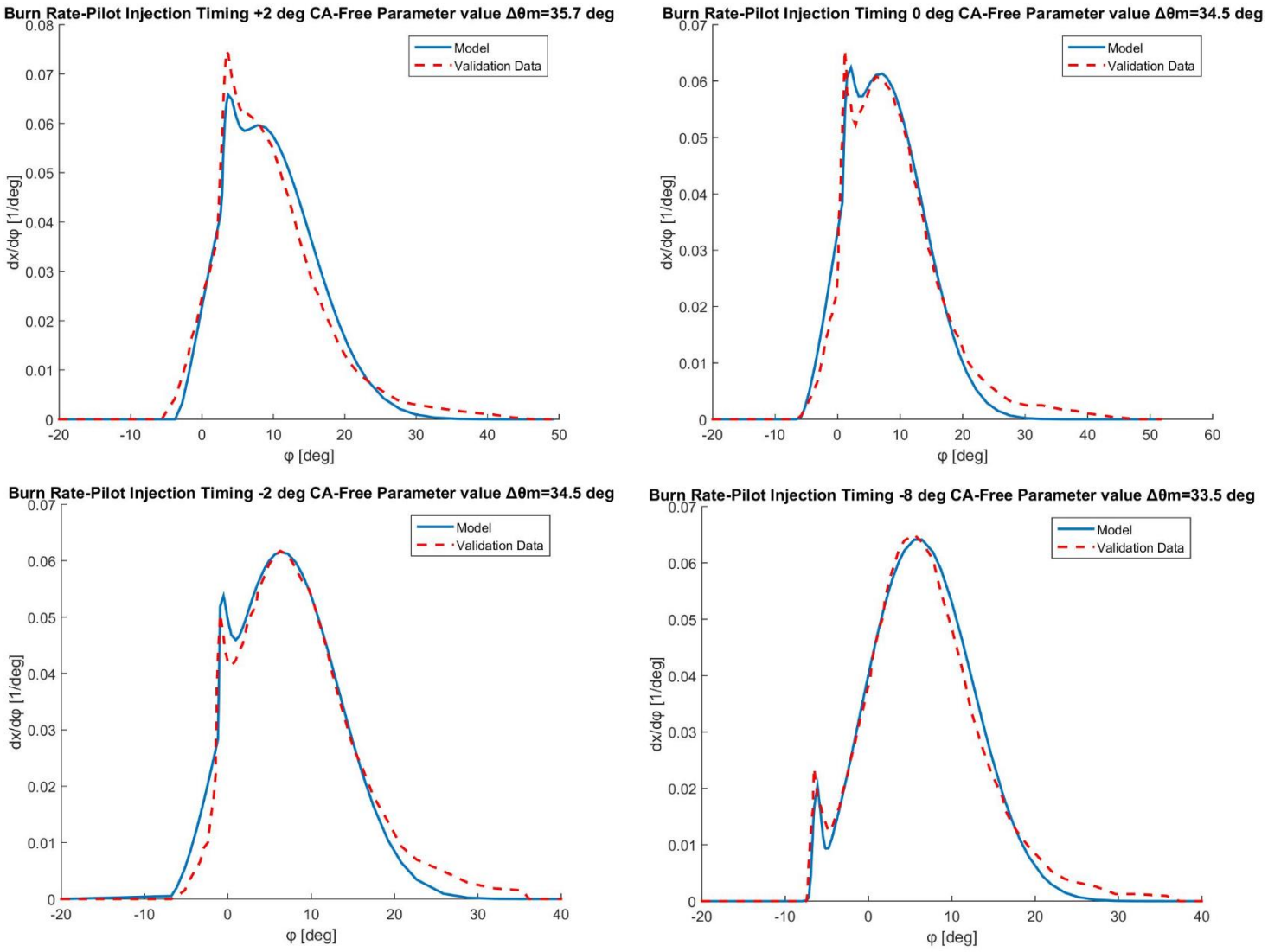

Figure 38: Model Validation for PIT variation

- *Model Validation for Pilot Injection Timing Variation:*
  The combustion model provides good fitting of the validation data for PIT variation in terms of both prediction of the pre-ignition phenomenon at PIT=2, 0 and -2 degrees and correct estimation of the combustion starting angles and durations.

- *Model Validation for Exhaust Valve Closing Variation:*
  While at all operation points tested for exhaust valve closing variation the fit provided by the model is adequate (Figures A17-A19), a critical deviation can be displayed at main fuel's ignition for EVC=264 deg. The reason for this lies at the way regression analysis works. Regression analysis, as a statistic tool, highly depends on the available data in order to produce the desired relationship between the predictors and the dependent variable.

  In particular, in a wide proportion of the data, corresponding to the equivalence ratio variation, the same load (50%) and a very close value of the EVC angle (266 deg) give a quite different value of the main fuel's ignition angle (about -6 CA degrees) than the one

calculated at EVC=264 deg (1 CA degree). As a result, the provided by the regression function of θ_{0m}, overestimates the pre-ignition of the main fuel in this case.

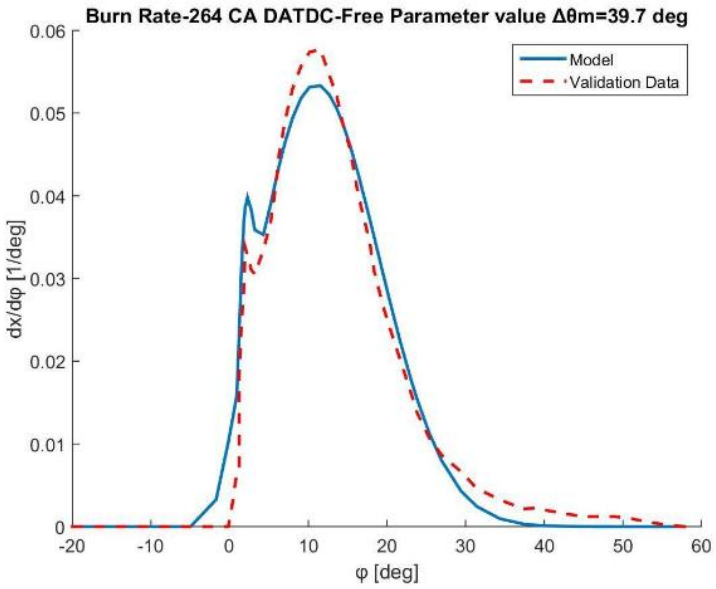

Figure 39: Over prediction of the pre-ignition phenomenon at EVC=264 degrees

- *Model Validation for Engine Speed Variation:*
  As indicated by Figures A18 and A19, the model achieves a very good fitting of the validation data in the whole spectrum of engine speeds it was tested on.

5 Chapter: Conclusions

5.1 Discussion

The aim of the present Diploma Thesis was to develop a combustion model for a large, dual fuel, two-stroke, low pressure, marine engine.

In this respect, a zero-dimensional, semi-empirical, phenomenological model was developed that describes the dual fuel combustion as a heat release phenomenon. For this purpose, the continuous analytical "Wiebe Function" was utilized which is a tool that approximates the burn rate and fraction in an internal combustion engine as a function of time or crank angle in a cost-effective way. More specifically, a double version of the Wiebe function was employed to model the combustion of pilot and main fuel respectively.

The model was developed and validated based on experimental and simulation results from available literature (1). By fitting the double-Wiebe equation to the existing model, a group of five equations was acquired for each of the Wiebe function parameters representing its variation as a function of each of the combustion parameters of engine load, overall equivalence ratio, pilot injection timing, engine speed and exhaust valve closing angle.

Subsequently, in order to combine each five-equation group into one multivariable function for every wiebe parameter, non-linear regression analysis was used. The outcome of this method was evaluated using the mathematical criteria of normal and adjusted "coefficient of determination" and "root-mean-square error". The combustion duration of the main fuel $\Delta\theta_m$ was set as a free parameter.

The accuracy of the model was validated against available data from a large two-stroke gas engine found in literature (1).

The main findings of the present work could be summarized in the following points:

- The maximum burn rate of both pilot and main fuel is reached faster at high engine loads and equivalence ratio values as a result of the increase of flame front propagation under these conditions. On the other hand, slower reach of the maximum burn rate is observed at high EVC values that correspond to low Compression Ratios and thus low flame velocities.

- Lower proportion of pilot fuel is required to trigger the air-fuel mixture at high engine load and speed because of the increased in-cylinder pressure that is caused at such operation points.

- The ignition delay phenomenon of the pilot fuel is reduced when the engine operates at high loads whereas it increases when the fuel-air mixture becomes richer making it harder for the pilot fuel to concentrate enough energy for its ignition.

- Concerning the pre-ignition of the main fuel, it becomes more pronounced at high engine speeds and overall equivalence ratios while it seems that the risk of pre-ignition can be reduced by early pilot fuel injection and late exhaust valve closing.

- The combustion duration of both fuels reduces at high engine load, equivalence ratios and engine speed as all three of them cause increase of the flame velocity. The main fuel combustion lasts longer at late pilot injection timing when pre-ignition is more likely to occur and so does at late exhaust valve closing because of the low temperature in-cylinder conditions it causes.

- Finally, it seems that the double-Wiebe function can sufficiently represent the complex combustion of a dual fuel marine engine. In particular, a good fit was achieved in terms of both combustion dynamics and deviation. The present model provided accurate results for over 90% of the tested operation points. Moreover, it could be calibrated to apply to any DF engine even at high pressure or four stroke concepts.

5.2 Recommendations for future research

The growing interest of the marine industry in the use of dual fuel engines for propulsion makes essential the development of adequate combustion models that can be used for simulating and further understanding the complicated dual fuel combustion process. In this scope, some recommendations for future research could be:

- A triple-Wiebe extension attempt of the present model could be made, with the third part of the function representing the end of combustion. This could eliminate the small under-prediction of the burn rate that the present model makes because of the slight change of the curve's form by the end of combustion which cannot be achieved by the single Wiebe function of the main fuel's combustion.

- The development of a pre-ignition model for the main fuel would be a very useful tool in terms of better understanding of the phenomenon and more accurate prediction of the main fuel's ignition angle depending on the values of the combustion parameters that cause it.

- The creation of an Ignition Delay model for the pilot fuel as a function of the combustion variables could eliminate the need to calculate the wiebe parameter of pilot fuel ignition angle θ_{0p} by fitting processes.

- In dual fuel, low pressure, two stroke engines extra care should be given in ensuring that the engine operates in the safe operation area between the knocking and misfiring zones. Thus, the design of a knock and misfiring detection methodology based on the in-cylinder conditions would be a substantial tool in terms of dual fuel engines studying and simulation.

References

1. **Černík, Filip.** *Phenomenological Combustion Modelling for Optimization of Large 2-stroke Marine Engines under both Diesel and Dual Fuel Operating Conditions.* Prague : CZECH TECHNICAL UNIVERSITY IN PRAGUE, 2018.

2. **Gas engine.** ***Wikipedia.*** **[Online] https://en.wikipedia.org/wiki/Gas_engine.**

3. Pearce, William. Otto-Langen Atmospheric Engine. ***OLD MACHINE PRESS.*** **[Online] https://oldmachinepress.com/2018/01/20/otto-langen-atmospheric-engine/.**

4. Hall, Mateos Kassa & Carrie. Dual-Fuel Combustion. ***The Future of Internal Combustion Engines.*** **s.l. : IntechOpen, 2018.**

5. ***Dual-Fuel Marine Engine (Highly Reliable Environmentally Friendly Engine).*** **Ohashi, Issei. s.l. : YANMAR, 2015.**

6. EEDI & SEEMP. ***MARPOL ANNEX VI.*** **[Online] https://www.marpol-annex-vi.com/eedi-seemp/.**

7. Carmelo Cartalemi, Winterthur Gas & Diesel. ***X-DF Low Gas Pressure Low-Speed Main Engines: The Game Changer for LNG-Fuelled ships.*** **s.l. : CIMAC CONGRESS, 2019.**

8. Upcoming environmental regulations for emissions to air – IMO NOx Tier III. ***DNV GL.*** **[Online] December 29, 2015. https://www.dnvgl.com/news/upcoming-environmental-regulations-for-emissions-to-air-imo-nox-tier-iii-45479.**

9. Ltd., Winterthur Gas & Diesel. ***Application of WinGD X-DF engines for LNG fuelled vessels.*** **2017.**

10. Shuonan Xu, David Anderson, Mark Hoffman, Robert Prucka and Zoran Filipi. ***A phenomenological combustion analysis of a dual-fuel natural-gas diesel engine.*** **2015.**

11. Hyunchun Park, Hyundai Heavy Industries / ETH Zurich. ***Combustion Modelling of a Medium-Speed Dual-Fuel Engine Using Double Vibe Function.*** **s.l. : CIMAC CONGRESS, 2019.**

12. Hua Zhou, Hong-Wei Zhao , Yu-Peng Huang , Jian-Hui Wei and Yu-Hui Peng. ***Effects of Injection Timing on Combustion and Emission Performance of Dual-Fuel Diesel Engine under Low to Medium Load Conditions.*** **2019.**

13. Dual fuel engines. ***WÄRTSILÄ.*** **[Online] https://www.wartsila.com/marine/build/engines-and-generating-sets/dual-fuel-engines.**

14. Four-Stroke Engines. ***MAN Marine Engines & Systems.*** **[Online] https://marine.man-es.com/four-stroke/engines.**

15. Hyundai Engines. ***Hyundai HiMSEN ENGINE programme 2018.*** **[Online] http://www.hyundai-engine.com/_board/upload/BOARD_A01/Cat/1532665542_37891/UPBA50E262FB7C4.pdf.**

16. Gas&Diesel, WIN GD Winterthur. ***Application of WinGD X-DF engines for LNG fuelled vessels.*** **2017.**

17. Turbo, Man Diesel and. ***The MAN ME-GI engine: From initial system considerations to implementation and performance optimisation.*** **s.l. : CIMAC Congress 2013, 2013.**

18. Marcel Ott, Winterthur Gas & Diesel. ***The 2-stroke Low-Pressure Dual-Fuel Technology: From Concept to Reality.*** **s.l. : CIMAC CONGRESS, 2016.**

19. Hannu Jääskeläinen. Natural Gas Engines. ***DieselNet.com.*** **[Online] November 2019. https://www.dieselnet.com/tech/engine_natural-gas.php.**

20. Arp, S. ***2-STROKE DUAL FUEL ENGINE SAFETY CONCEPT.*** **2014.**

21. Shuonan Xu, David Anderson, Amrit Singh, Mark Hoffman,Robert Prucka, and Zoran Filipi. ***Development of a Phenomenological Dual-Fuel Natural Gas Diesel Engine Simulation and Its Use for Analysis of Transient Operations.*** **s.l. : Clemson Univ., 2014.**

22. Papagiannakis, D. T. Hountalas and R. G. ***Development of a Simulation Model for Direct Injection Dual.*** **s.l. : National Technical University of Athens, 2000.**

23. Ivan Taritas, Darko Kozarac, and Momir Sjeric, Miguel Sierra Aznar and David Vuilleumier,Reinhard Tatschl. ***Development and Validation of a Quasi-Dimensional Dual Fuel (Diesel – Natural Gas) Combustion Model.*** **s.l. : SAE International, 2017.**

24. Lucas Eder, Marko Ban, Gerhard Pirker , Milan Vujanovic , Peter Priesching and Andreas Wimmer. Development and Validation of 3D-CFD Injection and Combustion Models for Dual Fuel Combustion in Diesel Ignited Large Gas Engines. ***Energies.*** **2018.**

25. Sochaczewski, Tytus Tulwin and Rafal. The dual-fuel CFD combustion model with direct and indirect CNG injection. ***Research Gate.*** **2017.**

26. Wiebe, Ivan Ivanovitch. ***Progress in engine cycle analysis: Combustion rate and cycle processes.*** **1962.**

27. Ghojel, Jamil. ***Review of the development and applications of the Wiebe function: A tribute to the contribution of Ivan Wiebe to engine research.*** **s.l. : Reaserchgate, 2010.**

28. Regression analysis. ***Wikipedia.*** **[Online] https://en.wikipedia.org/wiki/Regression_analysis.**

29. Coefficient of determination. ***Wikipedia.*** **[Online] https://en.wikipedia.org/wiki/Coefficient_of_determination.**

30. Root-mean-square deviation. ***Wikipedia.*** **[Online] https://en.wikipedia.org/wiki/Root-mean-square_deviation.**

31. regress. ***MathWorks.*** **[Online] https://www.mathworks.com/help/stats/regress.html.**

32. General Technical Data (GTD). ***WinGD.*** **[Online] https://www.wingd.com/en/engines/general-technical-data-(gtd)/.**

33. nlinfit. ***MathWorks.*** **[Online] https://www.mathworks.com/help/stats/nlinfit.html.**

34. Zhang, Y. ***Internal Combustion Engines: Improving Performance, Fuel Economy and Emissions.*** **s.l. : Science direct, 2011.**

35. ***THE EFFECT OF COMBUSTION DURATION ON THE PERFORMANCE AND EMISSION CHARACTERISTICS OF PROPANE-FUELED 4-Stroke S. I. ENGINES.*** **Jehad A. A. Yamin, H. N. Gupta and B. B. Bansal. s.l. : Emirates Journal for Engineering Research, 2003.**

36. ABB. ***A clean, efficient solution for IMO Tier 3: Gas and Dual-Fuel Engines.*** **Athens : s.n., 2014.**

37. Soylu, Seref. ***Prediction of knock limited operating conditions of a natural gas engine.*** **s.l. : ResearchGate, 2005.**

38. Woodyard, Doug. ***Pounders Marine Diesel Engines and Gas Turbines.*** **2009.**

39. Karim, Ghazi A. ***Dual-Fuel Engines.*** **2015.**

40. Hua Zhou, Hong-Wei Zhao , Yu-Peng Huang , Jian-Hui Wei and Yu-Hui Peng. Effects of Injection Timing on Combustion and Emission Performance of Dual-Fuel Diesel Engine under Low to Medium Load Conditions. ***Energies.*** **2019.**

41. Karim, Z Liu and G A. ***Simulation of combustion processes in gas-fuelled diesel engines.*** **s.l. : Department of Mechanical Engineering, The University of Calgary, Canada, 2016.**

42. Jehad A. A. Yamin, H. N. Gupta, and B. B. Bansal. ***THE EFFECT OF COMBUSTION DURATION ON THE PERFORMANCE AND EMISSION CHARACTERISTICS OF PROPANE-FUELED 4-Stroke S. I. ENGINES.*** **2003.**

APPENDIX

A1: Tables

Table A1: bi coefficients produced by non-linear regression

	m_p	m_m	f_p	ϑ_p [deg]	ϑ_m [deg]	$\Delta\vartheta_p$ [deg]	$\Delta\vartheta_m$ [deg]
b_1	9.524	4.575	-0.142	-20.547	-45.009	-25.990	-217.692
b_2	0.000	0.015	-0.122	6.920	-0.052	0.050	-58.957
b_3	6.139	0.932	0.018	0.040	1.046	1.322	0.117
b_4	32.256	-8,095,007.205	-0.719	13.994	191.450	-79,081,307.951	0.005
b_5	3.978	23.267	5.465	0.217	4.121	22.902	-7.330
b_6	-5.951	0.000	0.309	1.004	0.000	155.676	0.000
b_7	0.044	4.442	0.018	0.994	4.907	0.006	4.763
b_8	0.001	0.004	-0.029	-2.534	-0.010	-43.286	244.261
b_9	1.363	1.109	0.133	0.129	1.549	0.202	0.047
b_{10}	-0.011	-0.016	0.000	0.000	0.481	-9.133	0.006
b_{11}	1.042	0.996	1.013	1.728	0.833	0.192	1.555

A2: Figures

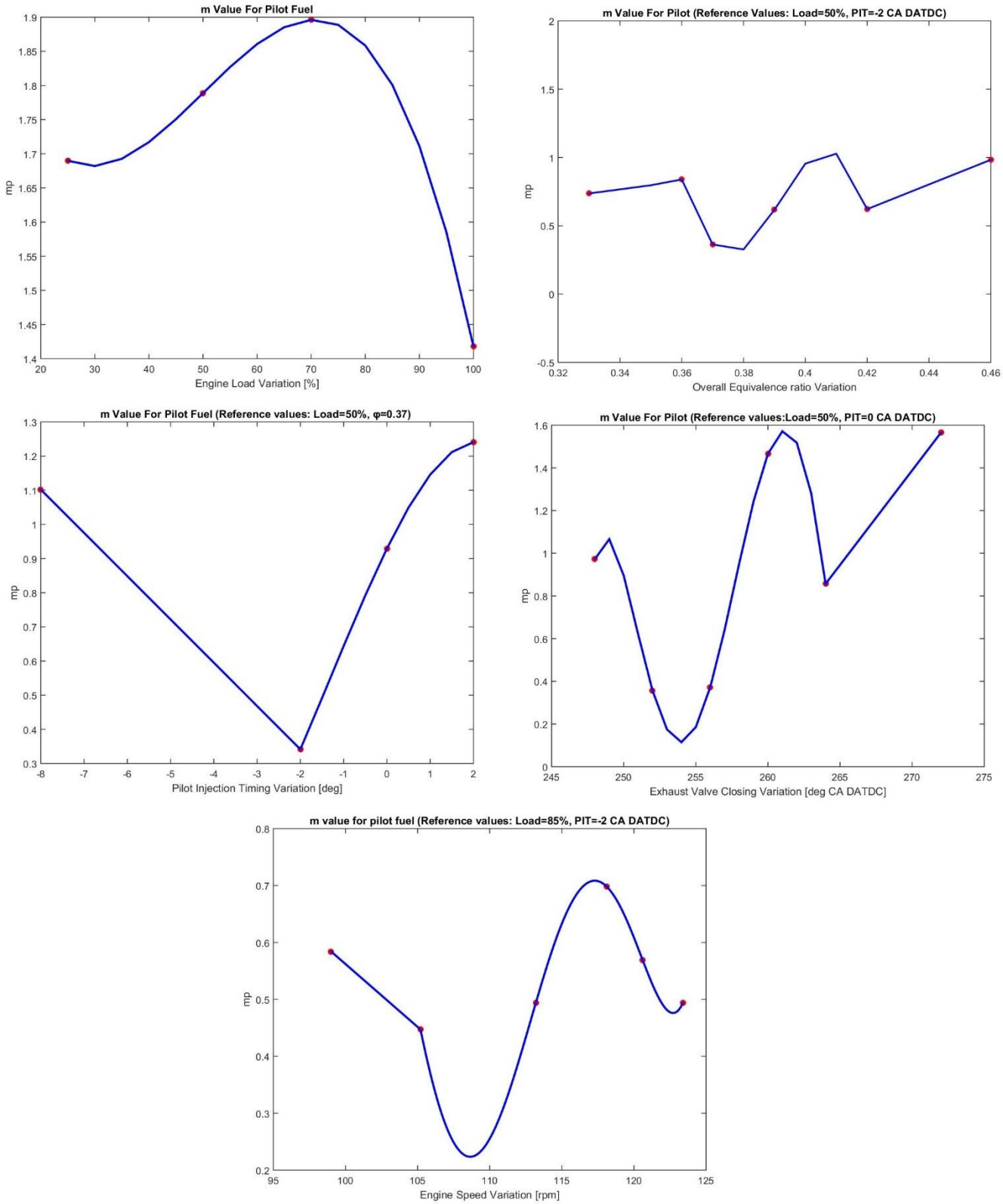

Figure A1: Pilot Fuel "form factor" variation

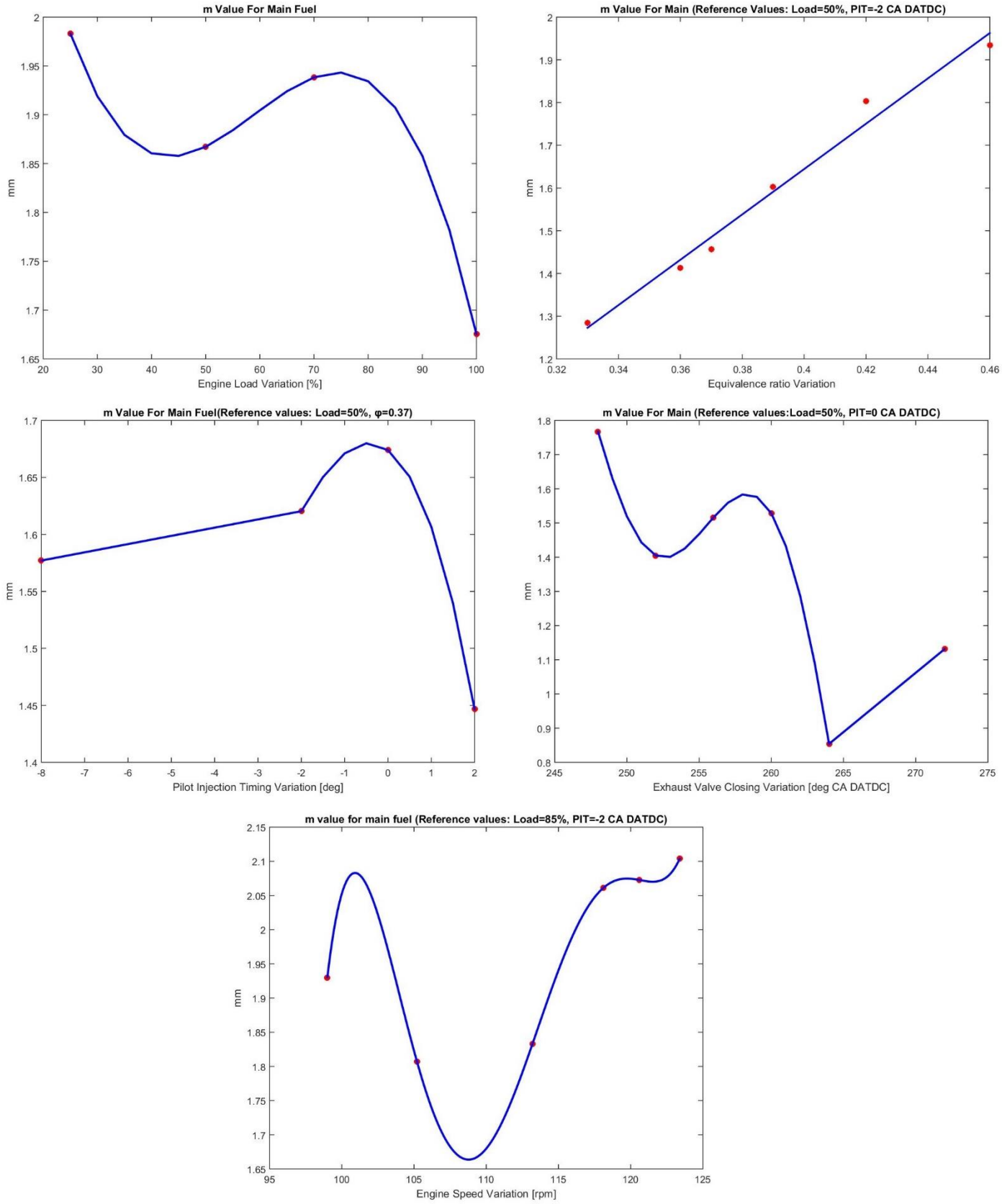

Figure A2: Main Fuel "form factor" variation

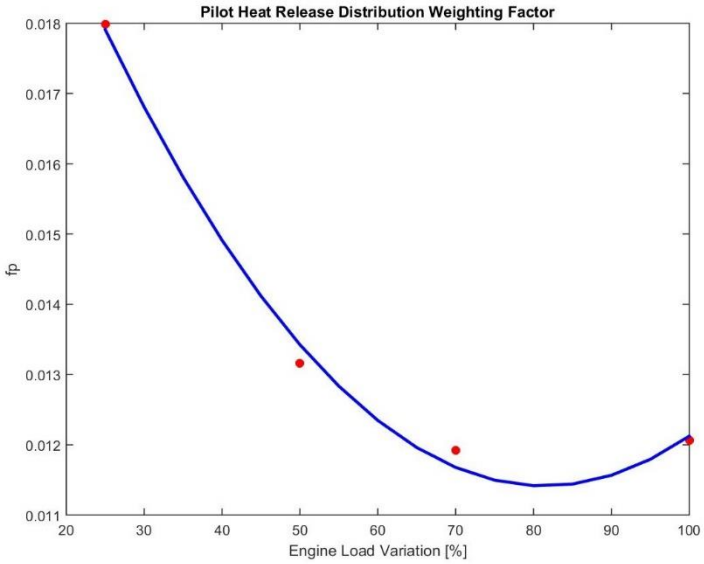

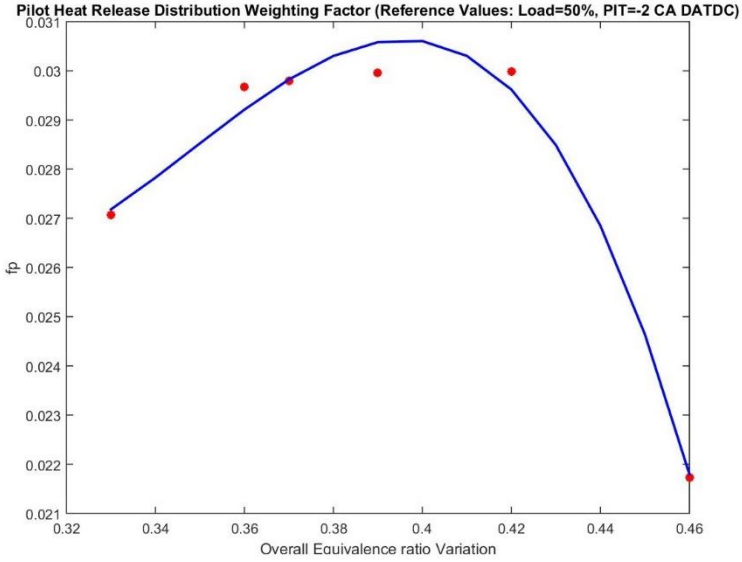

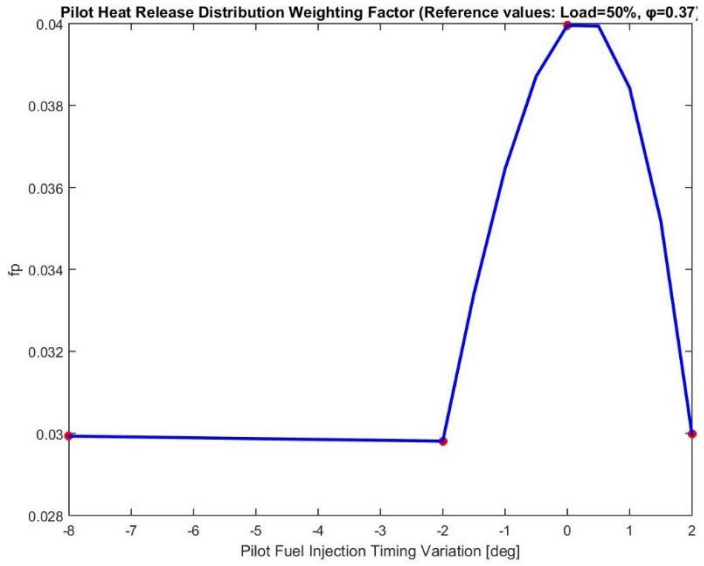

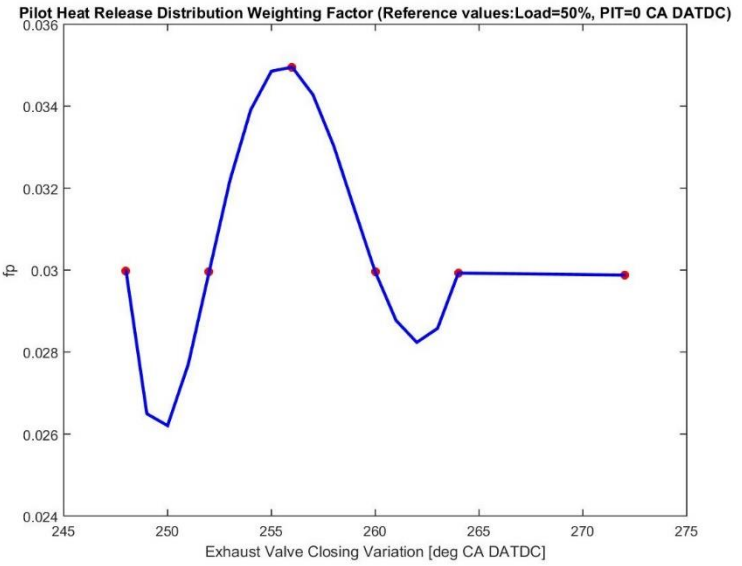

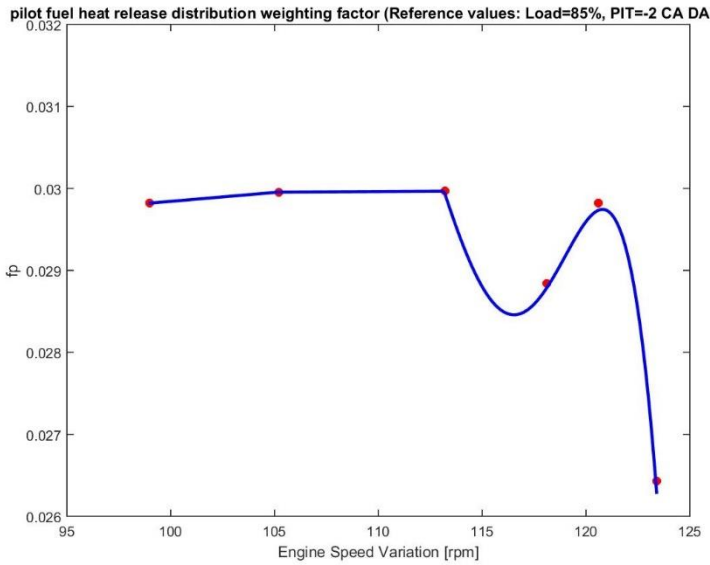

Figure A3: Pilot Fuel "Distribution Weighting Factor" variation

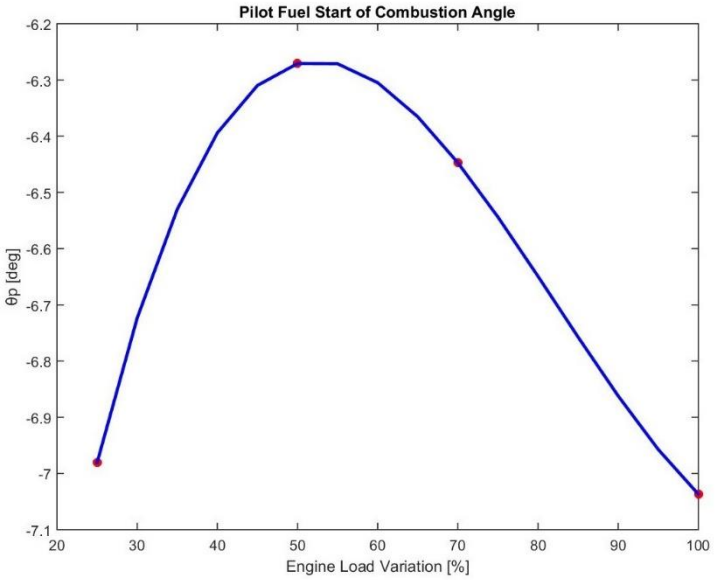

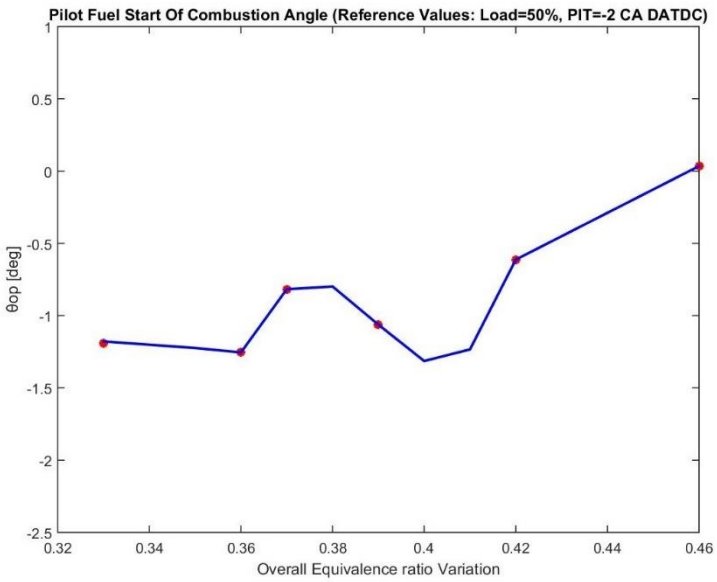

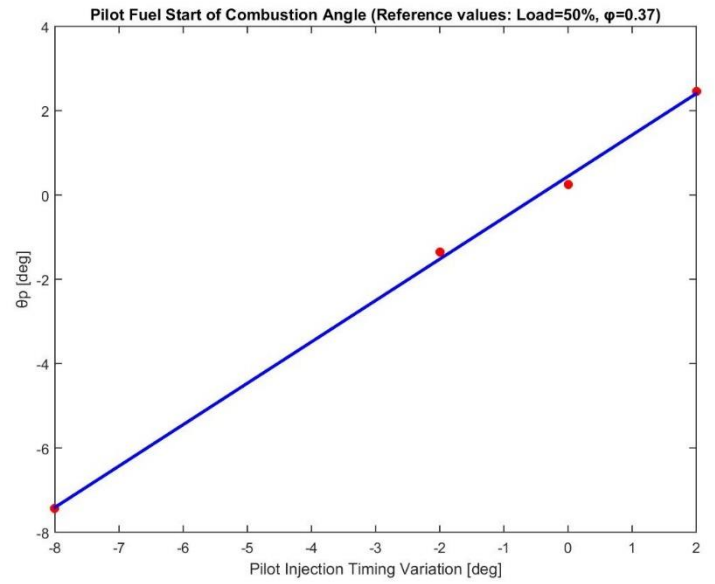

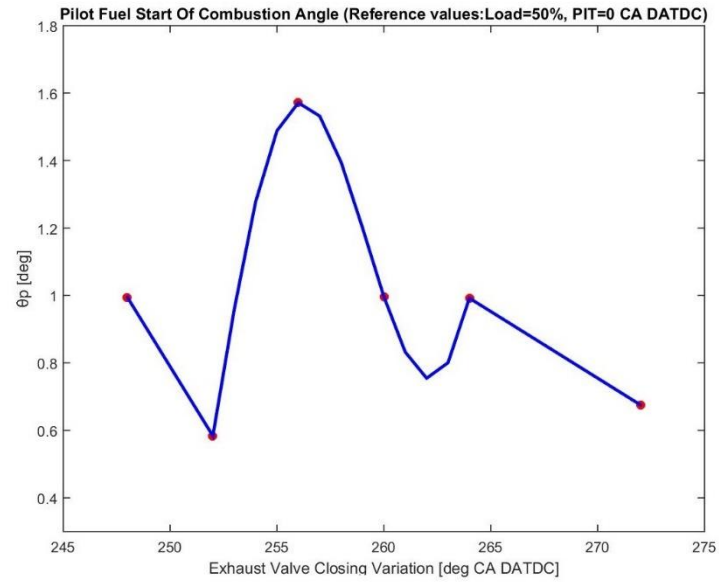

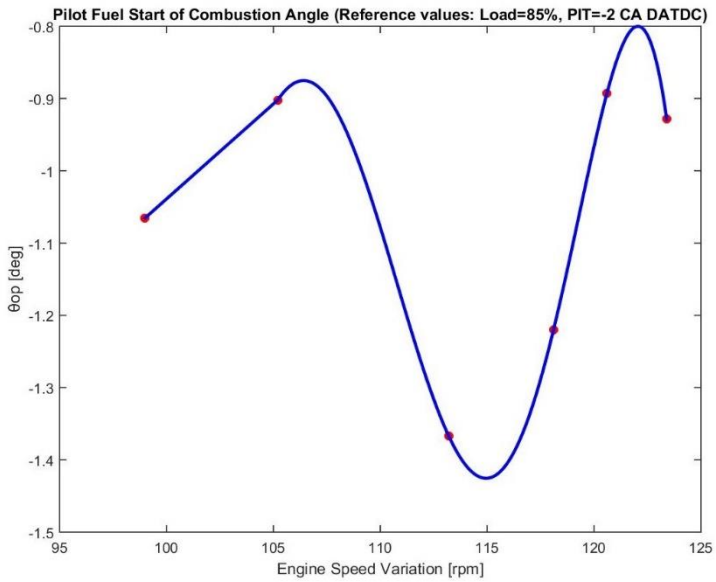

Figure A4: Start of pilot fuel combustion angle variation

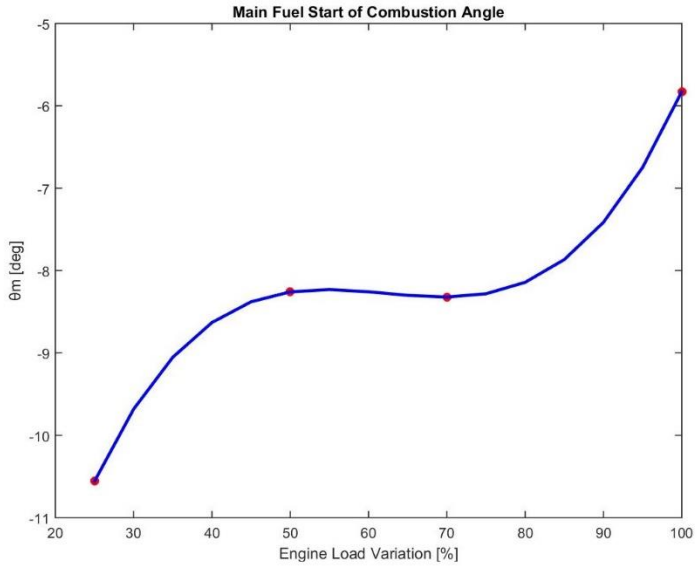

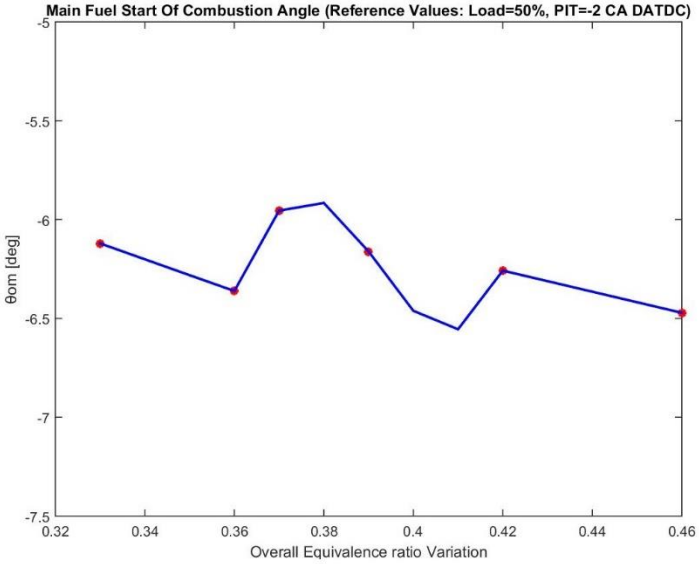

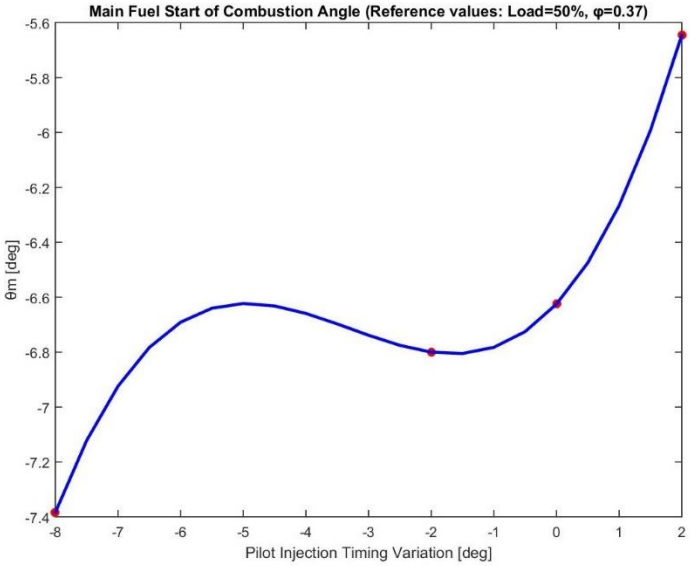

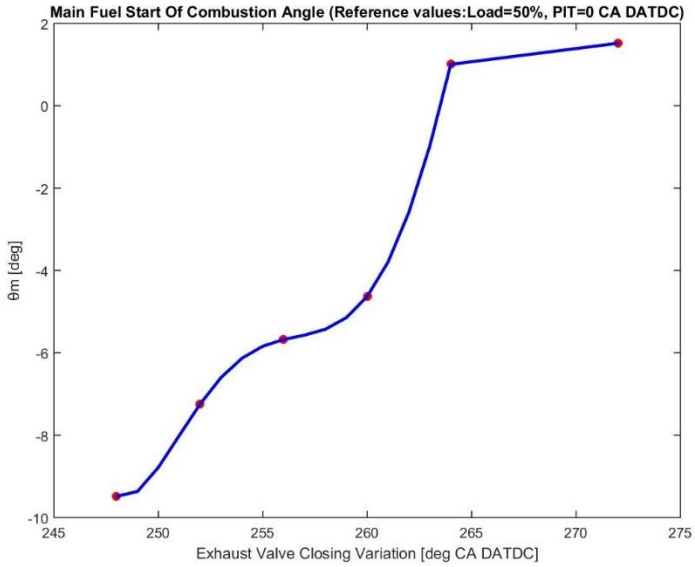

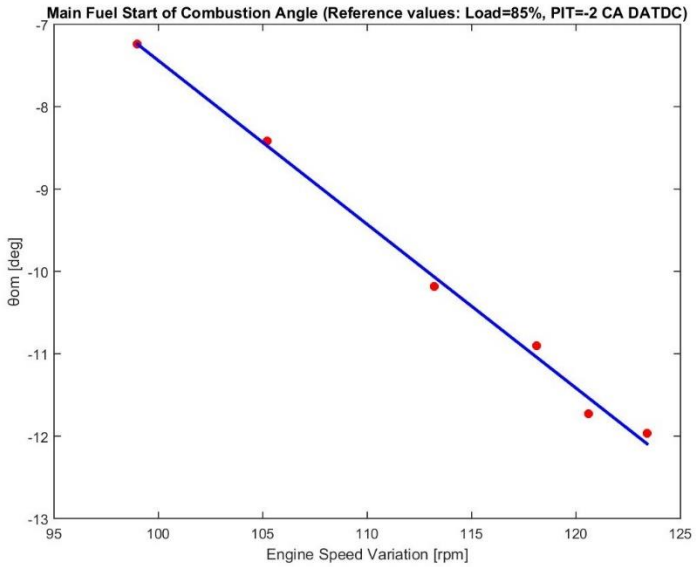

Figure A5: Start of main fuel combustion angle variation

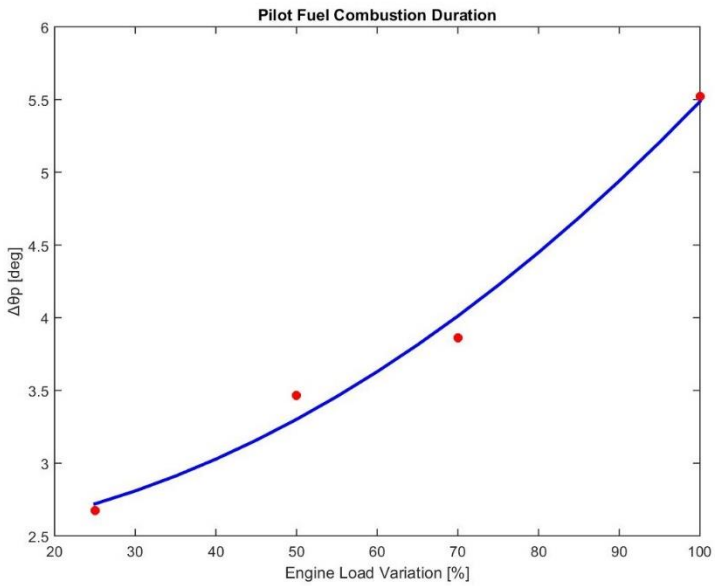

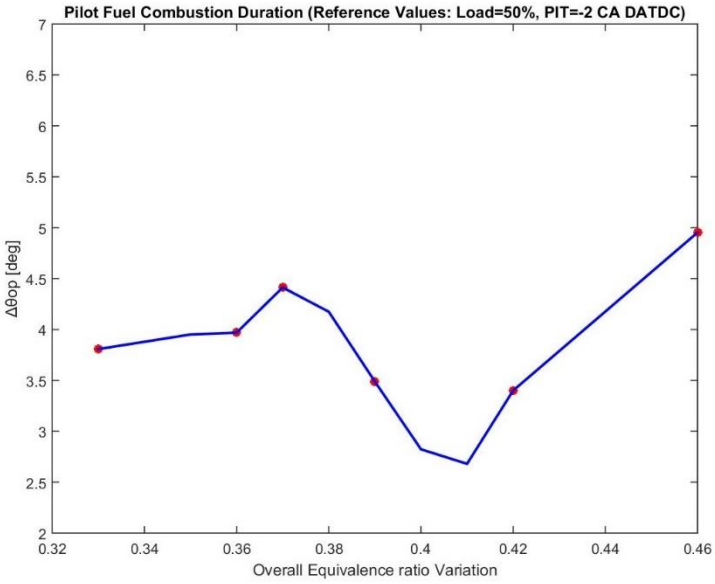

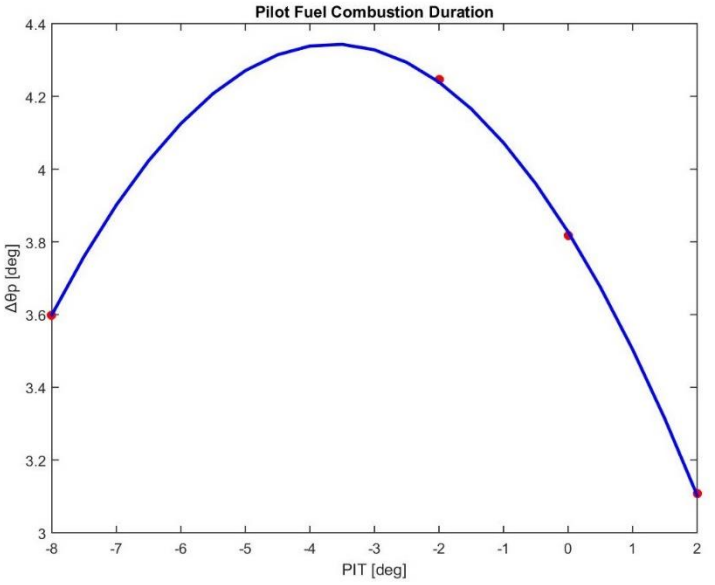

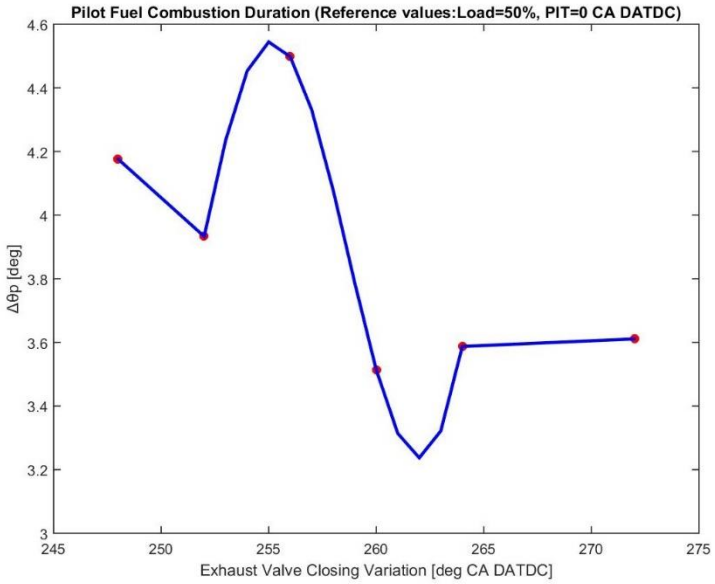

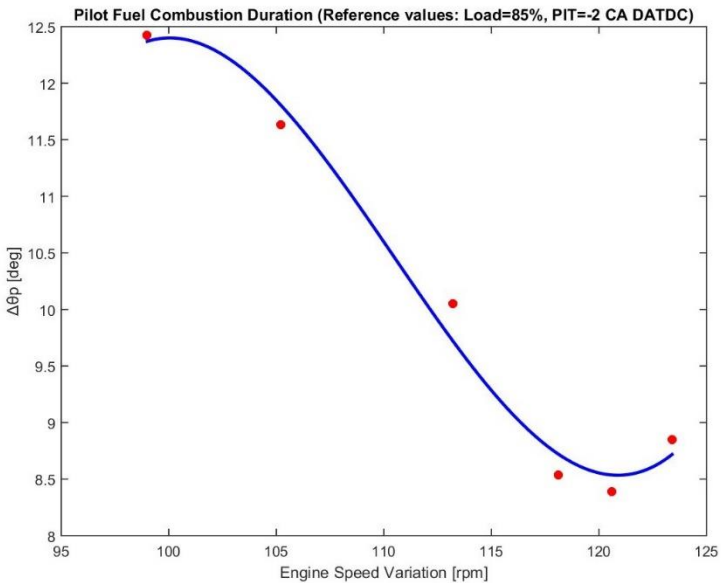

Figure A6: Pilot Fuel Combustion duration variation

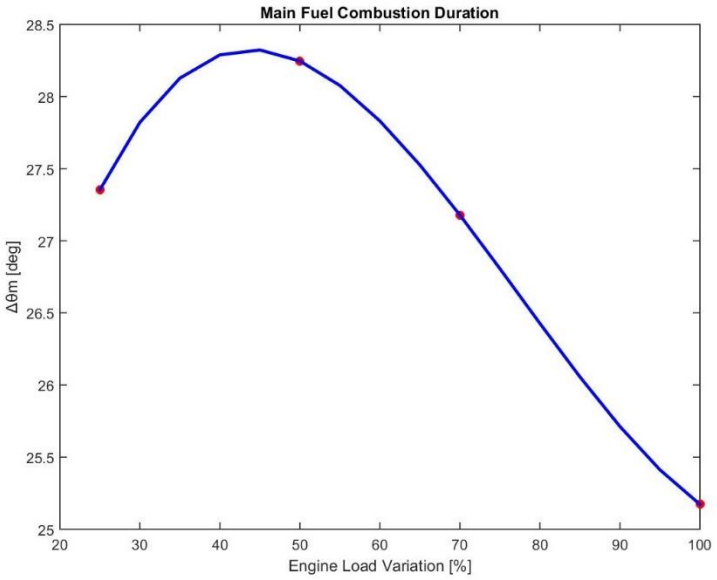

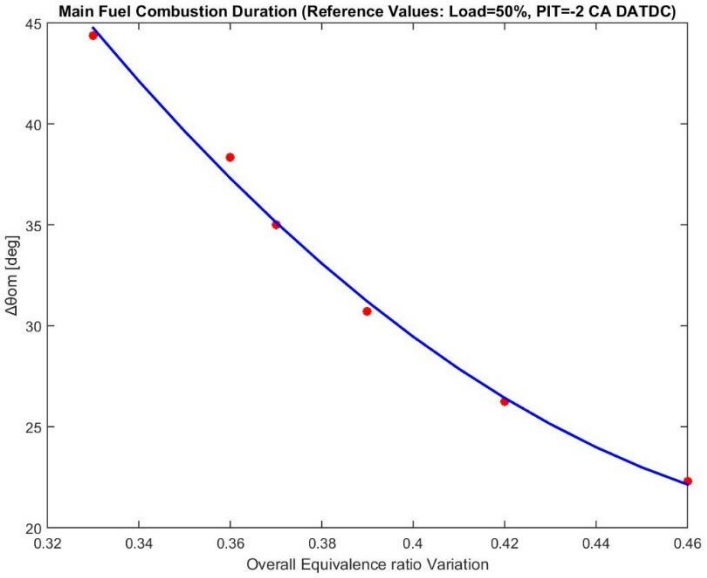

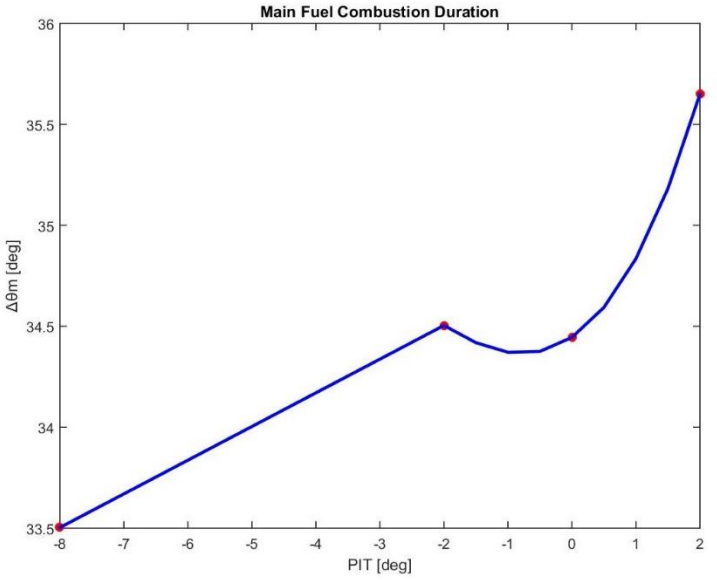

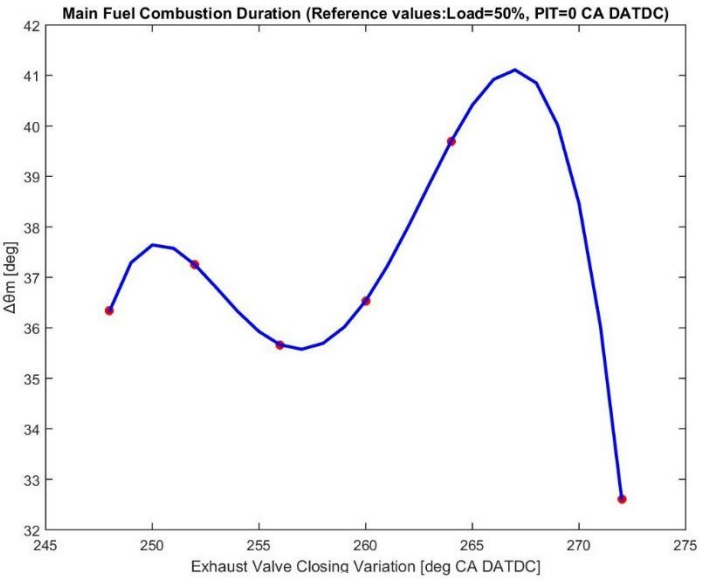

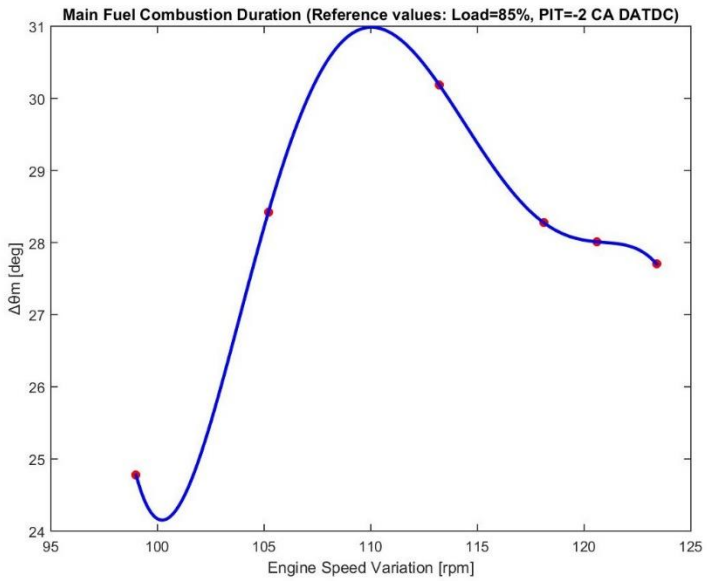

Figure A7: Main Fuel Combustion duration variation

Engine load variation results

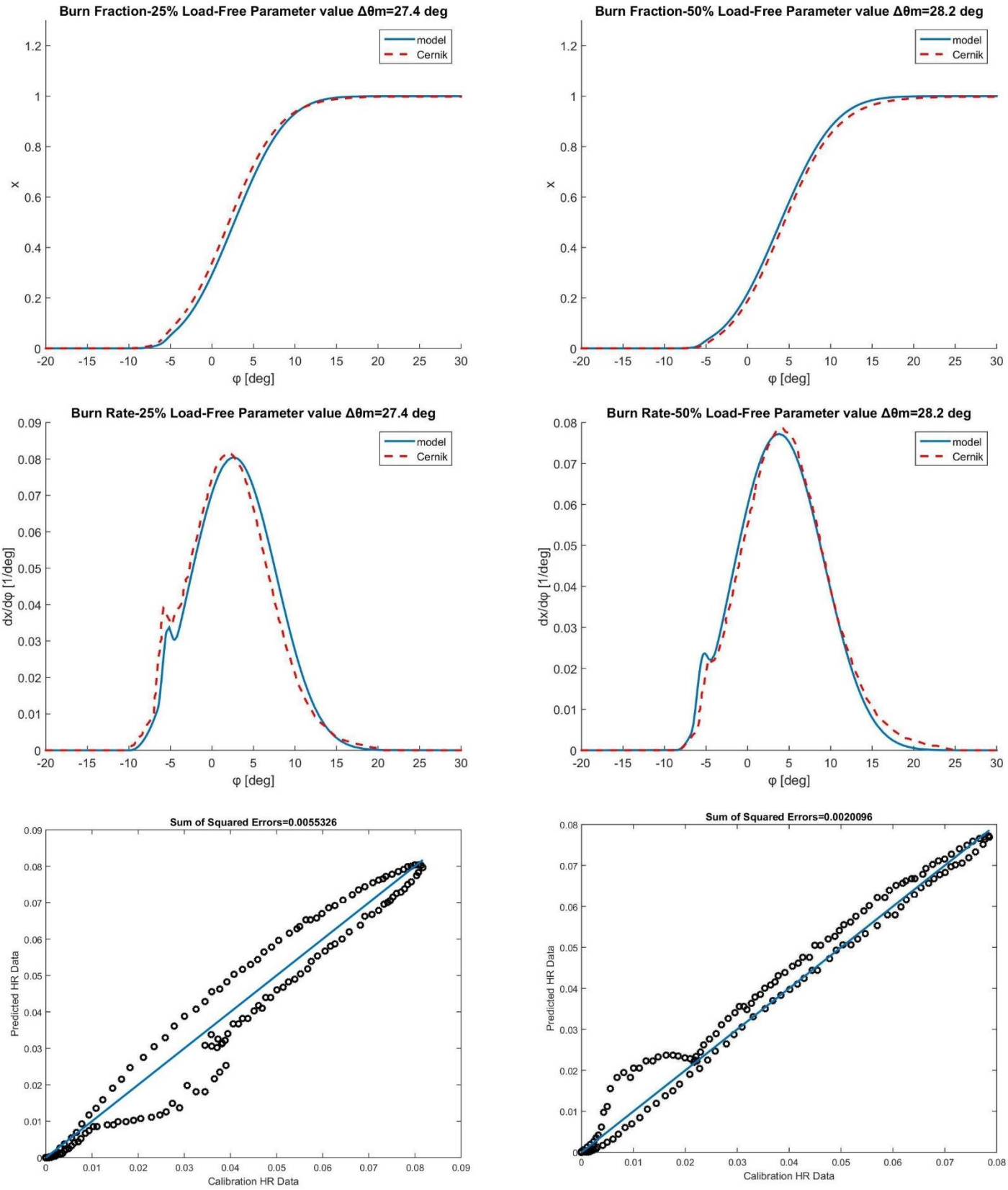

Figure A8: Model Validation at 25% and 50% Engine Load

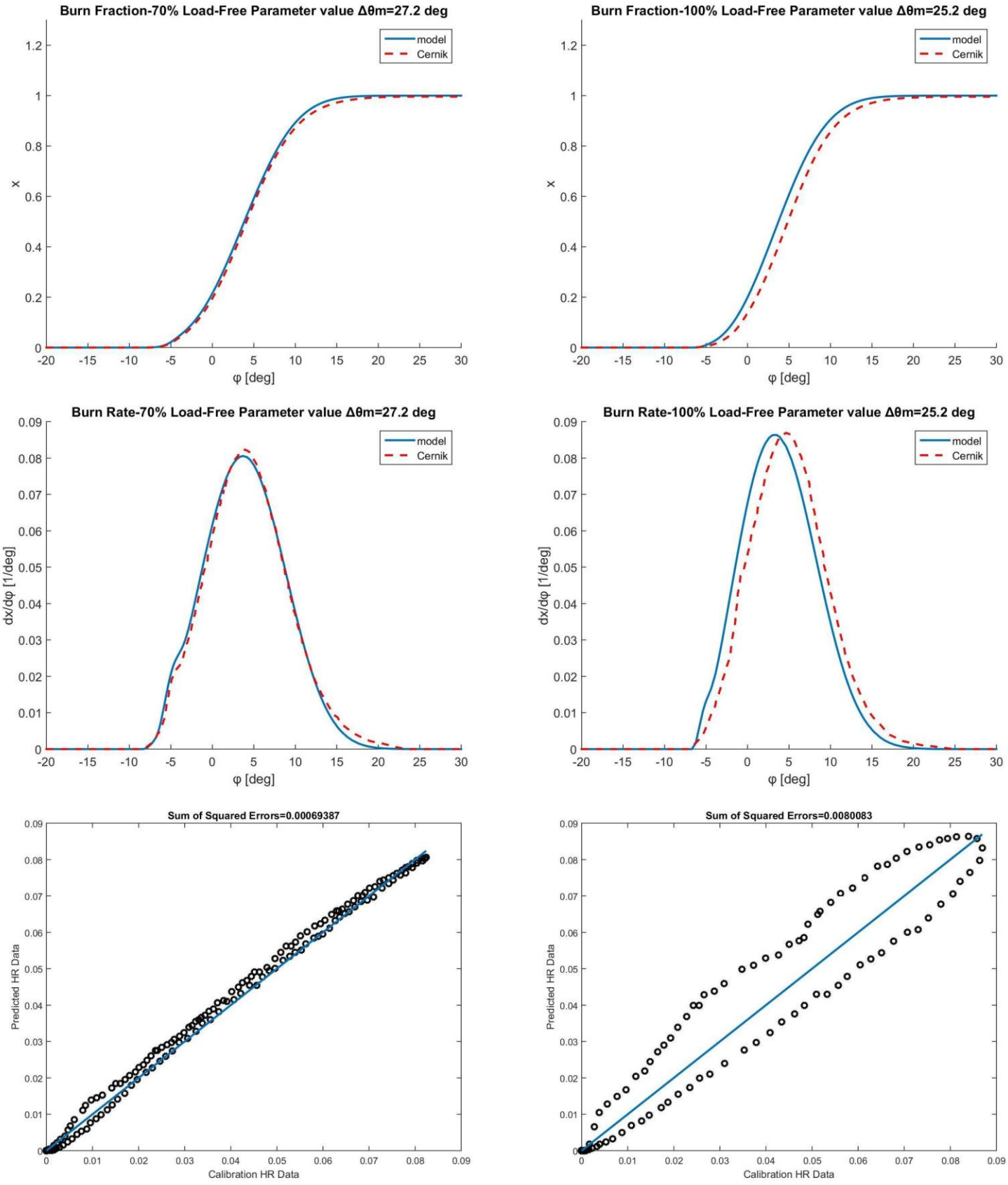

Figure A9: Model Validation at 70% and 100% Engine Load

Equivalence ratio variation results

(at 50% load, 99 rpm, Pit -2 deg, EVC 266 deg)

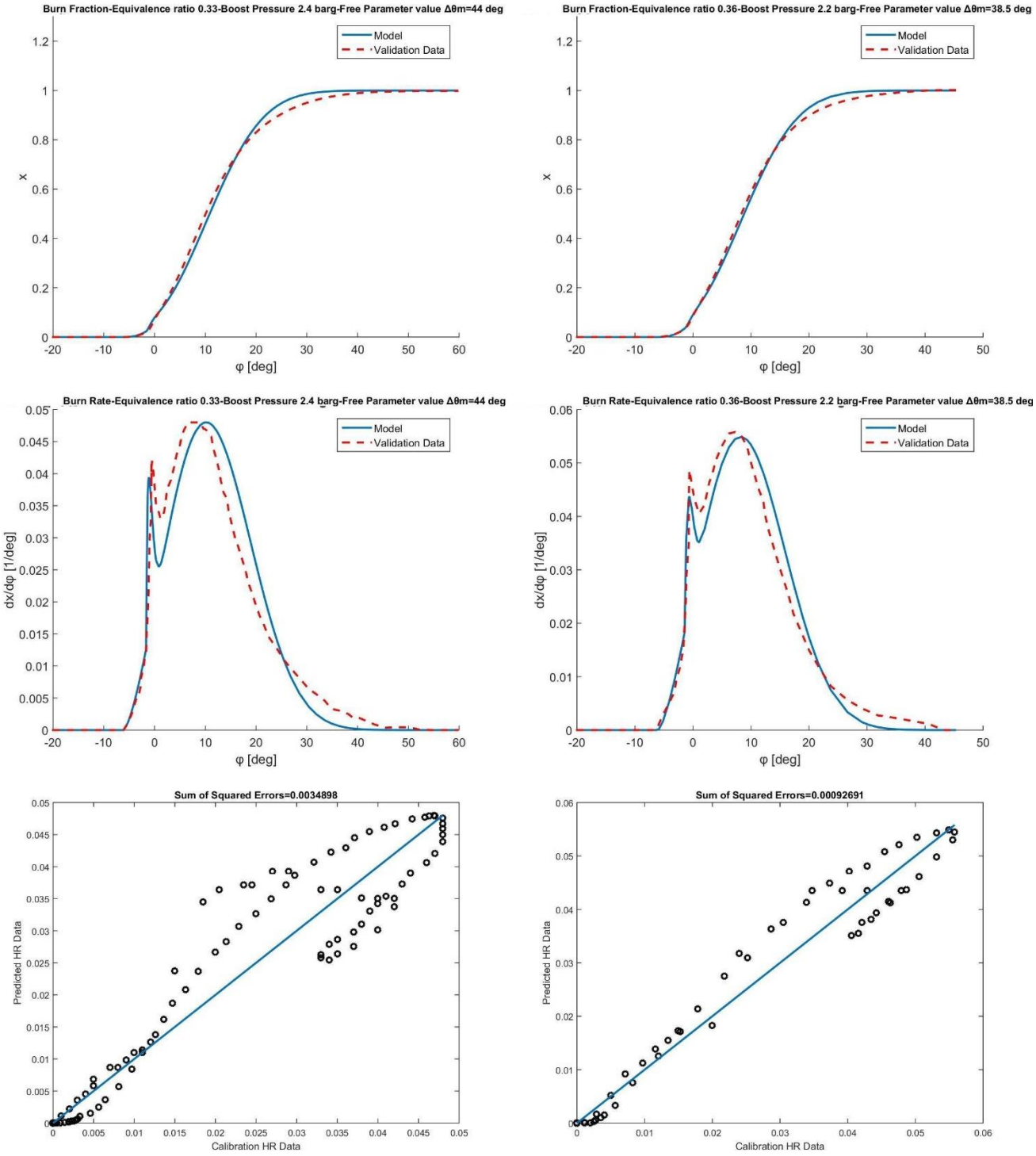

Figure A10: Model Validation at ϕ=0.33 and ϕ=0.36

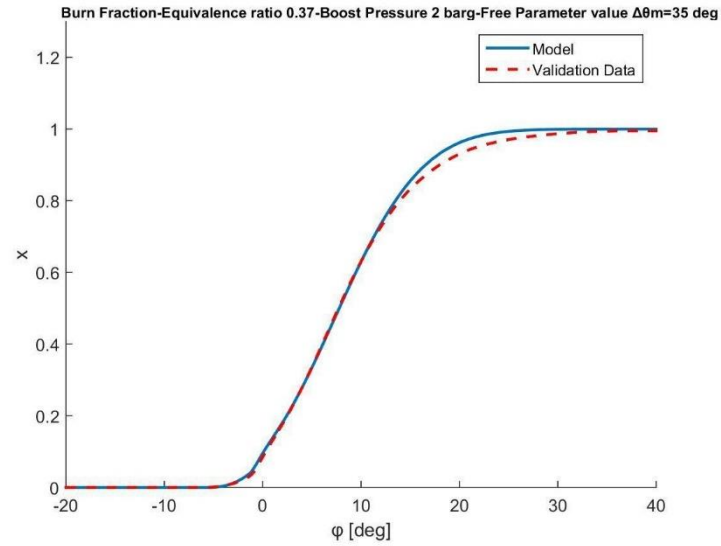

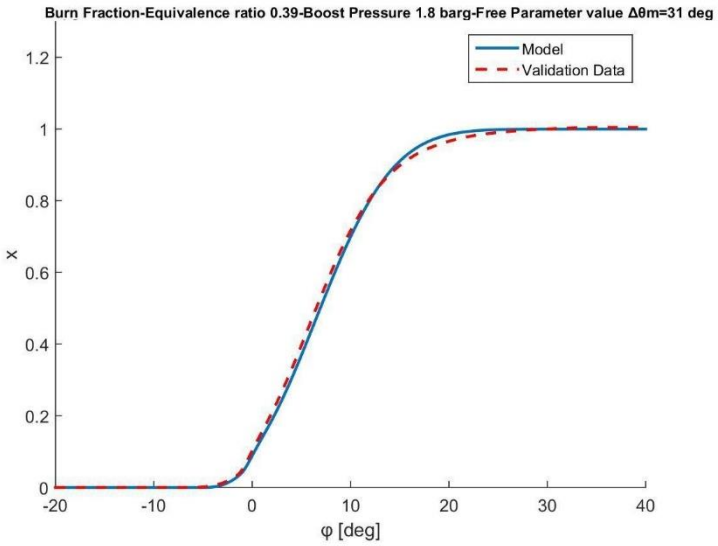

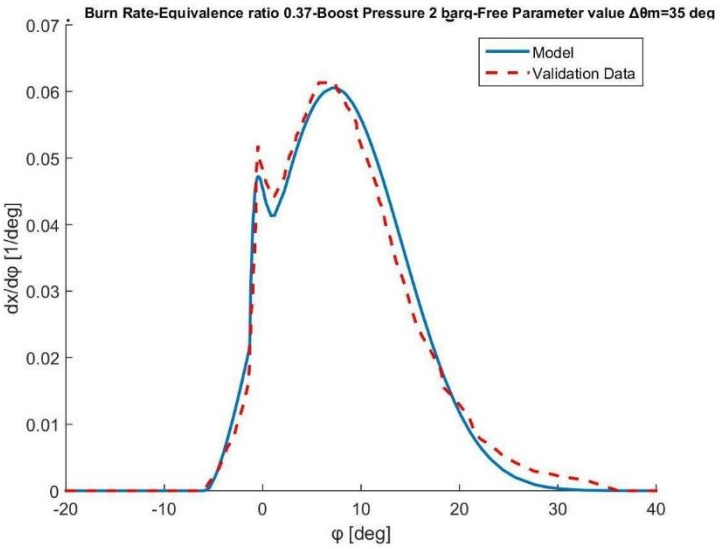

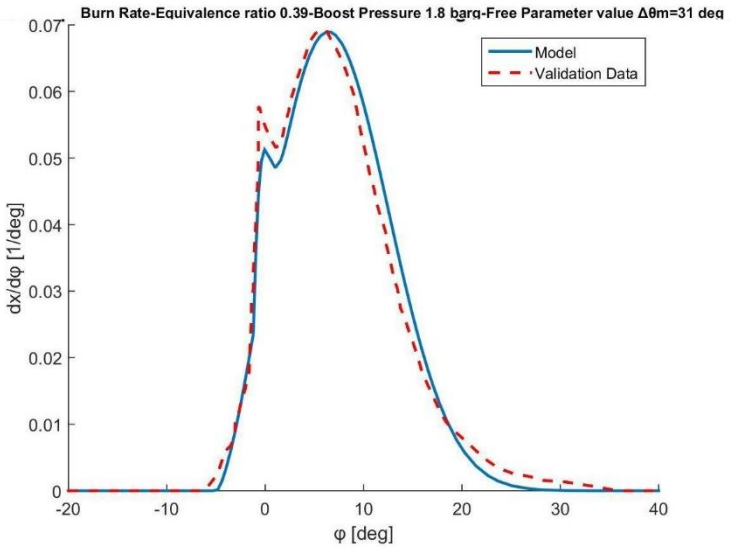

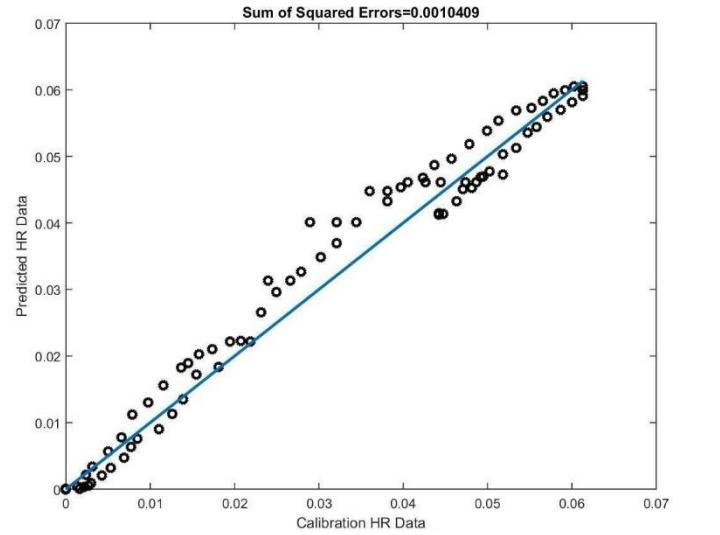

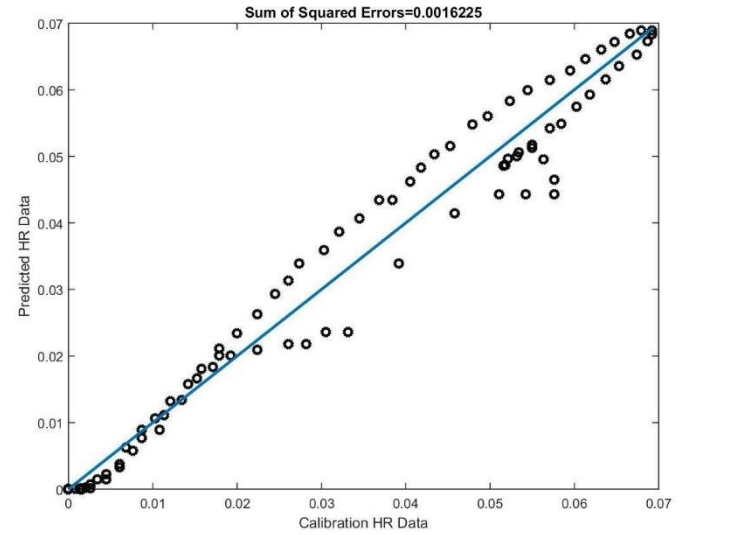

Figure A11: Model Validation at ϕ=0.37 and ϕ=0.39

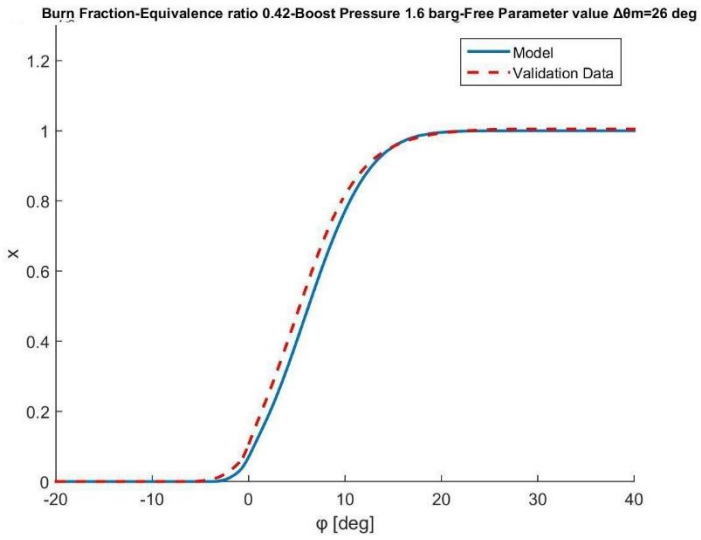

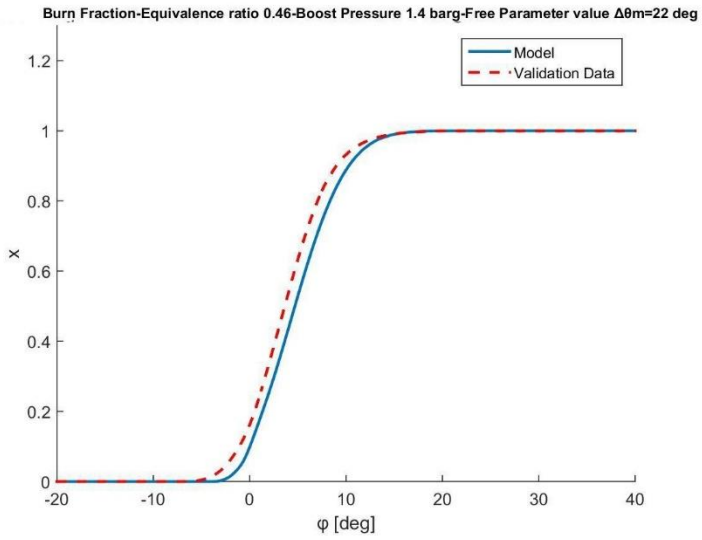

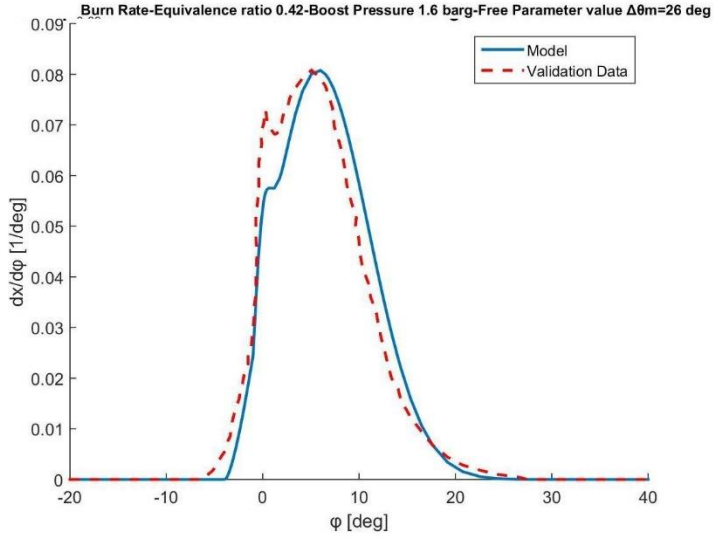

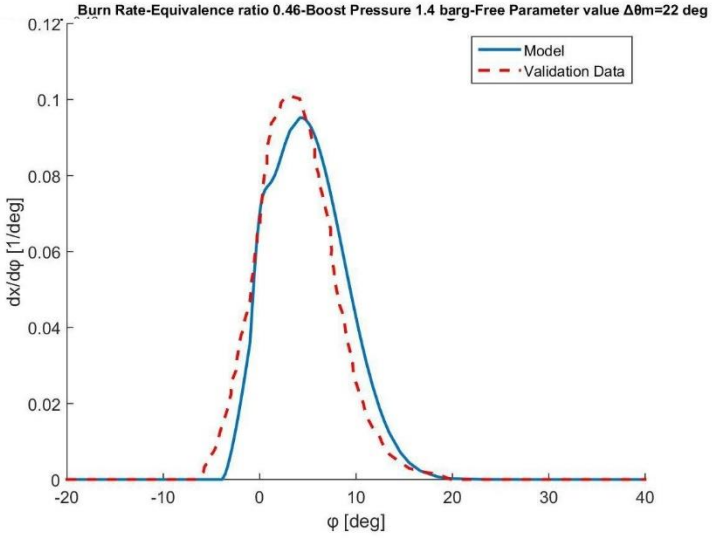

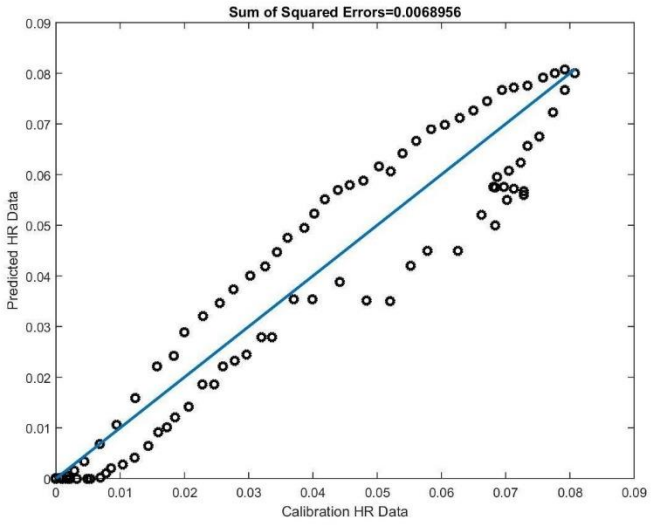

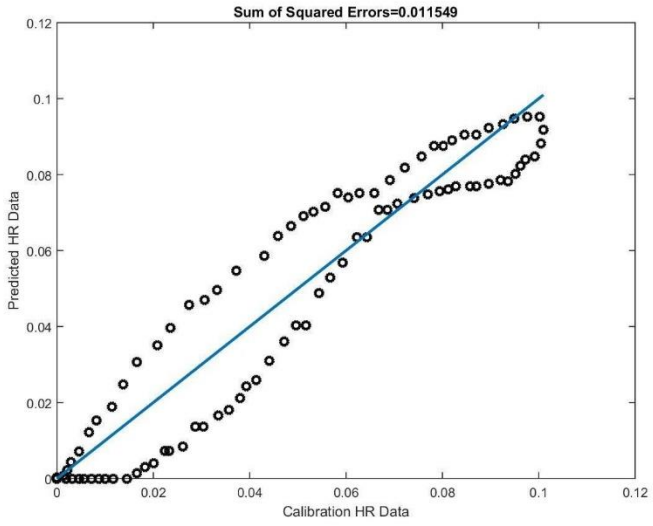

Figure A12: Model Validation at ϕ=0.42 and ϕ=0.46

Pilot fuel injection timing variation results

(at 50% load, 99 rpm, φ=0.37, EVC 256 deg)

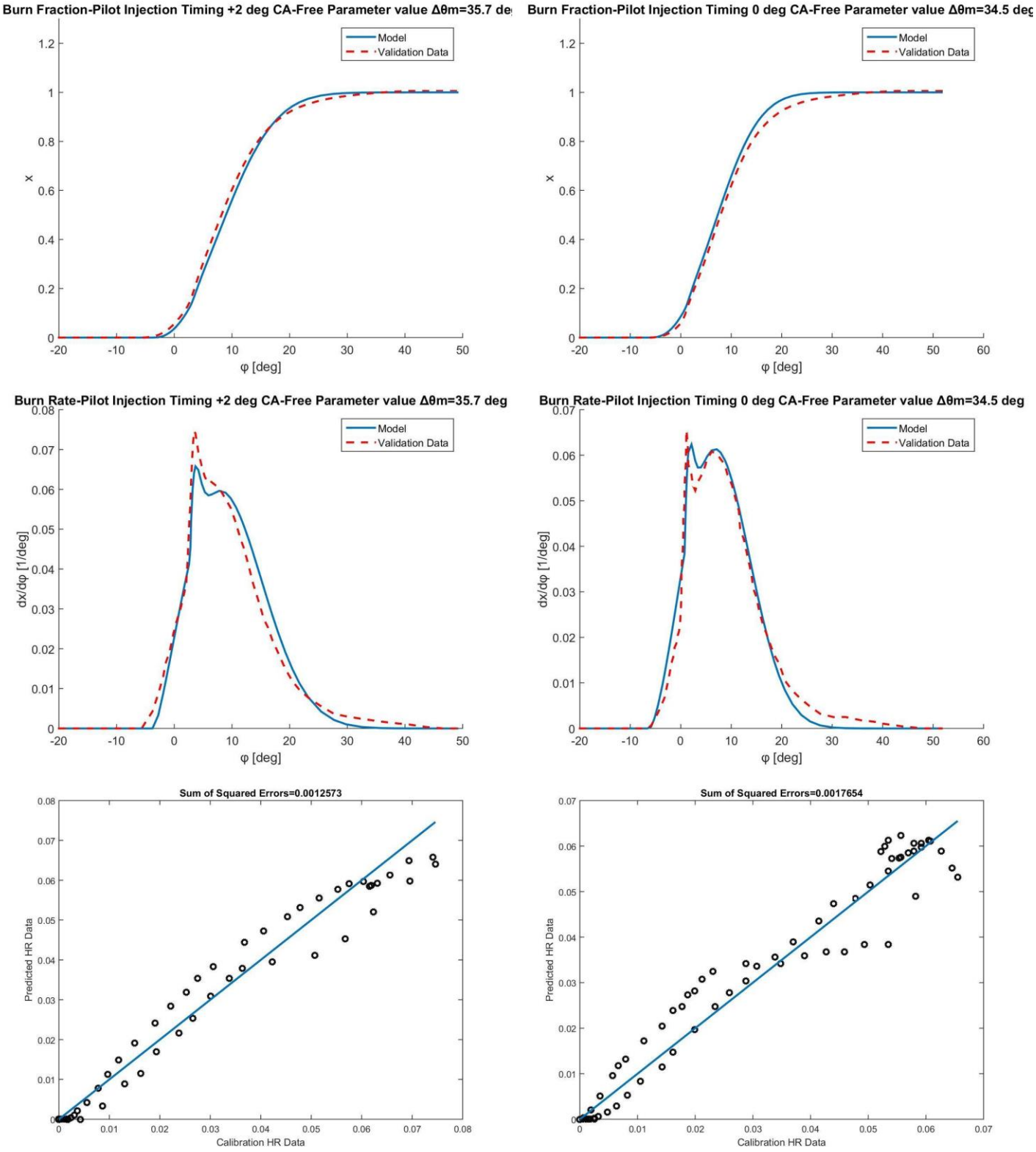

Figure A13: Model Validation at PIT=+2 and PIT=0 deg

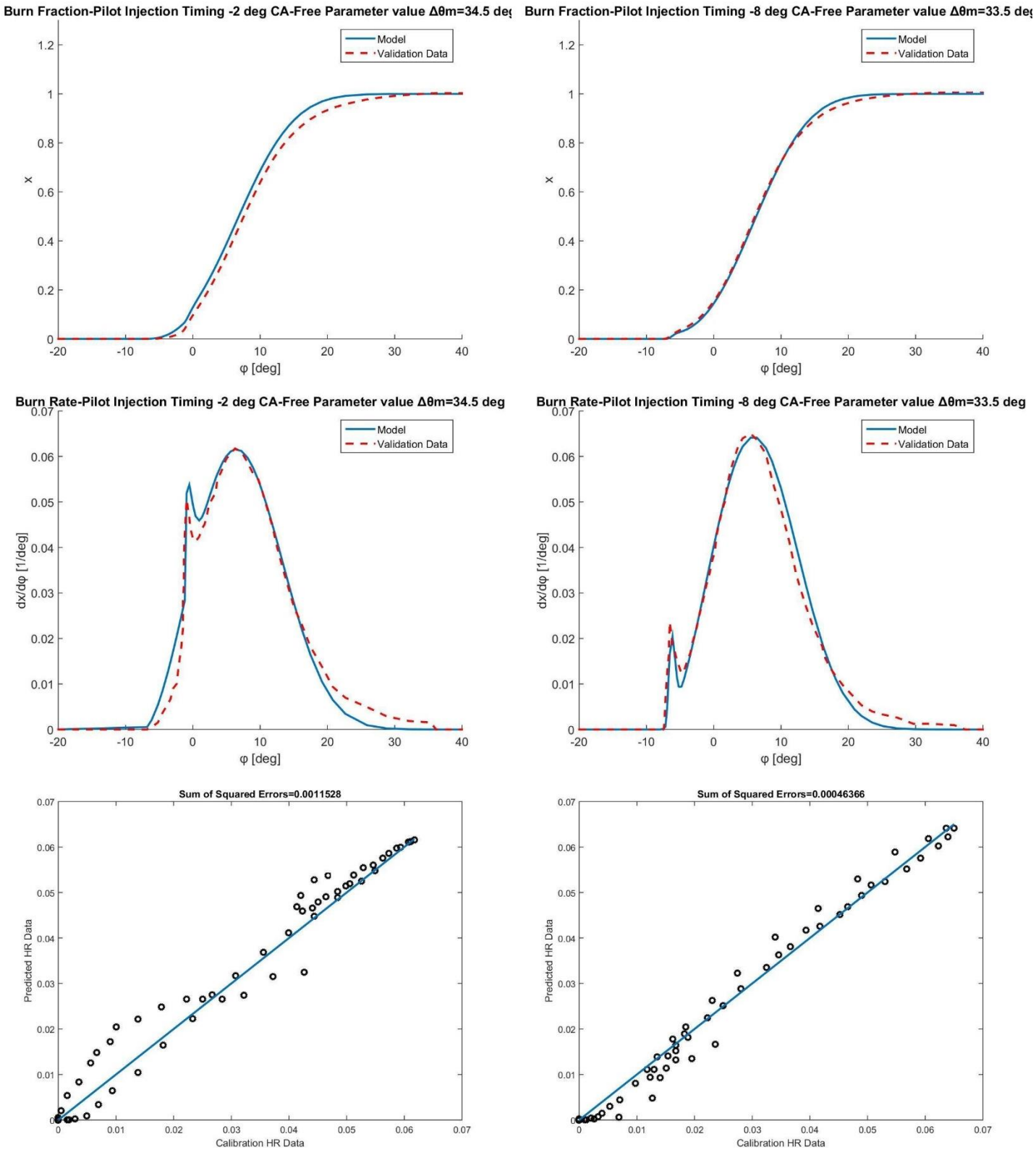

Figure A14: Model Validation at PIT=-2 and PIT=-8 deg

Engine speed variation results

(at 85% load, φ=0.39, Pit -2 deg, EVC 266 deg)

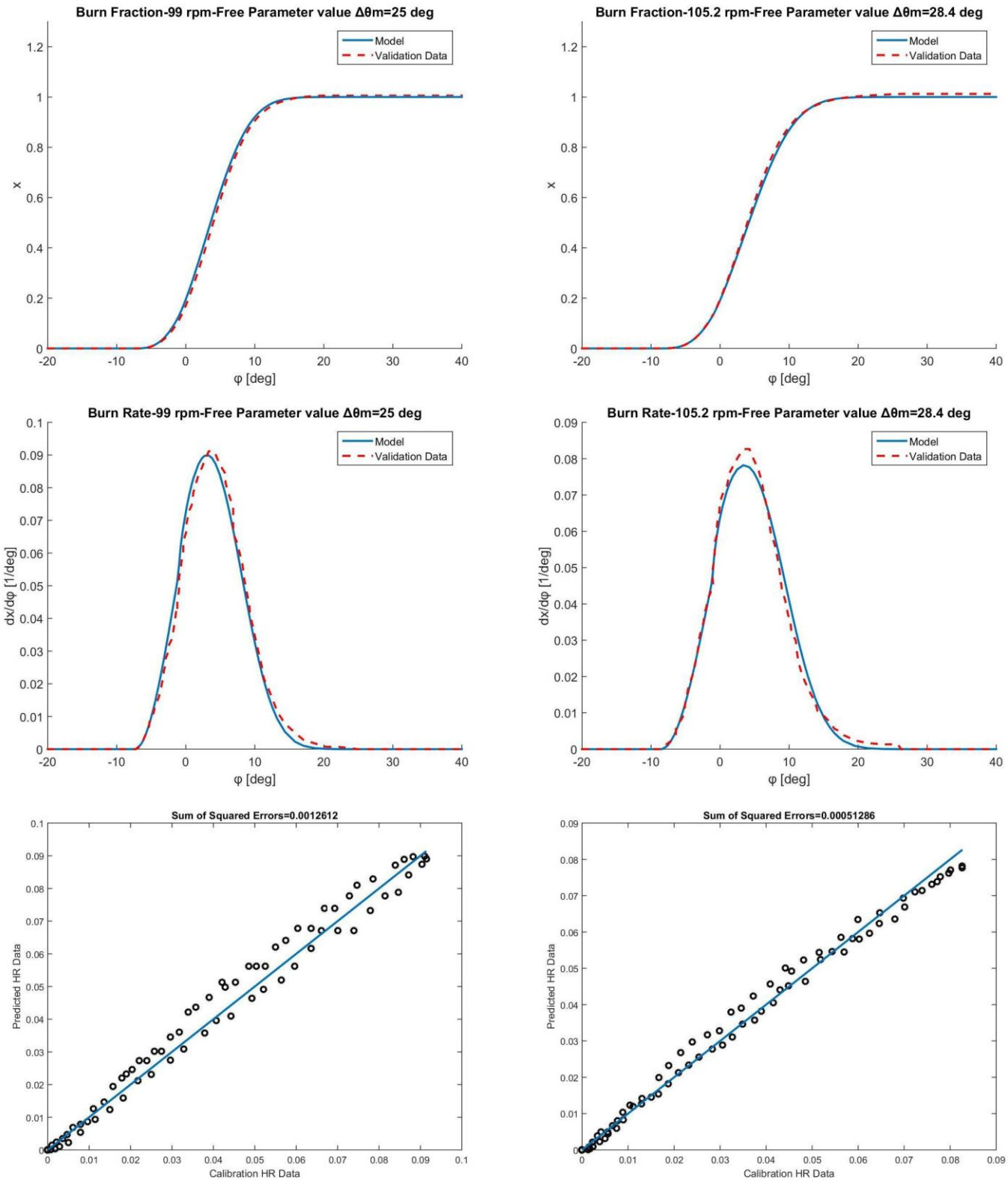

Figure A15: Model Validation at 99 and 105.2 rpm

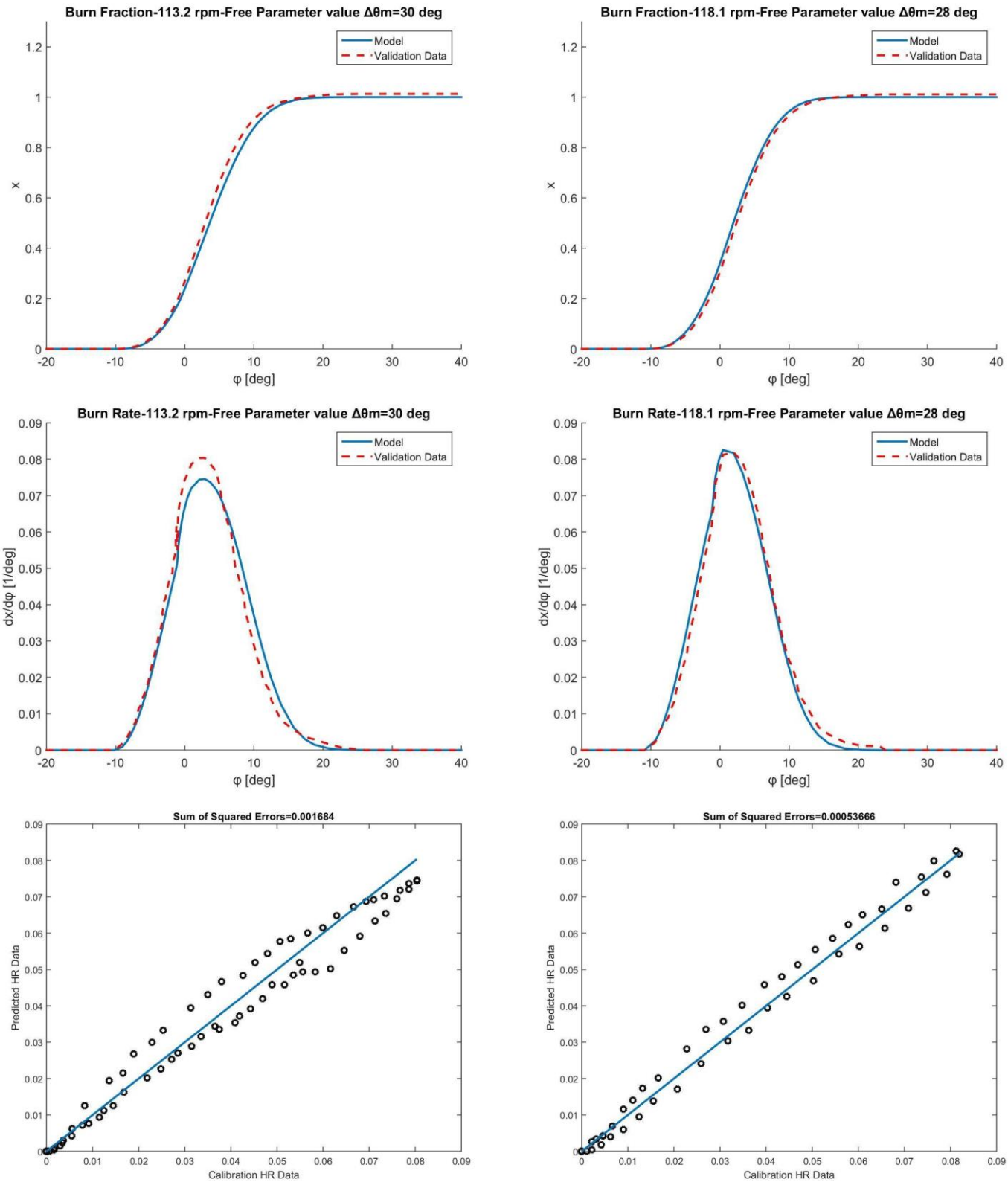

Figure A15: Model Validation at 113.2 and 1181.1 rpm

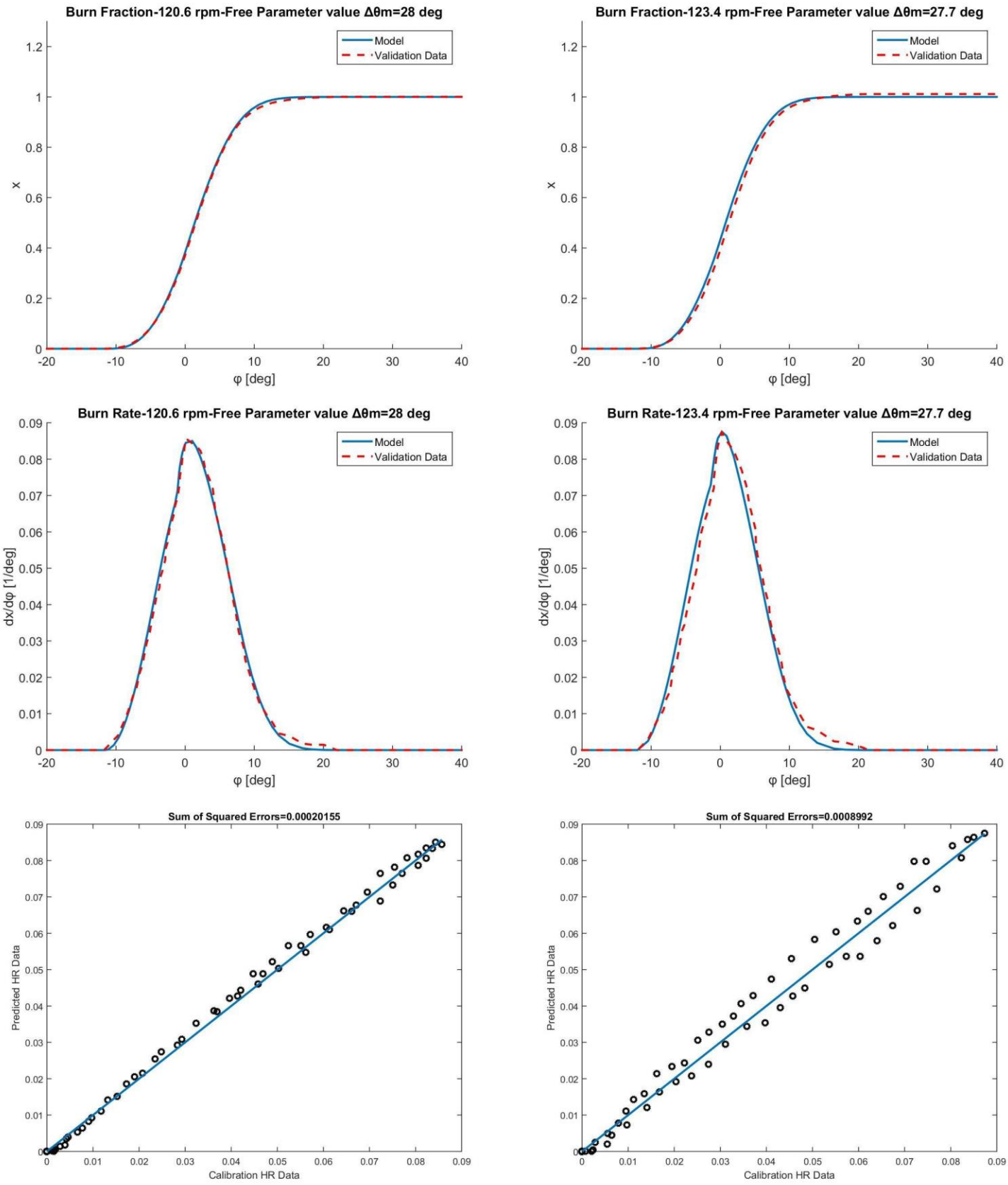

Figure A16: Model Validation at 120.6 and 123.4 rpm

Exhaust valve closing variation results

(at 50% load, 99rpm, Pit 0 deg)

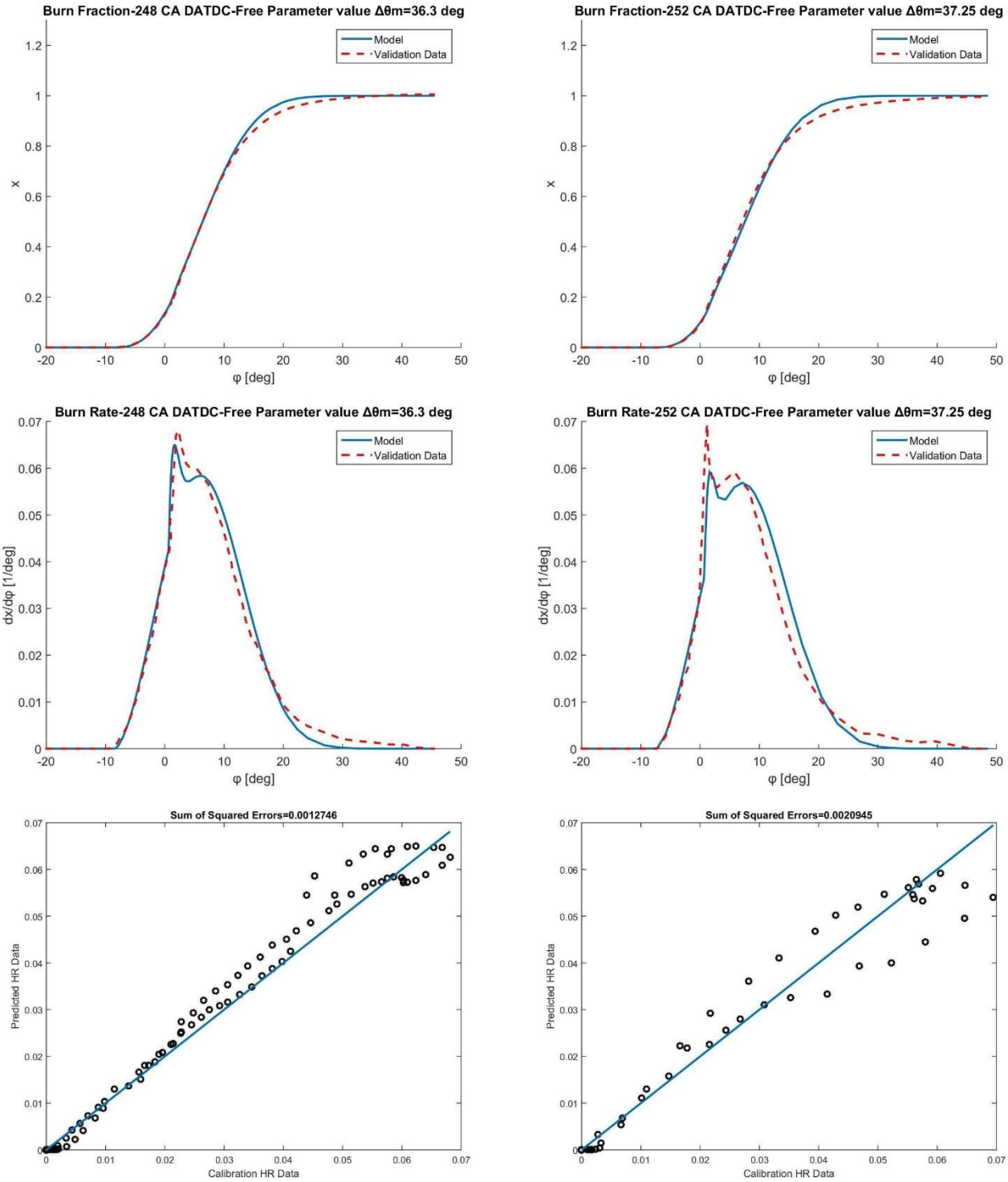

Figure A17: Model Validation at EVC=248 and EVC=252 deg

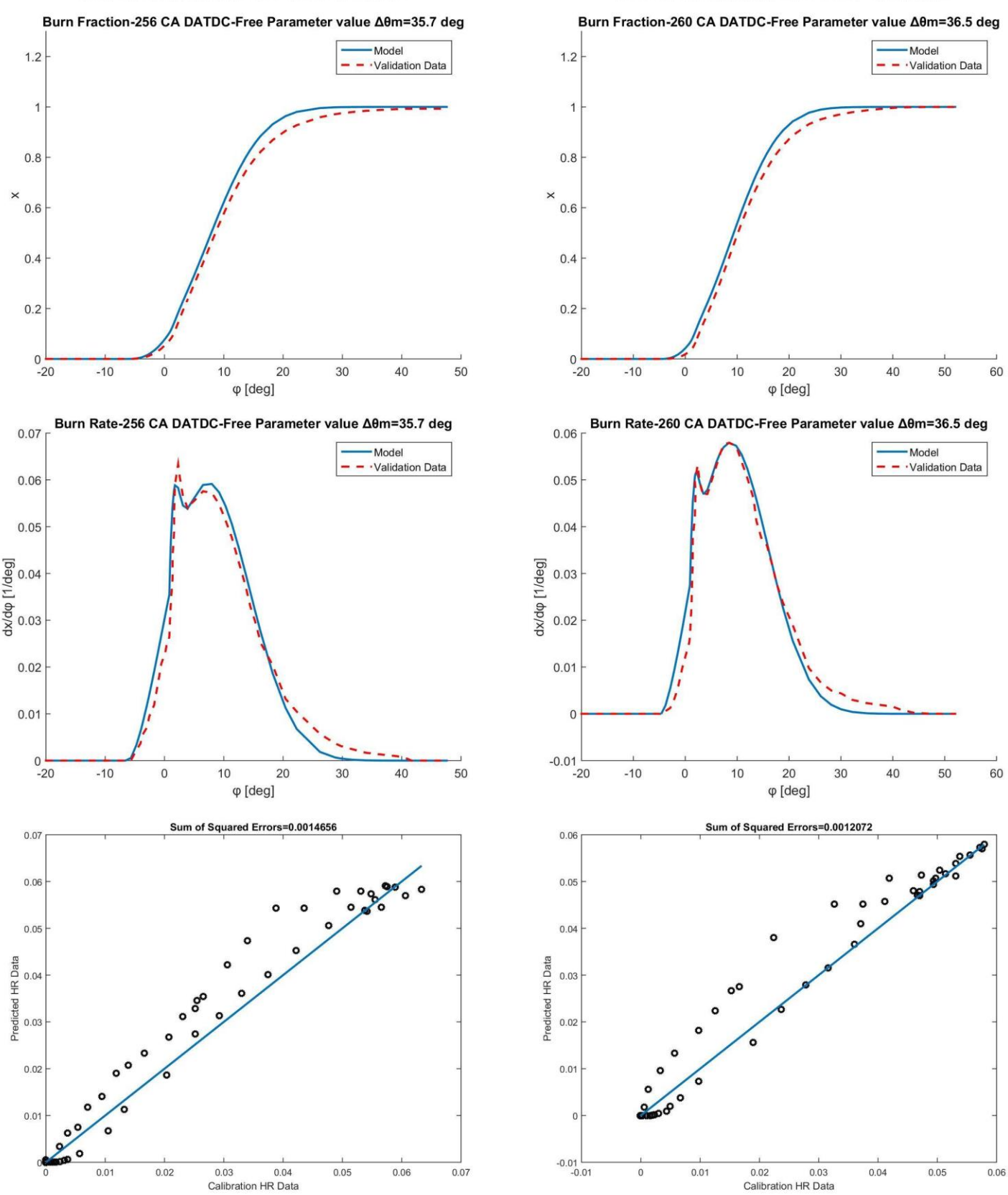

Figure A18: Model Validation at EVC=256 and EVC=260 deg

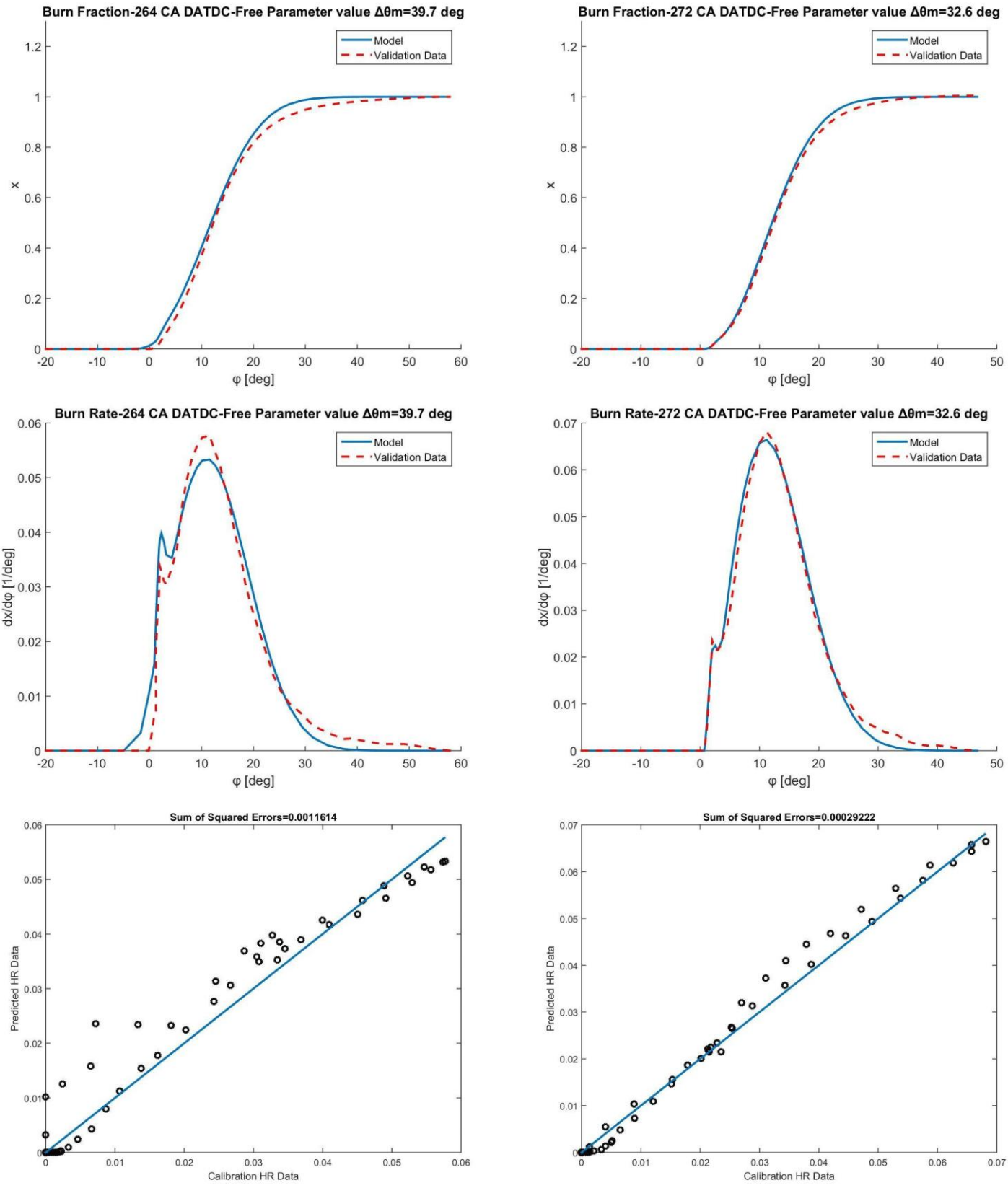

Figure A19: Model Validation at EVC=264 and EVC=272 deg